INFORMATION TO USERS

University of Alberta

Solubility of α-Olefins in Polyethylenes

by

Steven Jeremy Moore ©

A thesis submitted to the Faculty of Graduate Studies and Research in
partial fulfillment of the requirements for the degree of
Master of Science in Chemical Engineering

Department of Chemical and Materials Engineering

Edmonton, Alberta

Fall 2000

National Library
of Canada

Bibliothèque nationale
du Canada

Acquisitions and
Bibliographic Services

Acquisitions et
services bibliographiques

395 Wellington Street
Ottawa ON K1A 0N4
Canada

395, rue Wellington
Ottawa ON K1A 0N4
Canada

The author has granted a non-exclusive licence allowing the National Library of Canada to reproduce, loan, distribute or sell copies of this thesis in microform, paper or electronic formats.

The author retains ownership of the copyright in this thesis. Neither the thesis nor substantial extracts from it may be printed or otherwise reproduced without the author's permission.

L'auteur a accordé une licence non exclusive permettant à la Bibliothèque nationale du Canada de reproduire, prêter, distribuer ou vendre des copies de cette thèse sous la forme de microfiche/film, de reproduction sur papier ou sur format électronique.

L'auteur conserve la propriété du droit d'auteur qui protège cette thèse. Ni la thèse ni des extraits substantiels de celle-ci ne doivent être imprimés ou autrement reproduits sans son autorisation.

0-612-59852-7

Canada

<div align="center">

University of Alberta

Library Release Form

</div>

Name of Author: Steven Jeremy Moore

Title of Thesis: Solubility of α-Olefins in Polyethylenes

Degree: Master of Science

Year this Degree Granted: 2000

Permission is hereby granted to the University of Alberta Library to reproduce single copies of this thesis and to lend or sell such copies for private, scholarly or scientific research purposes only.

The author reserves all other publication and other rights in association with the copyright in the thesis, and except as herein before provided, neither the thesis nor any substantial portion thereof may be printed or otherwise reproduced in any material form whatever without the author's prior written permission.

Steve Moore

Apt. 900 – 131 Maxwell Street
Sarnia, Ontario
Canada N7T 7N9
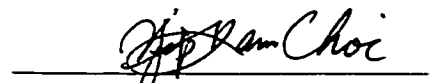
Date: *August 24, 2000*
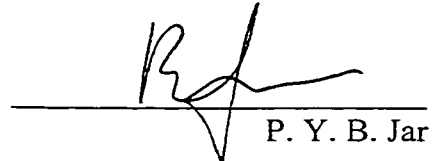
University of Alberta

Faculty of Graduate Studies and Research

The undersigned certify that they have read, and recommend to the Faculty of Graduate Studies and Research for acceptance, a thesis entitled **Solubility of α-Olefins in Polyethylenes** submitted by **Steven Jeremy Moore** in partial fulfillment of the requirements for the degree of **Master of Science in Chemical Engineering.**

S. E. Wanke (Supervisor)

P. Y. K. Choi

P. Y. B. Jar

August 23, 2000

Abstract

In this thesis, an accurate gravimetric procedure for the measurement of α-olefin solubilities in polyethylene is presented. This procedure was used to measure the solubilities of ethylene, 1-butene, and 1-hexene in four polyethylenes, at temperatures between 300 and 360 K and pressures up to 3.5 MPa for ethylene, and up to the saturation pressure for 1-butene and 1-hexene. The polyethylene samples studied were a high-density polyethylene, a low-density polyethylene, and two linear low-density polyethylene samples, one made with a Ziegler-Natta catalyst and the other made with a metallocene catalyst.

For the conditions of this study, ethylene solubility is well described by Henry's law; however, Henry's law is not valid for the sorption of 1-butene and 1-hexene. Olefin solubility was found to decrease with increasing temperature, and also with increased sample crystallinity. The solubility of α-olefins in polyethylene increases dramatically as the carbon number of the penetrant increases.

Acknowledgements

There are a number of people that I wish to thank for the help they have given me during the completion of this thesis and my time here at the University of Alberta.

First off, I am very grateful to my supervisor, Dr. Sieg Wanke, for his direction and advice in my research, and for providing me with valuable academic opportunities outside of the university.

I would also like to recognise Walter Boddez, Bob Scott, and the rest of the support staff in the Department of Chemical and Materials Engineering. These people deserve a share of the credit for all of the work that is done here.

Thank you to all my friends in the department, without whom my time here would probably have been more productive, but definitely not as much fun. And to Kathy Porter, for her friendship and love, and for continuing to make my life more and more interesting.

Finally, the greatest thanks must go to my parents, Jeremy and Marilyn Moore, for 25 years of love and support, and for helping to make me the person that I am.

Table of Contents

List of Tables

List of Figures

Nomenclature

a_1^c	combinatorial term in UNIFAC theory
a_1^{FV}	free volume term in UNIFAC theory
a_1^R	residual term in UNIFAC theory
a_2	activity of penetrant
$a(T)$	attraction parameter
amPE	amorphous polyethylene
b	hole affinity constant
$b(T)$	Van der Waals covolume
C_H	concentration of gas molecules in Henry's law sites
C_L	concentration of gas molecules in Langmuir type sites
C_L'	Langmuir capacity parameter
$F_{b,b}$	background buoyancy force
$F_{b,s}$	force due to sample buoyancy
$f_L(T)$	liquid fugacity at experimental temperature and one atmosphere
$f_L(T,P)$	liquid fugacity at experimental temperature and pressure
g	acceleration due to gravity
k	solubility constant
k*	Henry's law coefficient
k_H	Henry's law coefficient on concentration basis
$L_{T,P}$	sample length at experimental temperature and pressure
$L_{T,0}$	sample length under vacuum at experimental temperature
$L_{26,0}$	sample length under vacuum at 26°C

LLDPE	linear low-density polyethylene
M_c	chain length between crystallites
M_2	molar mass of penetrant
N_e	effective number of crosslinks
P	pressure
P_c	critical pressure of penetrant
P_s	deviation pressure
P_o	penetrant vapour pressure
P_1	initial equilibrium pressure
P_2	pressure after evacuation
P_3	final equilibrium pressure
QCM	quartz crystal microbalance
R	universal gas constant
S	solubility
T	temperature
T_c	critical temperature of gas
T_r	reduced temperature
v	molar volume of gas in Peng-Robinson equation
V_c	critical volume of gas
V_s	gas space volume
$V_{T,P}$	sample volume at experimental temperature and pressure
V_1	initial polymer volume
$V_1(T)$	specific volume of polymer at experimental temperature

V_2	molar volume of penetrant
V_2^L	molar liquid volume of penetrant
$V_{26,0}$	sample volume under vacuum at 26°C
W	sample weight
W_b	sample weight change
W_s	mass of amorphous polyethylene
α_T	thermal expansion coefficient
$\beta_{T,P}$	pressure expansion coefficient
χ_{12}	Flory-Huggins interaction parameter
$\dfrac{\varepsilon}{k}$	Lennard-Jones potential of penetrant
ϕ_1	volume fraction of polymer
ϕ_2	volume fraction of penetrant
ρ	sample density
ρ_a	density of amorphous polymer
ρ_g	gas density
ω	acentric factor

1. Introduction

By a considerable margin, polyethylene is the most widely produced polymeric material in the world. It is a polymer having the repeat unit $-(CH_2-CH_2)-$ but this description is not sufficient to characterise all of the different types of polyethylene that exist. By the substitution of alkyl chains for hydrogen atoms in polyethylene, branches off the main chain molecule can be formed. A classification system for the different kinds of polyethylene is based on the number and distribution of these branches. There are three main types of polyethylene:

1. High-density polyethylene; it has the simplest structure and consists predominantly of long straight chain molecules with little or no branching. This structure is shown in Figure 1-1.

Figure 1-1 - Structure of High-Density Polyethylene

2. Low-density polyethylene; it consists of long and short chains which are randomly connected. Figure 1-2 illustrates this structure.
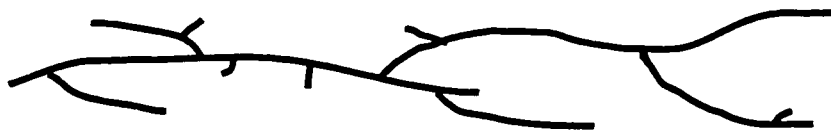
Figure 1-2 - Structure of Low-Density Polyethylene

3. Linear low-density polyethylene (LLDPE); its molecules consist of a main chain with a number of short branches. The structure of LLDPE is shown in Figure 1-3.

1

Figure 1-3 - Structure of Linear Low-Density Polyethylene

LLDPE is produced by the catalytic copolymerisation of ethylene and 1-alkenes, such as 1-butene, 1-hexene or 1-octene. The solubility of these olefin monomers in polyethylene is of interest for a number of reasons.

The polymerisation of LLDPE takes place in slurry or gas phase systems over solid catalyst particles. During the reaction, semicrystalline polyethylene forms inside the porous catalyst particle. For the reaction to continue, subsequent reactants must sorb into this polymer and then diffuse through the polymer to reach the catalyst surface (Hutchinson and Ray, 1990). The rate of polymerisation is dependent on the monomer concentration at the active sites of the catalyst, and this concentration is in turn dependent on the solubility of the monomers in polyethylene at the experimental temperature and pressure. Therefore, in order to analyse or model the polymerisation process, information on monomer solubility must be available (McKenna, 1998).

The solubility of α-olefin monomers in polyethylene is also important in the design of monomer removal equipment. Freshly produced polyethylene pellets contain large amounts of ethylene and other comonomers that must be removed in order to meet quality, safety, and environmental standards (Lutzow et al., 1999). Typically, monomer removal is accomplished by storing the freshly produced polymer in air-purged bins but this has led to some problems. A number of polyethylene producers have experienced bin fires resulting from inadequate purging and gaseous monomers reaching explosive levels above the polyethylene pellets (Beret et al., 1977). In order to have a rational basis

for the design of more effective monomer removal equipment, it is necessary to know the amounts monomer sorbed at different conditions (Beret and Hager, 1979).

Although useful for the aforementioned reasons, very few data are available on the solubility of olefins in polyethylene. There is a particular lack of data for higher olefins, which can likely be explained by the experimental difficulties of measuring solubilities of gases having low vapour pressures at ambient temperatures. Because it is difficult to predict the complex interactions between different monomers and polyethylenes having a wide variety of properties, experimental measurements are essential to obtain these solubilities. The objective of this work was to develop an accurate and reliable procedure for measuring olefin solubilities in polyethylene and to use this method to determine the solubilities of ethylene, 1-butene, and 1-hexene in a variety of different polyethylenes.

2. Literature Review

Previous work that has been done on the solubility of gases, with emphasis on olefins, in polymers is summarised in this section. Three main areas are reviewed; the focus of the first part is on the experimental techniques used to measure gas solubility; the second deals with models that have been developed to predict solubilities; and in the third, results for the solubility of ethylene, 1-butene, and 1-hexene in polyethylene are reported.

2.1 Review of Experimental Methods

Since the late 1950s, a number of research groups have examined solubility in a large number of fluid and polymer systems; a chronological summary of the experiments that have been done in this area is given by Mulder (1999). While there have been several methods used to determine solubilities, the vast majority of the experimental techniques can be grouped into the following three classifications:

1. Desorption analysis methods; these experiments begin with a polymer sample being saturated with a test gas. Solubility is then determined by measuring the amount of gas that is desorbed from the sample. Methods used to measure the desorbed gas include volumetric and chromatographic techniques.

2. Pressure decay methods; in these experiments a known amount of the test gas is admitted to a vessel of known volume containing the polymer sample. The pressure in the vessel is carefully monitored and once equilibrium is reached, a mass balance is performed to determine the amounts of gas contained in the vapour space of the vessel and inside the polymer.

3. Gravimetric methods; solubility is determined by the difference in mass of a polymer sample before and after saturation with the test gas.

2.1.1 Desorption Methods

Michaels and Parker (1958) were the first researchers to describe an accurate desorption analysis method that could be used to determine gas solubility in polymers. Their objective was to determine solubility constants for oxygen and nitrogen in different polyethylenes. Solubility measurements were made by placing approximately 150 g of polyethylene pellets into a glass bulb, which was attached to a vacuum system. The test gas was then introduced into the system up to atmospheric pressure and the researchers waited 12 hours for sorption equilibrium to be reached. After equilibrium, the system was rapidly evacuated using a rotary pump. The evacuation took approximately 1 minute to reach a pressure of less than 0.05 mm of mercury. Following evacuation, the sample bulb and the rest of the experimental system were sealed and allowed to reach equilibrium as the test gas desorbed from the polymer sample. The final pressure in the system was measured using a precision mercury manometer. The solubility constant, k, can be obtained from the following simple mass balance:

$$k\left(\frac{WP_1}{\rho}\right) + P_2 V_s\left(\frac{273}{T}\right) = P_3 V_s\left(\frac{273}{T}\right) + k\left(\frac{WP_3}{\rho}\right) \qquad (2\text{-}1)$$

where W and ρ are the weight and density of the polymer sample respectively. P_1 is the pressure at the initial equilibrium; P_2 the pressure immediately after evacuation; and P_3 the final equilibrium pressure. T is the gas temperature (Kelvin) and V_s is the gas space volume in the system.

An obvious problem with this and similar experiments is that some of the absorbed gas will desorb and be lost during the 1 minute evacuation. The researchers attempted to correct for this problem using diffusion constants for the gas-polymer system that had been determined in other studies. They estimated that for oxygen and nitrogen in polyethylene the magnitude of the correction is less than 10% of the gas originally present. In order to minimise the magnitude of the correction, Michaels and Bixler (1961) refined the technique so that an evacuation of approximately 10 seconds was needed to reach pressures between 0.1 and 0.2 mm mercury.

A similar but more refined desorption experiment was described by Robeson and Smith in 1967 and 1968. They measured the solubility of an ethane-butane mixture in polyethylene at temperatures between 20°C and 60°C. Their apparatus consisted of a cylindrical copper desorption chamber attached to a gas trapping system. The trapping system was made up of two u-shaped glass tubes, filled with gas spheres and immersed in liquid nitrogen baths. Polyethylene films were placed in the desorption chamber; the system was then evacuated and set to the desired temperature. After the sample had been completely degassed, the gas mixture was admitted to the cylinder until the system pressure was atmospheric. A sufficient amount of time was then taken to ensure sorption equilibrium. Then the cylinder was quickly evacuated and purged with a small controlled gas leak for 15 seconds. After 15 seconds, the cylinder was connected to the trapping system. During the desorption, the air leak was controlled so that the pressure in the cylinder was between 1 and 2 mm mercury. This helped to move the desorbed gas from the cylinder and into the traps. After the desorption, the traps were brought to room temperature and air was introduced to bring the contents to atmospheric pressure. When

the gas mixture in the traps was in equilibrium, a sample was injected into a gas chromatograph to determine its composition. From the composition, the amount of gas desorbed, and hence solubility, could be determined. As before, a correction for the gas lost during evacuation was made based on diffusion data.

In 1972 Deas et al. used a chromatographic desorption method to determine the solubility of hydrogen in polyethylene. This method was also used by Kubo and Dole in 1974 to determine the solubility of hydrogen and helium in a number of different polyethylenes. In their experiments, a Pyrex glass loop was filled with approximately 0.5 g of polyethylene. A vacuum system was assembled so that the loop could be evacuated, filled with hydrogen to a desired pressure, or rapidly purged by a blast of nitrogen. To begin the experiment, the sample loop was evacuated and placed into a constant temperature bath. Hydrogen was admitted to a pressure of exactly 1 atmosphere and the system was left for 24 hours to equilibrate. After equilibrium, ambient hydrogen in the system was removed by blast of nitrogen for approximately 5 seconds and the loop was removed from the temperature bath. Following another 24 hour wait, the glass loop was connected to a gas chromatograph, which was used to measure the amount of hydrogen that had been contained in the polyethylene.

In this method, two corrections were necessary to accurately determine the solubility of hydrogen. The first correction was used to account for the residual hydrogen that remained in the sample tube after the nitrogen purge. To determine this amount, the experimental procedure was performed using insoluble glass beads as a sample. A correction was also made to account for the loss of dissolved hydrogen during the purge. This correction was made by using a number of different purge times then preparing a

plot of the measured solubilities as a function of purge time. By extrapolating to a purge time of zero, an approximation of the true solubility can be obtained.

Another desorption experiment was performed by Beret and Hager in 1979. They measured the solubility of ethylene in low-density polyethylene, ethylene-vinyl acetate, and ethylene-ethyl acetate. In their experiment, approximately 7.5 g of spherical pellets were placed in a cylindrical glass sample holder. The sample holder was connected on one end to two gas inlets, and on the other end to a flame ionization detector. The pellets were degassed using a flow of nitrogen until the evolution of gas from the polymer was below recordable limits (10^{-11} g/min/g of polymer) and then saturated with ethylene for more than 48 hours. During this time, the temperature in the sample holder was controlled by heating tape around the system. To begin the measurements, the ethylene flow was replaced by a rapid purge blast (1000 cm^3/min) of nitrogen to remove all residual ethylene. After 30 seconds, the purge stream was replaced by a high purity nitrogen flow of 30 cm^3/min and the outlet flow was directed to the detector. From this point, the flame ionization detector continuously monitored the amount of ethylene in the nitrogen stream until it was below detectable levels. This took between 12 and 48 hours depending on the polymer. Solubilities were determined by measuring the total amount of ethylene evolved over the course of the experiment. However, no attempt was made to correct for ethylene evolution during the purge.

2.1.2 Pressure Decay Methods

The simplest example of solubility measurement by the pressure decay method is given by Lundberg et al. (1962). In this experiment, the researchers measured the

solubilities of nitrogen and methane in liquid polyethylene and polystyrene using a single-volume method. The liquid polymer was contained in a sintered glass cylinder, which permitted contact between the polymer surface and the surrounding gas. The cylinder was placed inside a pressure vessel of known volume, which was then brought to the temperature of the experiment. The test gas was then quickly admitted to the system and the system closed. The pressure inside the system was monitored as it decreased due to sorption into the polymer. When the pressure was constant, sorption equilibrium was considered to have been reached. Knowing the initial pressure immediately after the gas is admitted to the system, and the final pressure at equilibrium, a simple mass balance can be written to determine the amount of gas that has been sorbed by the polymer. However, there are problems with this type of experiment. When the gas is admitted, a short time is needed for the pressure gauge to stabilise. For some systems, a considerable amount of sorption may take place during this stabilisation. This makes it difficult to accurately determine the initial pressure, and hence the initial number of moles of gas in the system (Koros and Paul, 1976). It is possible to extrapolate the pressure decay data to zero time but this still introduces uncertainty into the experiment.

In order to overcome the problems associated with the single-volume method, a more advanced dual-volume pressure decay method was designed by a number of researchers. This type of experiment is well described by Koros et al. (1976), who measured the sorption of carbon dioxide in polycarbonate. The dual-volume sorption apparatus is shown schematically in Figure 2-1.

A polymer sample of known volume was placed inside Chamber B. The entire system was then evacuated for a period of 18 hours and kept at a constant temperature of
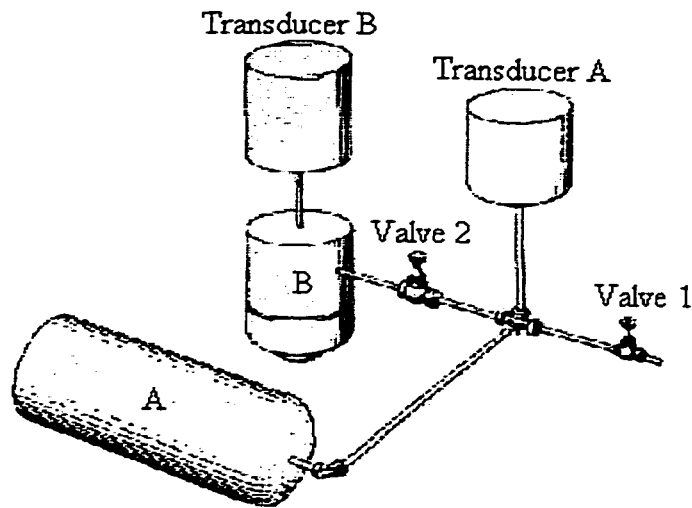
Figure 2-1 - Typical Dual-mode Sorption Apparatus (Koros et al., 1976)

35°C. After evacuation, Valve 2 was closed and carbon dioxide was admitted to the

system. Once the gas was admitted, Valve 1 was closed and the researchers waited for

the pressure in the system to equilibrate and recorded the pressure measured by

Transducer A. Knowing the volume of Chamber A and the temperature, the amount of

gas in the system could be accurately calculated. Valve 2 was then opened briefly to

allow gas into the sample Chamber B. The pressure in Chamber B was continuously

monitored until it was constant and equilibrium sorption had been reached. Following

equilibrium, the pressures in Chambers A and B were recorded and the amount of gas in

each chamber was calculated. The amount of gas sorbed in the polymer sample can be

determined from the difference between the number of moles of gas initially present in

the system, and the number of moles present after sorption equilibrium. Once a set of

measurements is complete, Valve 2 can be opened again to admit more gas into the

sample chamber and obtain solubility data at a higher pressure. This procedure can be

repeated until the pressure in Chamber B is equal to that in Chamber A.

The dual-volume method described by Koros et al. (1976) became a very popular method to determine solubilities and has been used by a number of researchers. Experiments using this pressure decay method to determine gas solubility in polymers include Sada et al. (1987), Chiou and Paul (1989), Hellums et al. (1989), and Del Nobile et al. (1995). According to Koros et al. (1976), the keys to obtaining accurate solubility results from this type of experiment are eliminating leaks from the system, allowing adequate time for equilibration, and determining the system volumes accurately.

A similar method was also used by Sato et al. (1996) to measure the solubilities of carbon dioxide and nitrogen in polystyrene. These researchers refined the method to take into account the fact that the volume of the polymer sample increases during the sorption process. In their experiment, the volume of the swollen polymer was predicted using the Sanchez-Lacombe (1978) equation of state.

2.1.3 Gravimetric Method

The third main category of solubility measurements are gravimetric measurements, where the amount of gas sorption in a polymer sample is determined by direct weighing of the sample. This method has the advantages that the data are easily analysed and there are few sources of uncertainty. The simplest method for gravimetric measurement of gas solubility in polymers was used by Crank and Park (1949) to investigate diffusion of organic vapours in polystyrene. In this experiment, a polymer specimen was placed in an atmosphere of constant penetrant vapour pressure, and was withdrawn and weighed at a number of time intervals. This intermittent removal and weighing could give rise to a large amount of error in the solubility values obtained

(Crank and Park, 1968). For gases that diffuse quickly, there would be some desorption during the weighing. Also, exposure to the air could lead to sorption of gas species other than the desired test gas. These errors can be overcome by more refined gravimetric techniques.

A much more accurate gravimetric technique makes use of a quartz helix microbalance to constantly measure the weight of the polymer sample under the controlled atmosphere. For such a balance, the weight of the load is proportional to the extension of the spring, which can be accurately measured with a cathetometer. A typical quartz spring sorption apparatus is described by Duda et al. (1973), who used their system to measure the solubility and diffusivity of ethylbenzene in polystyrene. The main sorption chamber of their experiment was a cylindrical glass column, approximately 4 feet long and with a diameter of 6 inches. Two quartz springs, with a sensitivity of 1.6 mm/mg, were hung inside the chamber. The polymer samples, in the form of flat disks, were placed in cylindrical quartz buckets, which were hung from the springs. The sorption chamber was connected to a vacuum system and also to a penetrant feed chamber, consisting of an insulated 1.5 litre flask with a temperature controller. The liquid penetrant in the feed chamber could be maintained at a constant temperature so that a constant vapour pressure of penetrant could be supplied to the sorption column. The temperature of the sorption column was maintained with a temperature control fluid flowing in an annulus around the main chamber. Pressure in the chamber was measured using a mercury manometer.

Before beginning an experiment, the polymer samples were heated and degassed in a vacuum oven to remove any internal stresses and volatiles that may have been

present. After the samples were placed in the sorption chamber, the chamber was evacuated and set to the experimental temperature. To start the sorption experiment, the system was sealed and the valve leading to the penetrant feed was opened. The weight change of the samples was measured by recording the extension of the springs over time.

The quartz spring apparatus developed by Duda et al. (1973) has been used by a number of other researchers. Typical examples include work by Faridi et al. (1994), who measured the solubility of various solvents in ethylene-propylene copolymers, and Lutzow et al. (1999), who examined the solubility and diffusion of toluene and n-heptane in polyethylenes of different crystallinity. Similar quartz balance measurements were made by Rogers et al. (1960), Li and Long (1969), Suwandi and Stern (1973), Kreituss (1981), and Yoon et al. (1992, 1994, and 1996).

A more recent advance in gravimetric solubility measurement is the use of electrobalances, interfaced with personal computers, which are able to continuously measure the weight change of a sample. An excellent example of the procedure used for this mode of gravimetric measurement is given by Kamiya et al. (1986b). In this experiment, the researchers measured the solubilities of nitrogen and carbon dioxide in low-density polyethylene; carbon dioxide in polycarbonate; and nitrogen, methane, ethane, and carbon dioxide in polysulfone. The apparatus consisted of a high-pressure stainless steel chamber containing Cahn model 2000 electrobalance. The pressure chamber was located inside a constant temperature air bath and connected to a gas supply system, which was composed of a rotary vacuum pump, cylinders of the test gases, pressure gauges, and flowmeters. A polymer sample, weighing approximately 200 mg, was hung directly from the balance beam using a Nichrome wire.

To begin the experiment, the system was evacuated until the weight of the sample was constant. The penetrant gas was then admitted to the system, in a stepwise manner, until the maximum pressure of 50 atmospheres was reached. After each pressure increment, the weight measured by the electrobalance was monitored until equilibrium had been reached. The researchers found that most of the sample weight change occurred within the first few hours after adding or removing the test gas. However some experiments, particularly those on carbon dioxide and ethane, showed persistent gradual weight changes continuing for at least four hours (Kamiya et al., 1986a). For cases where a slow weight change was observed, equilibrium was considered to have been reached in the rate of weight change became less than 0.3% of the total amount of sorbed gas per hour. After the maximum pressure of 50 atmospheres had been reached, the system was left for 24 hours and then desorption measurements were started. Here the pressure was decreased using the same steps and again ensuring that equilibrium is reached at each step.

Over the past 15 years, a number of different research groups have made use of a similar gravimetric method, based on a Cahn electrobalance. The most prolific group has been that of Kamiya. In addition to the experiment described above, they have investigated a number of other gas-polymer systems (Kamiya et al., 1986a, 1988a, 1988b, 1989a, 1989b, 1992, 1995; Hirose et al., 1986; Wang and Kamiya, 1995). Other groups that have used a similar method include: Castro et al. (1987); Liu and Neogi (1988); Lee and Flumerfelt (1995); and Hedenqvist et al. (1996).

One complication that arises in gravimetric solubility measurements is sample buoyancy. The sample weight change recorded by a microbalance is due not only to the

amount of sorbed gas but also to the difference in buoyancy of the sample under vacuum and under experimental pressures. In order to determine the magnitude of the buoyancy effect, the volume of the polymer sample must be accurately known. Furthermore, because a polymer sample will swell and increase in volume as gas is sorbed, it is necessary to know the sample volume after sorption equilibrium is reached at experimental temperature and pressure. In order to calculate buoyancy corrections, the swelling or dilation of polymers by gases has been of interest to researchers such as Hirose et al. (1986). In their experiment, a thin rectangular polymer sample was placed between two glass plates having a spacing of 100-150 μm. The plates were located in a stainless steel high-pressure chamber with a glass viewing window. To begin the experiment, the pressure chamber was evacuated and set to the chosen experimental temperature. After the sample was completely degassed, the length of the sample was measured using a cathetometer. The test gas was then admitted to the system using the same stepwise manner as that of Kamiya et al. (1986b). At each step, the length of the polymer sample was recorded after sorption equilibrium had been reached.

From this experiment, the change in length of a polymer sample due to swelling is determined. If it is assumed that the volume expansion of the polymer is isotropic, the sample volume can then be calculated from this length increase. The assumption that dilation is isotropic has been supported by the work of Fleming and Koros (1986) and Mulder (1999). For most work, including that done in this study, the accuracy of the sample volumes calculated using this assumption is acceptable. However, if greater accuracy is required, Pope et al. (1989) described an apparatus where the dilation of a sample can be measured in all three dimensions. Their apparatus consisted of a Jerguson

pressure cell with borosilicate windows, a TV camera and monitor, and a video micrometer. A polymer sample, measuring approximately 4 cm long by 1.5 cm wide, was hung inside the pressure cell and displayed on the monitor. In order to observe dilation in both width and thickness, the sample support was rotated so that an edge-on view could always be obtained. The video micrometer superimposed two pairs of lines on the monitor screen, one pair in the X direction and one in the Y direction. The pairs of lines made it easy to measure the length, width, or thickness of the sample. By simply aligning a pair of lines so that they were even with each side of the sample, the distance between the lines was automatically calculated by the micrometer. The experimental procedure concerning evacuation and filling of the pressure chamber was similar to that of Hirose et al. (1986).

Another apparatus used for gravimetric solubility measurement is the flow system described by Doong and Ho (1991). The advantage of this system is that it permits measurement of condensable vapour at high partial pressures without exposing the electrobalance to high temperatures. In their experiment, a polymer sample was placed in a pan hanging from a Cahn 2000 electrobalance. The pan was located in a sample tube with inlets for two gas streams. One of the streams was pure nitrogen, while the other consisted of nitrogen fed into a saturator containing liquid penetrant. Flows of both streams were controlled by mass flow controllers. By controlling the temperature of the saturator and the relative flow rates of the two streams, the partial pressure of penetrant in the system could be manipulated. Weight change, temperature, and pressure were recorded and stored by a personal computer. One complexity that arises from a flow system is the hydrodynamic effect, which influences the weight change measured by the

balance. To overcome this, once the system has reached sorption equilibrium (i.e. the weight change is constant), the gas flow is stopped and the equilibrium weight is quickly measured without the hydrodynamic effect.

Doong and Ho (1991) used their flow system to measure the solubilities of a number of aromatic vapours in semicrystalline polyethylene. A similar approach was used by Takeuchi and Okamura (1976) to measure the solubilities of benzene, cyclohexane, n-hexane, and toluene in polyethylene.

A more advanced gravimetric technique, that has been recently developed, is based on the use of a quartz crystal microbalance (QCM) (Siva et al., 1995; Miura et al., 1997). These experiments are begun by measuring the initial frequency of vibration of the quartz crystal. A thin film of polymer is then solution deposited onto the surface of the crystal. The weight of the deposited film can be determined by the change in vibration frequency of the crystal. After deposition, the polymer coated QCM is placed in a sorption chamber and sorption experiments are carried out in the same manner as has been previously described (Kamiya et al., 1986b). At each pressure step, the vibration frequency is measured until it is constant and equilibrium has been reached. The mass of sorbed gas can be calculated from this equilibrium frequency.

Solubility measurements using a QCM have a number of advantages over traditional gravimetric measurements. Because the polymer films on the crystal are very thin, a shorter time is needed for sorption equilibrium to be reached. Also, the mass of sorbed gas can be measured directly, without the need for a buoyancy correction (Miura et al., 1997).

2.2 Review of Solubility Models

For as long as researchers have been measuring the solubility of gases in polymers, there has also been research interest in developing mathematical models to explain the solubilities. These models have been developed both to fit existing data, and also to attempt to predict solubilities for solute-polymer systems where no experimental data are available. Because of the tremendous number of gas-polymer combinations that are present in industry, predictive models would be extremely useful. An overview of the models that have been used to describe gas solubility in polymers, and the development of these models is provided in this section.

2.2.1 Henry's Law

The simplest model for solubility is the case where the amount of sorbed material is directly proportional to the penetrant pressure. This relationship, known as Henry's law, is described by Equation 2-2

$$S=(k^*)P \tag{2-2}$$

where S and P are the solubility and pressure respectively and k^* is the solubility or Henry's law coefficient. Michaels and Bixler (1961), Hutchinson and Ray (1990) and Castro et al. (1987) all reported that Henry's law was applicable to the solubility of low molecular weight hydrocarbons in polyethylene at ambient temperatures and pressures close to atmospheric. Researchers including Stern et al. (1969) found that for simple gases including nitrogen, oxygen, and carbon dioxide, Henry's law behaviour was exhibited up to much higher pressures. Because of its simplicity and applicability, it is

not surprising that most of the first models for gas solubility in polymers were based on Henry's law.

Many of the first solubility models consisted of attempts to correlate the solubility coefficient, k^*, of a given penetrant to intrinsic thermodynamic properties of that penetrant. Such a correlation is given by Michaels and Bixler (1961), who used regression analysis to relate the solubility coefficient to the Lennard-Jones potential of the gas.

$$\ln k^* = 0.022\frac{\in}{k} - 5.07 \tag{2-3}$$

The Lennard-Jones potential was chosen because the researchers felt that it was "a more fundamental thermodynamic property than the normal boiling temperature for measuring the propensity of essentially spherical gas molecules to condense into a liquid-like matrix" (Michaels and Bixler, 1961). Also, it was found to yield a more successful correlation than boiling point or critical temperature. This model was found to accurately describe the solubility of 12 gases in low-density polyethylene.

A similar correlation was proposed by Stern et al. (1969), who examined solubility data for 28 different substances, having solubility values spanning 5 orders of magnitude. Stern et al. (1969) proposed that, according to the principle of corresponding states, one could expect that the Henry's law coefficient should be a unique function of the reduced temperature (i.e. system temperature divided by critical temperature). They demonstrated this relationship by plotting $\log k^*$ versus (T_C/T) and all 28 substances were found to delineate a single curve. A further investigation showed that $\log k^*$ was a linear function of $(T_C/T)^2$ and regression analysis led to the equation

$$\log k^* = -5.64 + 1.14\left(\frac{T_c}{T}\right)^2 \qquad (2\text{-}4)$$

The researchers point out that the correlation fails to describe the solubility of water vapour. It is likely that this failure results from the fact that the corresponding states correlation is not suitable for strongly polar, hydrogen-bonded species. They also note that using a correlation based on (T_c/T) has advantages over those of Michaels and Bixler (1961), based on (ϵ/k). The primary advantages being that values for the critical temperature of species are much more widely available than (ϵ/k), and the temperature dependence of k^* is built into the correlation.

A correlation with the same form as Equation 2-4 was proposed by Hutchinson and Ray (1990).

$$\log k^* = -2.38 + 1.108\left(\frac{T_c}{T}\right)^2 \qquad (2\text{-}5)$$

This equation was found to fit a wide range of literature data. Following the observations of Stern et al. (1969), Castro et al. (1987) found that the correlation parameters are linear functions of the penetrant molecular weight. They found that Henry's law coefficient is well correlated by the equation

$$\log k^* = (-5.265 + 0.00203M_2) + (0.855 + 0.00142M_2)\left(\frac{T_c}{T}\right)^2 \qquad (2\text{-}6)$$

where M_2 is the molecular weight of the penetrant.

2.2.2 Deviation Pressure

While Henry's law is a useful starting point for solubility modelling, it is only applicable for certain systems under certain conditions. At higher pressures, all gases

20

begin to deviate from Henry's law and in these cases, penetrant solubility is no longer a linear function of penetrant pressure. Furthermore, Henry's law cannot usually be applied to heavier hydrocarbon vapours, which swell and plasticize the polymer to a greater extent (Hutchinson and Ray, 1990). Examining solubility data from a number of researchers, Stern et al. (1969) concluded that the pressure at which deviation from Henry's law behaviour becomes significant decreases as critical temperature of the penetrant increases. They defined the deviation pressure, P_S, to be the pressure at which a 5% deviation from Henry's law solubility would be observed. Following the method used in their previous correlation for the solubility constant, Stern et al. (1969) showed that log (P_S/P_C) was a linear function of (T_C/T) and linear regression gave the equation

$$\log\left(\frac{P_S}{P_C}\right) = 3.025 - 3.50\left(\frac{T_C}{T}\right) \tag{2-7}$$

where P_C is the critical pressure of the penetrant. This correlation is useful not only for predicting the deviation pressure for different substances, but also for predicting deviation pressures for the same penetrant at different temperatures.

Castro et al. (1987) used the same definition of deviation pressure and determined it to be a function of P_o, the vapour pressure of the penetrant, and the penetrant molecular weight. They found that

$$P_S = \frac{0.0212P_o}{-0.94 + 0.0356M_2 - 0.0002296M_2^2} \tag{2-8}$$

Both Equations 2-7 and 2-8 are useful for determining at what point Henry's law is no longer a suitable model for gas solubility. At pressures above the deviation pressure, more complex thermodynamic models must be used to predict or correlate solubility.

2.2.3 Flory-Huggins Theory

The most widely used models for gas solubility in polymers are based on the Flory-Huggins equation, which can be used to predict the activity of a penetrant dissolved in a polymer lattice. While many researchers have used slightly different forms of the equation, it is commonly given as

$$\ln a_2 = \ln \phi_2 + \phi_1 + \chi_{12}\phi_1^2 \qquad (2\text{-}9)$$

where a_2 is the activity of the penetrant; ϕ_1 and ϕ_2 are the volume fractions of polymer and penetrant respectively; and χ_{12} is the Flory-Huggins interaction parameter. Details of the derivation of this equation are given by Flory (1953) as well as in many polymer textbooks.

The Flory-Huggins equation has been used to model solubility data by a number of research groups. Castro et al. (1987) measured the sorption of n-alkane vapours in polyethylene and found that the solubility data was well fit by the Flory-Huggins equation. It was found that the value of χ_{12} varies with the volume fraction of the polymer. Because of this variation, no single value of χ_{12} was sufficient to describe sorption over their entire range of experimental conditions. However, they found that for temperatures greater than 30°C, the value of the interaction parameter remains approximately constant. Lee and Flumerfelt (1995) investigated the solubility of nitrogen in molten low-density polyethylene at temperatures up to 450 K and pressures up to 125 atmospheres. They found that the Flory-Huggins relationship represented the experimental results quite well at higher pressures where Henry's law was no longer applicable. Furthermore, Yoon et al. (1996) found that the solubilities of 1-butene, 1-hexene, and 1-octene could be represented by Equation 2-9 with fixed values for the

interaction parameter. The results of Yoon et al. (1996) are particularly relevant to the current study.

It is has been postulated that for semicrystalline materials such as polyethylene, gas sorption takes place only in the amorphous regions (Michaels and Bixler, 1961). For this reason, the amorphous volume fractions of penetrant and polymer are typically used in the Flory-Huggins equation. However, although sorption does not occur in crystallites, their presence does affect sorption in the amorphous regions. Crystallites act as physical crosslinks, tying the amorphous regions together and restricting the movement of the polymer chains (Hutchinson and Ray, 1990).

To account for the effect of crystallites on gas sorption in the amorphous region, a number of modifications to the original Flory-Huggins theory have been suggested. Rogers et al. (1959) suggest the addition of an "elastical-entropy" term, which yields the equation

$$\ln a_2 = \ln \phi_2 + \phi_1 + \chi_{12}\phi_1^2 + \frac{\phi_1^{1/3}V_2\rho_a}{M_C} \tag{2-10}$$

where V_2 is the molar volume of the penetrant, ρ_a is the density of the amorphous phase, and M_C is the chain length between crystallites. A similar correction was suggested by Flory (1969) to give the equation

$$\ln a_2 = \ln \phi_2 + \phi_1 + \chi_{12}\phi_1^2 + \frac{V_2 N_e}{V_1}(\phi_1^{1/3} - \frac{\phi_1}{2}) \tag{2-11}$$

where V_1 in the initial polymer volume and N_e is the effective number of crosslinks. Similar extensions to the Flory-Huggins theory are given by Liu and Neogi (1988) and Budzien et al. (1998a).

While the Flory-Huggins equation has proven to be a very useful tool for predictions of gas solubility in polymers, it has a number of limitations that should be considered (Fried, 1995). The equation is only valid for systems that are sufficiently concentrated that there is uniform segment-density; there is no volume change of mixing during the sorption process; and there are no energetically preferred arrangements of polymer segments and penetrant molecules.

2.2.4 Dual Mode Sorption

Sorption isotherms for gases in rubbery polymeric materials are usually seen to have upward curvature, concave to the sorption axis. As discussed above, this behaviour is well modelled using the Flory-Huggins equation. However, for a glassy polymer, sorption isotherms typically possess downward curvature and thus a different model must be used (Lipscomb, 1990).

The most commonly used model for sorption in glassy polymers is the dual mode model (Vieth, 1991). This model is based on the idea that there are two types of sites which penetrant molecules may occupy. The first type of sorption occurs within the polymer matrix, while the second takes place in the excess free volume of microvoids present in the material (Lipscomb, 1990). Sorption into the denser polymer matrix is assumed to obey Henry's law. In the dual mode model, sorption is calculated in terms of gas concentration in the polymer so Henry's law is given as

$$C_H = k_H P \qquad (2\text{-}12)$$

where C_H is the concentration of gas molecules occupying Henry's law sites, and k_H is the Henry's law coefficient on a concentration basis. Sorption into the microvoids can be described by a Langmuir isotherm to yield the equation

$$C_L = \frac{C_L' bP}{1 + bP} \qquad (2\text{-}13)$$

where C_L is the concentration of gas in Langmuir type sites, C_L' is the Langmuir capacity parameter, and b is the Langmuir or hole affinity constant. The total concentration of sorbed gas is the sum of the Henry's law and Langmuir components

$$C = C_H + C_L = k_H P + \frac{C_L' bP}{1 + bP} \qquad (2\text{-}14)$$

The presence of the Langmuir absorption component greatly enhances the total solubility in glassy polymers compared to rubbery materials (Lipscomb, 1990).

2.2.5 UNIFAC Model

In 1975, Fredenslund et al. developed a group contribution method to predict activity coefficients in nonideal liquid mixtures. Their model is known as UNIFAC (UNIQUAC Functional-group Activity Coefficient) and is an extension of the quasi-chemical theory of liquid mixtures (UNIQUAC). The UNIFAC model provides a procedure to calculate activities based on constants representing the sizes and surface areas of individual functional groups, and parameters reflecting the energetic interactions between groups. The UNIFAC method was modified by Oishi and Prausnitz (1978) so that it could be applied to estimate solvent activities in polymers. The advantage of using a functional group contribution model for this estimation is that while there are a

tremendous number of penetrant-polymer systems, the number of functional groups which constitute these species is much smaller.

Solvent activities in the UNIFAC method are calculated as the sum of contributions from three sources

$$\ln a_i = \ln a_i^C + \ln a_i^R + \ln a_i^{FV} \qquad (2\text{-}15)$$

The first term, a_i^C, is a combinatorial or entropic term that takes into account the number, size, and shape of the functional groups involved. The second term, a_i^R, is the residual or enthalpic term; it accounts for the interactions between functional groups. The final term, a_i^{FV}, takes into account changes in the free volume of the system due to mixing. Such free-volume effects are significant because the polymer molecules are much more tightly packed than penetrant molecules. Because of this free volume term, the Oishi and Prausnitz model is sometimes referred to as the UNIFAC-FV model.

The UNIFAC-FV method has been used to study a number of binary penetrant-polymer mixtures. It has been found to give good estimates of penetrant activities in nonpolar systems, while less accurate results are obtained for polar systems (Oishi and Prausnitz, 1975). The method also permits estimation of penetrant activities in ternary systems, which could be of use to predict the solubility of gas mixtures in polymers.

Doong and Ho (1991) suggested the addition of a fourth term, the "elastic factor", to the UNIFAC-FV method. This term is similar to the additions made to the Flory-Huggins theory to take into account the crystallinity of the polymer. The crystalline domains restrain the amorphous chains and this introduces an elastic free energy contribution. The researchers used this modification to the UNIFAC-FV method to model the solubility of organic vapours in semicrystalline polyethylene. Castro et al.

(1995) used the same model to analyse solubility data for n-pentane and n-hexane in polyethylene and polypropylene.

2.2.6 PRISM Theory

The final model to be discussed was developed by Curro and Schweizer in 1987. It is known as the polymer reference interaction site model (PRISM). Similar to the UNIFAC method, PRISM theory predicts the activity of a penetrant molecule in polymers using an entropic and enthalpic contribution (Budzien et al., 1998b). In the model, each repeat unit in a polymer chain is considered to be an independent interaction site. Penetrant molecules are randomly inserted into these sites as point particles and then "grown" to a characteristic diameter. The reversible work associated with this growth provides the entropic contribution to the activity. The enthalpic contribution is found using a perturbation method approach to determine the energetics of interaction between the penetrant molecule and the interaction site.

PRISM theory was first used to predict the solubility of monatomic solutes in polymer melts (Curro et al., 1997). Its use was then extended to describe the solubility of noble gases in semicrystalline polyethylene (Budzien et al., 1998b). However, it has still not been successfully applied to larger, non-spherical penetrants. Work toward refining the theory so that solubilities of larger gases, such as hydrocarbons, could be predicted is currently being pursued.

2.3 Previous Olefin Solubility Results

There have been four research groups that have reported values for the solubility of ethylene in polyethylene. Their results will be summarised in this section. For the sake of comparison, the results have been converted to Henry's law coefficients, having units of grams of ethylene per gram of amorphous polyethylene (amPE) per atmosphere. The first group to study ethylene in polyethylene was Li and Long (1969). Using a quartz spring gravimetric technique, they reported a solubility of 1.2×10^{-3} g/(g amPE·atm) in a 45% crystalline, low-density polyethylene at 25°C. Beret and Hager (1979) used a chromatographic desorption method and measured a much lower value of 6.5×10^{-5} g/(g amPE·atm) for low-density polyethylene, having a crystallinity of 48%, at 23°C. It should be noted that there is some uncertainty in both these values as they were obtained from figures in the respective papers. In 1983, Kulkarni and Stern measured ethylene solubility using a unique volumetric method and reported a value of 1.3×10^{-3} g/(g amPE·atm) for a 55% crystalline, low-density polyethylene at 20°C. Finally, McKenna (1998) reported a coefficient of 1.2×10^{-3} g/(g amPE·atm) for a low-density polyethylene at 70°C. This value was also estimated from a figure, as was the crystallinity of approximately 52%.

There is quite good agreement between the values of Li and Long (1969), Kulkarni and Stern (1983), and McKenna (1998), despite the range of experimental conditions that were used. It should not be a surprise that the value of McKenna (1998) is similar to the others even though it was measured at a higher temperature. McKenna (1998) found that the solubility of ethylene has only a weak dependence on temperature, with the solubility decreasing slightly as the temperature is increased. The value of Beret

and Hager (1979) however, is substantially lower than the other three. This may be a result of the chromatographic method that these researchers used. One of the major flaws of this type of technique is that some of the desorbed ethylene is often lost at the beginning of the chromatographic measurement. It is probable that such a loss occurred in this case, resulting in a lower than expected solubility value.

Two research groups have investigated the solubility of higher α-olefins in polyethylene. To compare their results, it is convenient to look at the solubility, in terms of grams of olefin penetrant per gram of amorphous polyethylene, as a function of penetrant activity. Penetrant activity is usually approximated as the ratio of penetrant pressure to the penetrant saturation pressure at the given temperature. Yoon et al. (1996) measured the solubility of 1-butene and 1-hexene in linear low-density polyethylene. For 1-butene, the solubilities reported for a number of different polymers ranged between 0.0065 g/g amPE and 0.0085 g/g amPE, at a maximum activity around 0.1. They measured these solubilities at temperatures between 70°C and 85°C and found little variation with temperature. For 1-hexene, the solubilities ranged from 0.04 g/g amPE to 0.05 g/g amPE, at a maximum activity of 0.4. McKenna (1998) reported the solubility of 1-butene in polyethylene to be 0.025 g/g amPE at 80°C and an activity of 0.09. The values for both studies were estimated from figures in their respective papers.

3. Experimental Details

3.1 Polyethylene Samples

One of the major objectives of this study was to examine the effects that polyethylene chain structure and crystallinity have on olefin solubility. To this end, it was necessary to study polyethylene samples having a wide variety of different structures. Four polyethylene samples were selected in an attempt to encompass the range of different properties and characteristics available in industrial polyethylene. The samples studied were: a high-density polyethylene; a low-density polyethylene that results from production by the high pressure process; and two linear low-density polyethylene (LLDPE) samples, one made with a Ziegler-Natta catalyst and the other made with a metallocene catalyst. The two catalyst types available to produce LLDPE give rise to very different structures with the metallocene catalyst capable of producing samples with extremely low crystallinities. The properties of the polyethylene samples used in this experiment are shown in Table 3-1. The crystallinities were determined by x-ray diffraction (Mulder, 1999).

Table 3-1
Properties of Polyethylene Samples

Sample	Type	Comonomer	Mn (g/mol)	Polydispersity	Density (g/cm^3)	Crystallinity (%)
MM003	LDPE	-	22011	4.73	0.923	50.4
MM013	HDPE	-	11481	9.61	0.954	70.2
MM029	LLDPE	1-butene	25894	3.29	0.917	47.0
MM019	LLDPE	1-hexene	40356	2.14	0.885	18.5

The polyethylene samples were received from the manufacturers in pellet form and were pressed into sheets using a Carver Laboratory press. These sheets measured 100

mm by 100 mm with a thickness of approximately 0.5 mm. The procedure for pressing the sheets was as follows:

1. The press plates were closed loosely and heated to a temperature of 170°C.

2. Approximately 5 g of polyethylene pellets were arranged evenly throughout the mould. The mould was a 0.5 mm thick piece of brass with a 100 mm by 100 mm square hole, that was placed between two, 2 mm thick, smooth Teflon sheets. The mould and sheets were then placed between two heavy metal plates with thickness of 3 mm.

3. The mould assembly was placed between the press plates and heated without applying pressure for 10 minutes.

4. The sample in the mould was pressed for 5 minutes at a pressure of 13.8 MPa.

5. The pressure was increased to 32.2 MPa for a further 5 minutes.

6. Without decreasing the pressure, the press plates and mould assembly were quenched to 25°C by turning off the heaters and running cold water through the plates for approximately 10 minutes.

7. The pressure was released and the mould assembly removed from the press. The sample sheet was then removed from the mould.

The sheets produced by this method were generally of uniform thickness and free of bubbles or other imperfections. There was some slight surface roughness as a result of the texture of the Teflon sheets encasing the mould.

3.2 Gravimetric Solubility Measurement

The procedure used to determine solubilities in this experiment is a gravimetric method based on that used by Kamiya et al. (1986a, 1988a, 1988b, 1989a, 1989b, 1992, 1995; Hirose et al., 1986; Wang and Kamiya, 1995). This method was chosen because it is simple to perform, yet versatile enough to determine solubilities under a wide variety of conditions. In this experiment, solubility is determined by measuring the change in weight of a polyethylene sample exposed to a penetrant vapour. The weight change is measured by a Cahn electrobalance, controlled by a personal computer.

3.2.1 Experimental Equipment

The experimental setup used for the gravimetric solubility measurements is shown schematically in Figure 3-1. The microbalance used for the gravimetric solubility measurements was a Cahn D-110 Digital Pressure Balance. At the pressures used in this study, the balance has a sensitivity of ± 10.0 μg. The balance was mounted in a 316 stainless steel housing which was certified for pressures up to 13.8 MPa. The polyethylene samples were hung from the balance beam on a nichrome wire and contained in a stainless steel reactor tube having an inside diameter of 25 mm. Experimental pressure and temperature were measured by an Omega PX425-600GV pressure transducer and a Fluke 52 K/J Thermometer respectively.

The Cahn microbalance was enclosed in a constant temperature air bath. The air bath is important because it assures that there are no temperature gradients present in the system. Any thermal gradients in the reactor tube or balance housing would lead to
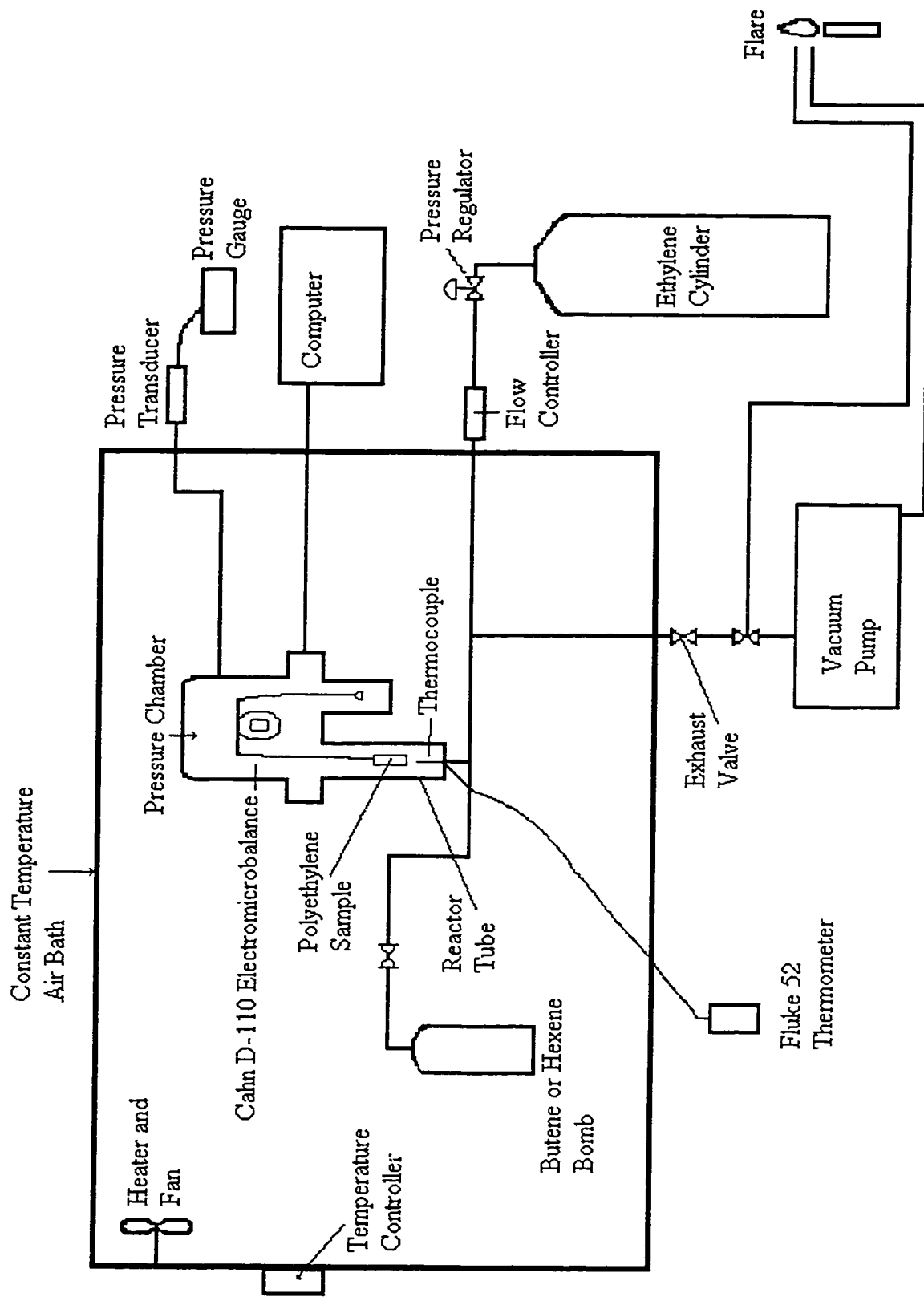
Figure 3-1 - Solubility Measurement Apparatus

33

convection currents that could affect the measured weights. The location of the cylinders of different gases should also be noted. Because ethylene is above its critical temperature at ambient conditions, it can be introduced to the system directly from a cylinder at room temperature. The flow of ethylene into the system was controlled by a Matheson Model 8250 Series Modular Dyna Blender. To carry out measurements at higher pressures and elevated temperatures with 1-butene and 1-hexene, it was necessary to preheat these fluids before they were introduced to the Cahn balance system. The simplest way to accomplish this was to locate a reservoir containing the desired hydrocarbon inside the air bath so the gas source was at the same temperature as the weight measurement system. To this end, 500 cm^3 stainless steel bombs were filled with 1-butene and 1-hexene. Gas flow from these bombs to the Cahn balance was controlled manually using a needle valve.

3.2.2 Experimental Procedure

The following section contains the detailed procedures used for the measurement of ethylene solubility in the polyethylene samples. The changes made to this procedure for 1-butene and 1-hexene are also discussed. Further instructions on the use of the Cahn software are given in Appendix 1.

Software Setup

1. From the operating directory C:\Cahn, the program D100-02.exe was loaded. From the Main Menu, option 1, Setup Mode was selected.

2. The operating parameters found in the file "newmeth.met" were loaded. The only parameter requiring adjustment was the Display Weight Range. A range from −0.01

g to 0.001 g was used for ethylene and a range of −0.001 g to 0.2 g for 1-butene and 1-hexene.

Calibration

1. Option 2, Run Mode was selected from the Main Menu.

2. After ensuring that the pressure inside the system was atmospheric, the pipe fittings attached to the stainless steel tube were removed and the tube unscrewed from the balance assembly. Care was, and must be, taken to remove the stainless steel tube directly downward so as not to disturb the hangdown wire from the balance.

3. A 12 mm diameter quartz pan was hung from the hangdown wire using tweezers; care was taken not to touch quartz pan with bare hands. After the weight recorded by the balance stabilised, the balance was tared.

4. A calibration mass of 1.000 g was entered. The calibration standard was then placed into the quartz pan with the tweezers. When the weight was stable, the Calibrate Balance option was selected.

5. With the balance calibrated, the quartz pan and calibration standard were removed from the hangdown wire, again taking care not to touch the quartz pan or the calibration mass.

Sample Placement

1. A rectangular sample measuring approximately 15 mm by 55 mm was cut from the previously pressed polyethylene sheet. Approximately 3 mm from the end, a paper clip was used to make a small hole in the middle of the sample. A wire hook, to attach the sample to the hangdown wire, was inserted into the hole.

2. The sample was hung on the hangdown wire and the stainless steel tube was carefully put into place over the sample. It was then screwed into place and the feed tubes on the side of the tube were connected.

3. The outlet line was directed to the vacuum pump and the outlet valve was opened slowly to evacuate the system.

4. The front panel of the air bath was closed and the air bath fan turned on. The bath temperature controller was set to 30 °C.

5. The sample was left under vacuum overnight to ensure that it was completely degassed.

Performing an Experiment

1. The outlet valve was closed.

2. Option 2, Run Mode was selected from the Main Menu of the Cahn software. The name of the new data file was entered and the balance was zeroed. The run was then started.

3. After checking that the flow controller was closed, the valve on the ethylene cylinder was opened and the regulator set to 100 psi.

4. The flow control valve was then opened slowly until the controller gave a reading of 0.5 V. After the experimental pressure reached atmospheric, the flow was increased to between 1.5 V and 2 V.

5. The system was left to fill until the system pressure was equal to that supplied by the ethylene cylinder regulator.

6. After the pressure in the system had stabilised, the weight recorded by the balance was monitored to determine when equilibrium had been reached. Equilibrium was

assumed to have been reached if no changes greater than ± 0.00005 g in the sample weight were observed over a 30 to 60 minute period. On some occasions it was not practical to monitor the weight change as the experiment ran so the system was left overnight to equilibrate.

7. After equilibrium was reached, the following data were recorded: the temperature and pressure inside the reactor tube, the atmospheric pressure in the room, and the measured equilibrium weight change.

8. The ethylene cylinder regulator pressure was then increased to 300 psi and Steps 5, 6, and 7 of this procedure were repeated.

9. After equilibrium was reached at a gauge pressure of 300 psi, the regulator pressure was increased to 500 psi and Steps 5, 6, and 7 were again repeated.

10. The experimental run at the given temperature was complete after Steps 5 to 7 were done at 500 psi.

Changing Temperatures

1. The valve on the ethylene cylinder was closed and the box outlet line was directed to the flare.

2. The outlet valve was opened slowly to allow the ethylene to escape to the flare.

3. After the pressure had decreased to atmospheric, the outlet valve was closed and the outlet line was directed to the vacuum pump. The valve was then opened again.

4. The air bath temperature was set to 50 °C and the system left to heat under vacuum overnight.

The experimental procedure described above under "Performing and Experiment" was then done at this temperature. The above procedure was repeated for temperatures of

70°C and 90°C. For the sample MM019, the metallocene produced LLDPE, the 90°C run was omitted because the sample had a melting temperature of approximately 85°C.

Modifications for 1-Butene and 1-Hexene

There were a number of minor modifications made to the above procedure for measuring the solubility for the higher α-olefins. As already mentioned, the gases were admitted to the experimental system from a gas reservoir that was contained inside the constant temperature air bath. Unlike the case of ethylene, neither a flow controller nor pressure regulator was used to limit the entry of the higher olefins to the system. Instead, the rate of flow, and system pressure, were controlled manually with a needle valve. One effect of this is that the time taken to fill the system to a given pressure was considerably shorter; usually the system was filled in approximately 10 to 20 minutes. Also, because of the low vapour pressures of 1-butene and 1-hexene at the temperatures of interest, the experimental pressures for these gases were considerably lower than those used with ethylene. The following table shows the approximate temperatures and pressures that were used in this study.

Table 3-2
Experimental Conditions for 1-Butene and 1-Hexene

Temperature (°C)	1-Butene Pressures (kPa)	1-Hexene Pressures (kPa)
30	120, 230, 290	not measured
50	210, 370, 530	not measured
69	290, 570, 820	50, 70, 110
88	560, 890, 1240	75, 130, 190

It should be stressed that these pressure values are approximate. It was often difficult to achieve a set pressure as the system pressure changes due to sorption by the polyethylene.

This is especially the case for 1-hexene because the system pressures were very low and the amount sorbed by the polymer was considerable. Under these conditions, the experimental pressure decreased significantly from the initial pressure when the system is closed to the final pressure when equilibrium was reached.

3.3 Buoyancy Corrections

One cannot simply assume that the change in sample weight measured by the balance is equal to the amount of gas that has been sorbed by the sample. When the test gas is admitted to the system, both the polyethylene sample and the balance beam itself will have buoyancy; this buoyancy will affect the measured weight change and therefore must be corrected for.

The buoyancy of the beam can be determined by following the procedure for solubility measurement at each temperature and pressure without a sample present. Any weight change that is seen can be attributed to the buoyancy of the beam and can be added to the weight change of a sample in solubility experiments under the same conditions.

Correction for sample buoyancy is considerably more complicated as the buoyancy of the sample is a function of its volume. Because the sample volume changes as the polymer is swollen with penetrant, one must know the volume at experimental temperatures and pressures. Determination of sample volumes at experimental conditions was the objective behind a series of dilation measurements performed by Mulder (1999).

The apparatus used for the dilation measurements is shown in Figure 3-2. The apparatus was similar to that used for the solubility measurements, except that the microbalance, pressure chamber, and reactor tube were replaced by a Jerguson pressure cell. This cell had a glass face so that the sample could be seen and its length could be measured using a cathetometer. The experimental procedure was also similar to the

40
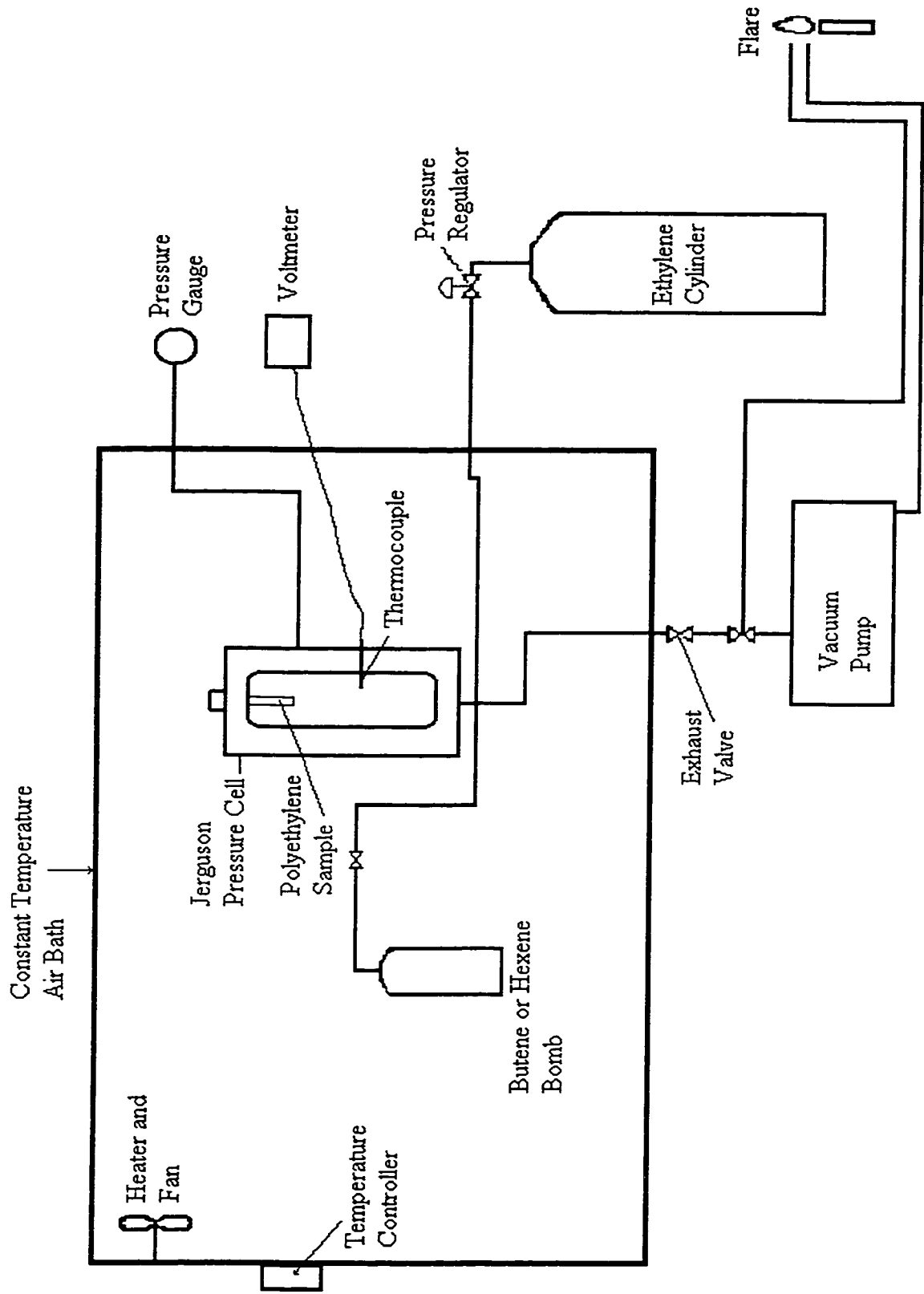
Figure 3-2 - Dilation Measurement Apparatus

41

solubility measurements; at each temperature and pressure, the length of the sample was measured after sorption equilibrium was reached.

The first dilation experiments performed by Mulder (1999) were done to determine the change in sample volume with temperature. From these measurements, thermal expansion coefficients were determined for each of the four polyethylene samples following Equation 3-1.

$$\alpha_T = \left(\frac{L_{T,0} - L_{26,0}}{L_{26,0}} \right) \frac{1}{T} \qquad (3\text{-}1)$$

where $L_{T,0}$ is the sample length under vacuum at the experimental temperature, $L_{26,0}$ is the sample length under vacuum at the reference temperature of 26°C and T is the experimental temperature.

The second group of dilation experiments was done to measure volume change due to polymer swelling. These measurements led to pressure expansion coefficients, which are calculated by Equation 3-2.

$$\beta_{T,P} = \left(\frac{L_{T,P} - L_{T,0}}{L_{T,0}} \right) \qquad (3\text{-}2)$$

where $L_{T,P}$ is the sample length at a given temperature and pressure and $L_{T,0}$ is the sample length under vacuum at the same temperature. Different pressure expansion coefficients must be determined for each polymer at each temperature and pressure combination. Because solubility measurements were often carried out at slightly different pressures than those at which the pressure expansion coefficients were obtained, the pressure expansion coefficients at a constant temperature were fit to a polynomial equation as a function of pressure. This allowed the estimation of a pressure expansion coefficient at

each experimental pressure. Further details about the determination of thermal and
pressure expansion coefficients can be found in Mulder (1999).

Once the thermal and pressure expansion coefficients were determined, sample
volume was calculated using Equation 3-3 (Hirose et al., 1986).

$$V_{T,P} = V_{26,0}[1 + 3\alpha_T(T - 26)](1 + 3\beta_{T,P}) \qquad (3\text{-}3)$$

where $V_{T,P}$ is the sample volume at the experimental temperature and pressure and $V_{26,0}$
is the sample volume under vacuum at the reference temperature of 26°C. There is an
assumption inherent in Equation 3-3 that sample expansion is isotropic; this assumption
has been supported by the work of Fleming and Koros (1986) and Mulder (1999).
Further details on the calculation of sample volume and the buoyancy corrections are
given in a sample calculation in Appendix 2.

3.4 Solubility Calculation

Once the weight change measurements had been completed, it was a relatively easy task to calculate the solubility of the α-olefins in polyethylene.

1. The gas density was determined from the experimental temperature and pressure using the Peng-Robinson (1976) equation of state. The constants used in the calculation of the attraction parameter and van der Waals covolume of ethylene were those given by Bu et al. (1995).

2. The volume of the swollen polymer sample was estimated from Equation 3-3. The initial volume of the polymer sample was determined by dividing the mass of the sample by its density. Pressure expansion coefficients were determined as a function of pressure by Mulder (1999).

3. The buoyancy force exerted on the sample was determined by the equation

$$F_{b,s} = \rho_{gas} g V_{T,P} \tag{3-4}$$

where $F_{b,s}$ is the buoyancy force and ρ_g is the gas density.

4. The mass of amorphous polyethylene, W_s, was determined by multiplying the mass of the sample by the amorphous fraction.

5. The solubility of gas in the polyethylene sample was determined by Equation 3-5

$$S = \frac{W_b + F_{b,s} - F_{b,b}}{W_s} \tag{3-5}$$

where S is the solubility in grams of penetrant per gram of amorphous polyethylene, W_b is the weight change measured by the balance, and $F_{b,b}$ is the background buoyancy.

A sample solubility calculation is given in Appendix 2.

4. Results and Discussion

4.1 Ethylene Solubility

The solubility of ethylene in the different polyethylene samples is shown as a function of temperature and pressure in Figures 4-1 to 4-4. The units for solubility are grams of ethylene per gram of amorphous polyethylene. These units were chosen because gaseous penetrants do not have significant solubility in the crystalline regions of polyethylene (Michaels and Bixler, 1961).
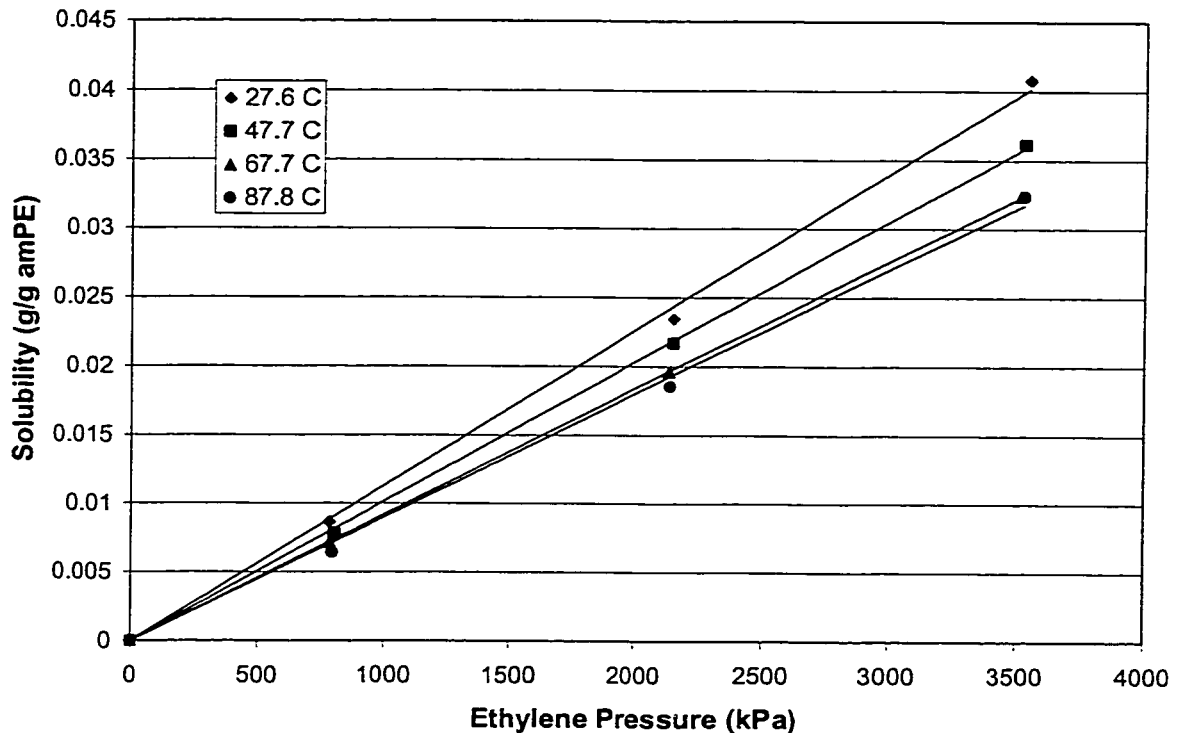
Figure 4-1 - Solubility of Ethylene in MM003, 50% Crystalline LDPE

At each of the different temperatures, the amount of sorbed ethylene is directly proportional to the ethylene pressure; therefore, Henry's law is applicable. Because of this relationship, linear regression was used to fit the lines that are shown in Figure 4-1. It can also be seen from Figure 4-1 that the solubility of ethylene in low-density

polyethylene decreases with an increase in temperature. The maximum solubility of

0.041 g/g amPE was recorded at a temperature of 27.6°C. However, this temperature

effect seems relatively small as all four of the sorption isotherms are quite close together.

The solubility of ethylene in the high-density polyethylene sample is shown in

Figure 4-2. Despite the considerable differences in molecular structure and crystallinity,

ethylene solubility in HDPE is similar to that in LDPE on an amorphous basis. It can be

seen in Figure 4-2 that Henry's law is applicable in HDPE and ethylene solubility again

decreases with increasing temperature. The maximum solubility of ethylene in sample

MM013 is 0.036 g/g amPE.
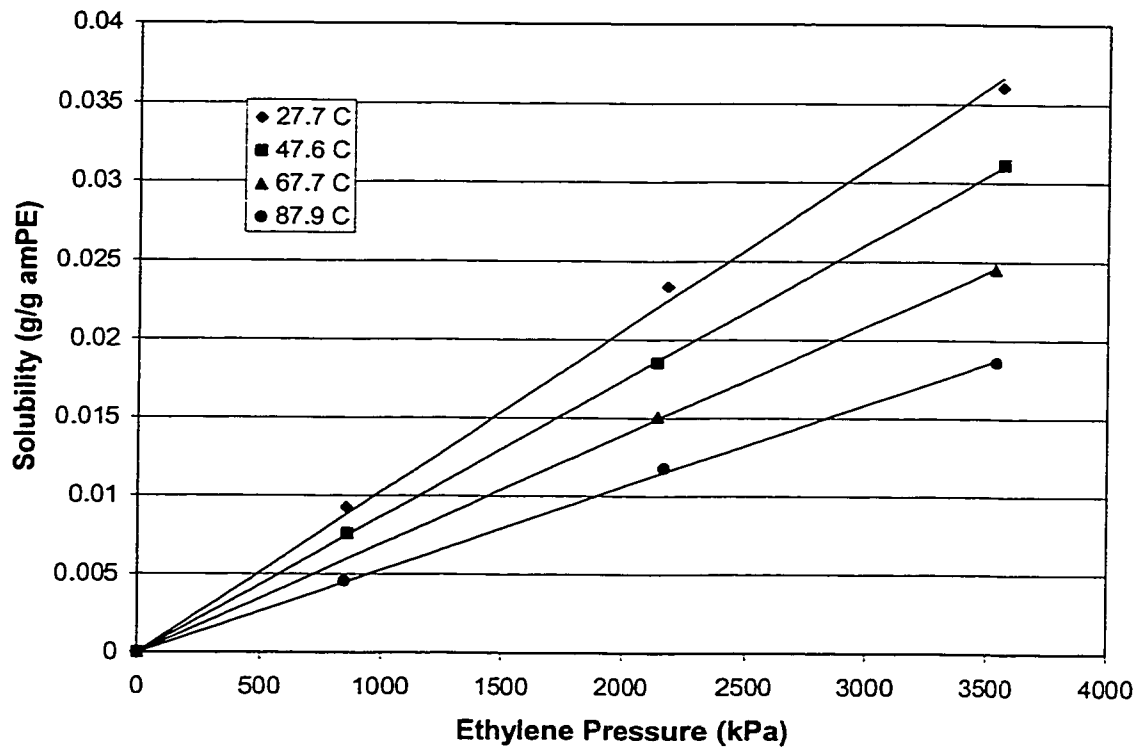
Figure 4-2 - Solubility of Ethylene in MM013, 70% Crystalline HDPE

The solubility of ethylene in the two linear low-density polyethylene samples is

shown in Figures 4-3 and 4-4.
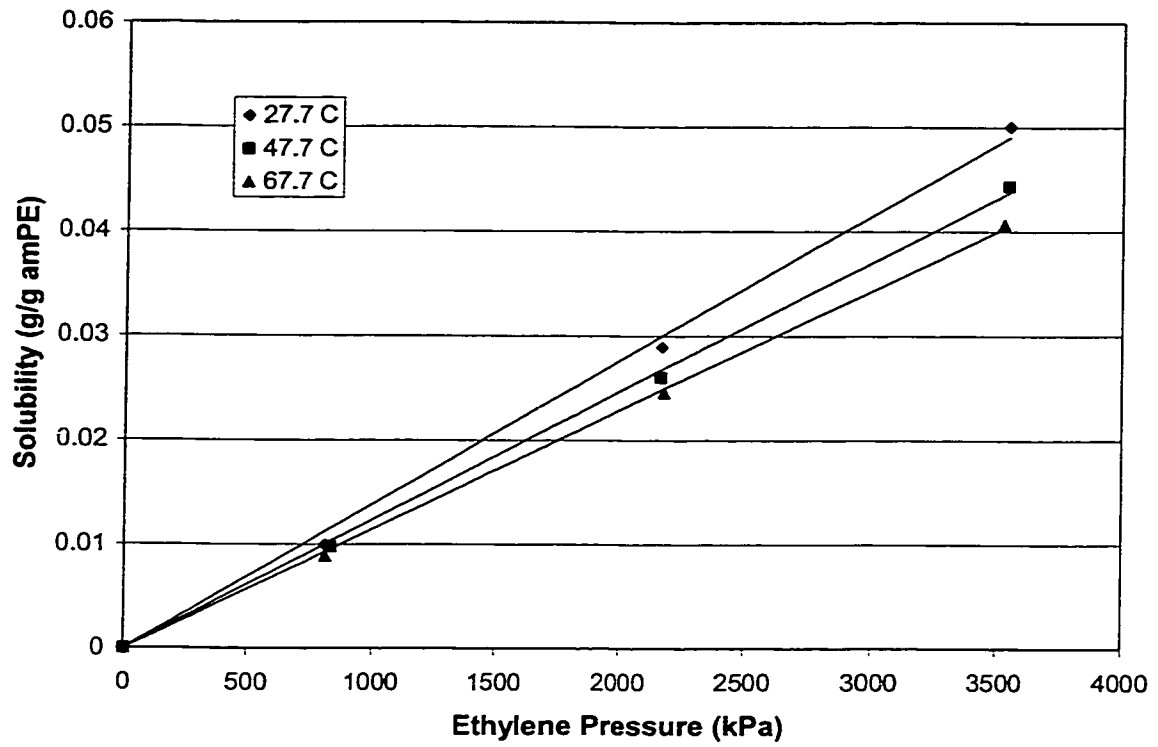
Figure 4-3 - Solubility of Ethylene in MM019, 18% Crystalline LLDPE
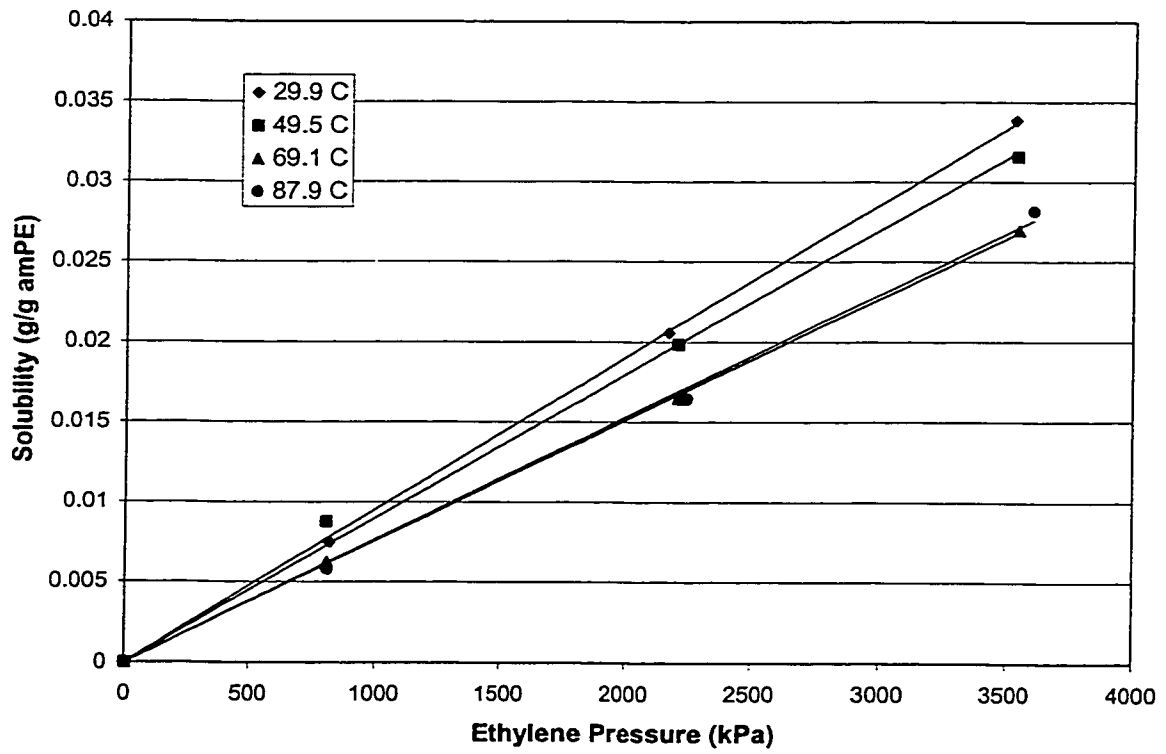
Figure 4-4 - Solubility of Ethylene in MM029, 47% Crystalline LLDPE

47

Both of the LLDPE samples exhibit similar ethylene solubility characteristics as seen in LDPE and HDPE. The maximum ethylene solubility was recorded for sample MM019, an LLDPE produced with a metallocene catalyst. This sample had a maximum ethylene solubility of 0.050 g/g amPE. In contrast, the lowest ethylene solubility was seen in the Ziegler-Natta catalysed LLDPE, sample MM029. This sample had a maximum ethylene solubility of only 0.034 g/g amPE.

4.1.1 Henry's Law Coefficients

Ethylene solubility obeyed Henry's law for all of the polyethylene samples tested. Henry's law coefficients were determined from the slopes of the fit lines shown in Figures 4-1 to 4-4. These coefficients are given in Table 4-1

Table 4-1
Henry's Law Coefficients for Ethylene

Sample	Henry's Law Coefficient [g/(g amPE·atm)]			
	Temperature (°C)			
	28	48	68	88
MM003	11.4×10^{-4}	10.3×10^{-4}	9.32×10^{-4}	9.13×10^{-4}
MM013	10.4×10^{-4}	8.83×10^{-4}	7.05×10^{-4}	5.37×10^{-4}
MM019	14.0×10^{-4}	12.5×10^{-4}	11.5×10^{-4}	not measured
MM029	9.66×10^{-4}	9.12×10^{-4}	7.67×10^{-4}	7.76×10^{-4}

For 3 of the 4 polyethylene samples, the Henry's law coefficients decrease as the temperature is increased. In the fourth sample, MM029, the coefficients at 68°C and 88°C are almost equal. The temperature effect is most noticeable for the high-density polyethylene sample, MM013. For this sample, the Henry's law coefficient at 88°C is approximately 48% lower than at 28°C. The magnitude of the temperature effect on

MM013 can also be seen in Figure 4-2 as the sorption isotherms are more widely spaced than for the other samples.

4.1.2 Comparison to Literature Values

The solubility of ethylene in low-density polyethylene has been measured by four other research groups. Their findings are summarised and compared to the current study in Table 4-2.

Table 4-2
Ethylene Solubility in LDPE: Comparison to Previous Results

Research Group	Temperature (°C)	Crystallinity (%)	Henry's Law Coefficient [g/(g amPE·atm)]
Li and Long (1969)	25	45	1.2×10^{-3}
Beret and Hager (1979)	23	48	6.5×10^{-5}
Kulkarni and Stern (1983)	20	55	1.3×10^{-3}
McKenna (1998)	70	52	1.2×10^{-3}
Current Study – MM003	28	50	1.14×10^{-3}

It can be seen from Table 4-2 that the Henry's law coefficient for LDPE found in this study is in reasonable agreement with those found by other researchers. A possible explanation for the lower value of Beret and Hager (1979) is given in Section 2.3.

4.1.3 Effect of Polyethylene Crystallinity on Ethylene Solubility

The ethylene solubilities in this study are given in terms of grams of amorphous polyethylene because the crystalline regions are considered to be essentially impermeable. Therefore, one might expect that, on an amorphous basis, ethylene

solubility would be close to constant for samples of different molecular structure and crystallinity. However, as discussed by Hutchinson and Ray (1990), even though solubility occurs only in the amorphous phase, the crystallites still play an important role in the process. Figure 4-5 shows the solubility of ethylene in the polyethylene samples as a function of sample crystallinity.
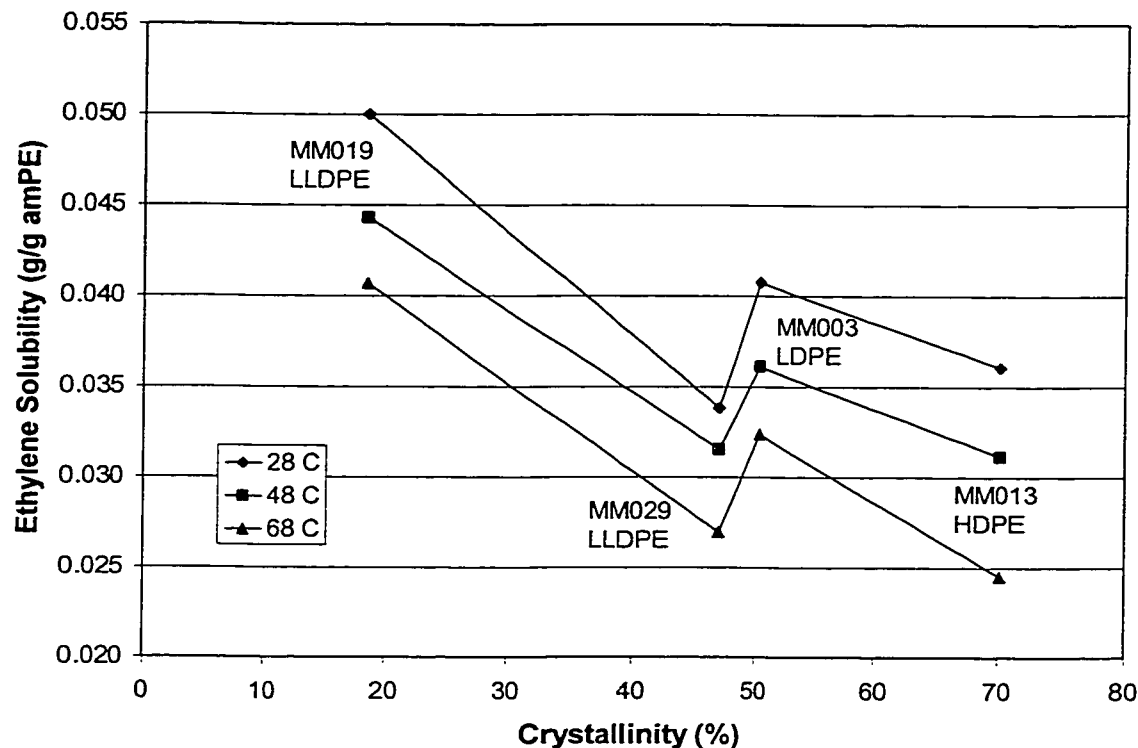
Figure 4-5 - Solubility of Ethylene in Polyethylene Samples of Different Crystallinity at 3550 kPa

It can be seen from Figure 4-5 that sample crystallinity plays a role in ethylene solubility in polyethylene. Even when considered on an amorphous basis, solubility generally decreases with increasing sample crystallinity. This result is in agreement with the findings of Doong and Ho (1991) and Yoon et al. (1996).

It can also be seen that solubility in amorphous polyethylene is not only a function of crystallinity. Ethylene was considerably less soluble in the Ziegler-Natta catalysed linear low-density polyethylene, MM029, than in MM003, the low-density polyethylene, despite similar crystallinities. This suggests that the molecular structure of the polyethylene is also an important factor in ethylene solubility.

4.1.4 Comparison of Experimental Methods at High Temperature

The Cahn D-110 balance was not designed to be used at temperatures above ambient conditions. During the course of this study, the balance failed after continued exposure to the high temperatures that it was subjected to. It was subsequently fixed and the experiments were continued. This failure raises the possibility that measurements made at high temperatures may be unreliable. While it is suspected that the balance failed instantaneously during one particular experiment, it is possible that it could have failed gradually and thus affected the ethylene solubility measurements that were made prior to the outright failure.

In an attempt to check the validity of the ethylene measurements that were made, a slightly different experimental method was used that avoided exposing the balance to high temperatures. For one set of experiments, the air bath enclosing the balance (see Figure 3-1) was turned off and the sorption temperature was controlled by putting a band heater around the reactor tube. This method would not work for the higher α-olefins because of their low vapour pressures but it is acceptable for use with ethylene. Ethylene solubility was measured using this method over the entire range of temperatures and

pressures for the high-density polyethylene sample, MM013. The results of this experiment are shown in Figure 4-6.
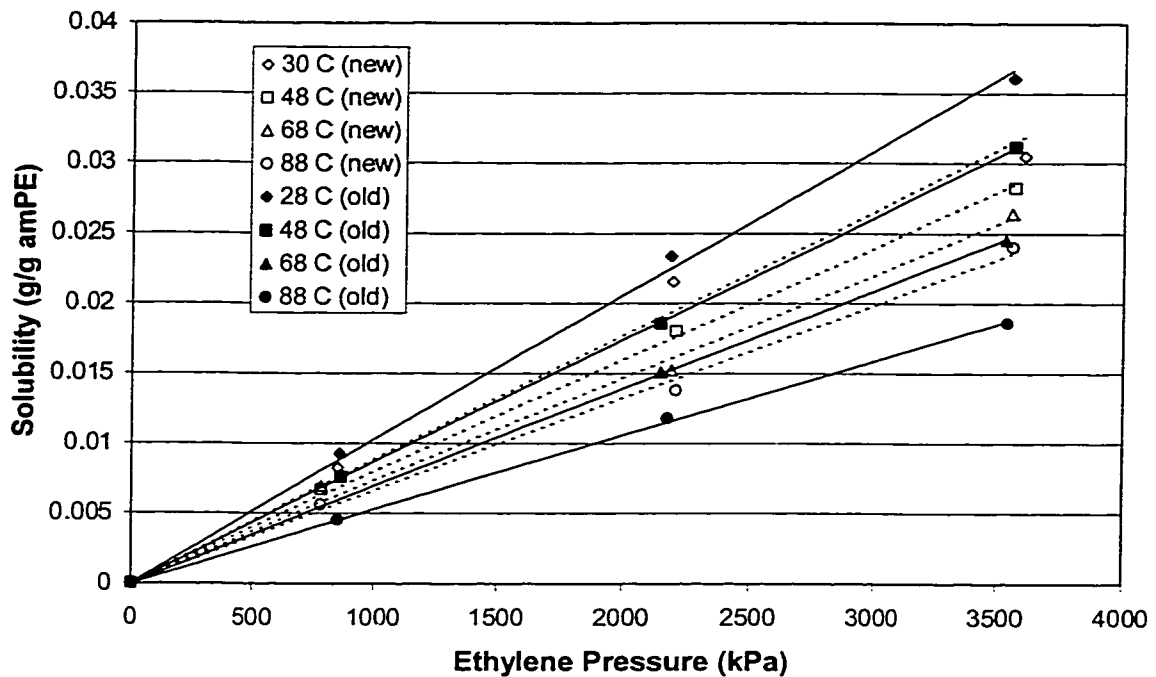
Figure 4-6 - Comparison of Ethylene Solubility Measurement Techniques in MM013, 70% Crystalline HDPE

In Figure 4-6, the solid points and lines represent measurements that were made using the air bath with the balance at the same temperature as the reactor tube. The open points and dashed lines represent the new method, with the reactor tube temperature controlled by the heating band. There is little difference between the points obtained using the original method and those obtained with the new method. This suggests that, although the high temperatures do damage the balance over time, measurements made prior to balance failure are reliable. It is good that this is the case because there is no alternative to high air bath temperatures for 1-butene and 1-hexene. For these gases, the balance must be kept at the same temperature as the reactor tube or condensation would take

place in the balance. Furthermore, even though the heating band method can be used for ethylene measurements, it is still not desirable to do so because this method introduces a considerable amount of noise to the weight change measurements. This noise is a result of convection currents, that form in the reactor tube due to temperature gradients between the surface and the inside of the tube, and cause the measured weight of the sample to fluctuate. For this reason, it is preferable to use the air bath, which minimises temperature gradients.

4.1.5 Sensitivity Analysis

Because there are a number of parameters involved in the solubility calculation, it is sometimes difficult to predict how the uncertainty in a particular parameter would be propagated throughout the calculation. For this reason, it is useful to systematically vary each of the parameters and observe the effect that each has on the final solubility value. Table 4-3 lists a number of the parameters for which the values could be uncertain and the effects that these uncertainties have on the calculated solubility. These calculations were made on the sample MM019, the metallocene catalysed linear low-density polyethylene, at a temperature of 47.7°C and an ethylene pressure of 3550 kPa. The measured solubility under these conditions was 0.0443 g/g amPE.

Solubility measurements were often carried out at slightly different pressures than those at which the pressure expansion coefficients were obtained. For this reason, the pressure expansion coefficients at a constant temperature were fit to a polynomial equation as a function of pressure. The uncertainty in the pressure expansion coefficient arises from this polynomial fit and is estimated to be up to approximately 40%.

Table 4-3
Sensitivity of Ethylene Solubility Calculation

Parameter	Parameter Uncertainty (%)	Solubility Uncertainty	
		Absolute (g/g amPE)	Percentage
Pressure Expansion Coefficient	40	± 0.0015	3.5
Thermal Expansion Coefficient	40	± 0.00045	1.0
Gas Density	2	± 0.0013	3.0
Weight Change	6	± 0.0013	3.0
Total Uncertainty (sum of all parameters)		± 0.0046	10.4

The uncertainty on the thermal expansion coefficient was estimated in a similar manner to that of the pressure expansion coefficient and was also estimated to be up to 40%. As can be seen in Table 4-3, even an error of this magnitude in the thermal expansion coefficient leads to very little uncertainty in the final solubility value.

Uncertainty in the value for the gas density could have been introduced in two ways: errors in the temperature and pressure used in the calculation and error from the Peng-Robinson equation itself. The latter error would be quite small and should be less than 1%. The uncertainties in temperature and pressure were determined to be 0.2°C and 14 kPa respectively; these uncertainties lead to an error of approximately 1%. Therefore, the total uncertainty on the gas density was estimated to be 2%.

The uncertainty of the weight change measurements came from the error involved with the balance, as well as from any uncertainty in determining when equilibrium was reached. Equilibrium was considered to have been reached if the balance did not vary more than ± 0.00005 g over a 30 to 60 minute period. Therefore the uncertainty in the

equilibrium weight change value was considered to be 50 micrograms. The ultimate repeatability of the balance was 10 micrograms. At the smallest measured weight change (-0.00103 g), an uncertainty of 60 micrograms represents approximately 6%.

The Total Uncertainty value of 10.4% in Table 4-3 was determined as a sum of all the previous uncertainties. This uncertainty can be considered a "worst case scenario" because in order for a calculated solubility value to be this far off its true value, all of the parameters would have to have their maximum error. Furthermore, all parameters would have to have errors in the same direction. In a more realistic case, one would expect some of the parameter values to be slightly high and others to be slightly low. Therefore, it is very unlikely that measured values would approach an uncertainty of 10.4%.

4.2 Background Buoyancy for 1-Butene and 1-Hexene

Buoyancy effects will cause the apparent weight of the balance beam and hangdown assembly to change as the pressure increases from vacuum in an experimental run. To compensate for this effect, the experimental procedure was carried out without a sample present. Any weight change measured is a result of the buoyancy of the beam and hangdown assembly, and was used to correct the weight change due to solubility. Mulder (1999) measured the background buoyancy for ethylene; the results for 1-butene and 1-hexene are presented in Tables 4-4 and 4-5.

Table 4-4
Background Buoyancy for 1-Butene

Temperature (°C)	Pressure (kPa)	Weight Change (g)
30.1	121	0.00003
30.0	229	0.00005
30.0	283	0.00007
49.6	205	0.00002
49.6	349	0.00002
49.6	510	-0.00004
69.1	286	-0.00001
69.1	383	0.00003

The measurements were stopped at 69.1°C because the 1-butene cylinder was empty. The experiment was not restarted because the measured weight changes were insignificant. At the higher temperatures, 49.6°C and 69.1°C, the background buoyancy values were within the ± 0.00005 g uncertainty on the solubility weight measurements.

For this reason, the buoyancy correction for 1-butene was only applied to the runs at 30°C.

The background buoyancy values for 1-hexene are greater than those for 1-butene and are also greater than the weight measurement uncertainty of ± 0.00005 g. The background buoyancy values, shown if Table 4-5, were used to correct the measured weight changes during 1-hexene sorption.

Table 4-5
Background Buoyancy for 1-Hexene

Temperature (°C)	Pressure (kPa)	Weight Change (g)
69.2	49.0	0.00003
69.2	69.6	0.00010
69.2	110	-0.00026
87.7	71.0	-0.00001
87.9	130	-0.00013
87.9	163	-0.00018

4.3 1-Butene Solubility

Solubility isotherms for 1-butene in the four polyethylene samples are shown in Figures 4-7 to 4-10. The units for solubility in these figures are grams of 1-butene per gram of amorphous polyethylene.
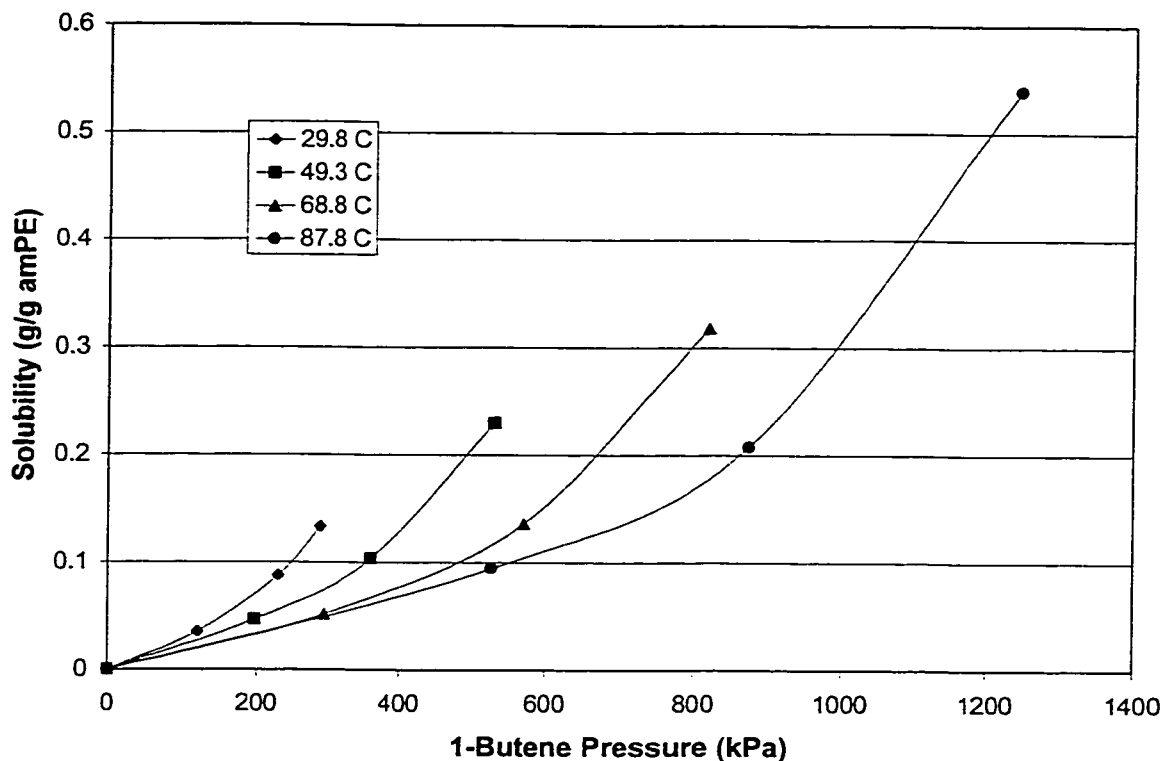
Figure 4-7 - Solubility of 1-Butene in MM003, 50% Crystalline LDPE

The solubility behaviour of 1-butene in low-density polyethylene is considerably different than that of ethylene. The most obvious difference is that the sorption isotherms are no longer linear. As can be seen in Figure 4-7, Henry's law certainly does not apply to the solubility of 1-butene in LDPE. 1-Butene is also much more soluble than ethylene; the maximum 1-butene solubility of 0.54 g/g amPE in the LDPE sample is an order of magnitude greater than that of ethylene. The increase in solubility is even more dramatic

considering the maximum 1-butene pressure of 1240 kPa is much lower than the pressures reached in the ethylene solubility measurements.

The pressures at which 1-butene solubility measurements were made were dependent on the vapour pressure at each given temperature. Therefore, a different set of pressures was used for each temperature. This makes it somewhat more difficult to see the effect that temperature has on 1-butene solubility; the greatest solubility will obviously occur at the maximum temperature because of much higher penetrant pressure. However, if one examines the isotherms in Figure 4-7 at a constant pressure, it can be seen that solubility decreases with increasing temperature. This temperature dependence is similar to that seen for ethylene.

Figure 4-8 shows the solubility of 1-butene in high-density polyethylene.
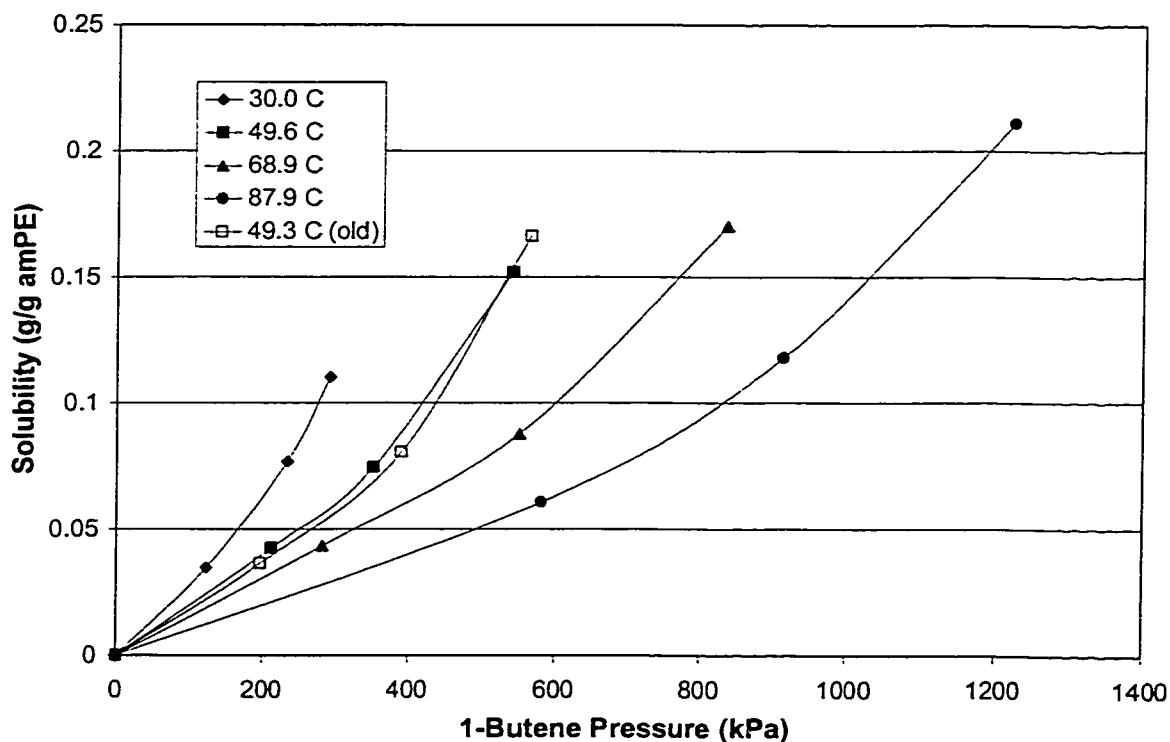
Figure 4-8 - Solubility of 1-Butene in MM013, 70% Crystalline HDPE

Even with a basis of amorphous mass, 1-butene is considerably less soluble in the HDPE sample than in LDPE. The solubility in the MM013 sample was 0.21 g/g amPE which was less than half that in the LDPE sample. However, this solubility is still considerably greater than that of ethylene in the same high-density polyethylene sample.

One of the data series in Figure 4-8 is labeled "49.3 C (old)". These solubility values were the first ones that were measured for 1-butene. Shortly after they were made, the balance broke due to high temperatures and the experiments were stopped for some time. When the balance was returned, a complete new set of measurements was performed on another sample of the MM013 high-density polyethylene. The values obtained from this first measurement are included in the figure to show the reproducibility of the experimental method. There is little difference between the "old" values and those obtained in the later series of measurements. These repeat measurements show the reproducibility on different samples of the same polymer. After adjusting for the pressure differences between the data sets, the average difference between the new and old values was 5.4%. As expected, this percentage difference is considerably less than the "worst case" uncertainty of 10.4% that was described in Section 4.1.5.

The solubility of 1-butene in the two linear low-density samples is shown in Figures 4-9 and 4-10. The solubility in the Ziegler-Natta catalysed LLDPE, MM029, is very similar to the solubility in the LDPE sample. The sorption isotherms for the two samples exhibit similar curvature and the maximum amounts of 1-butene sorbed are also very close. As with the low and high-density samples, both of the LLDPE samples
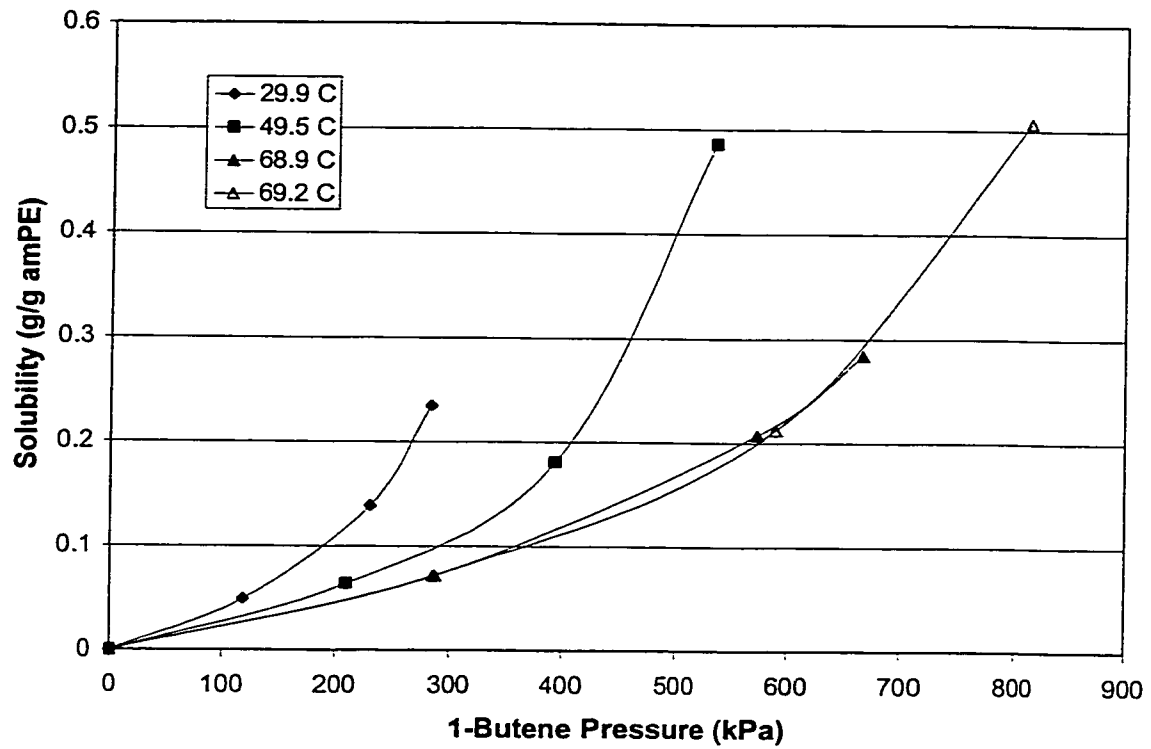
Figure 4-9 - Solubility of 1-Butene in MM019, 18% Crystalline LLDPE
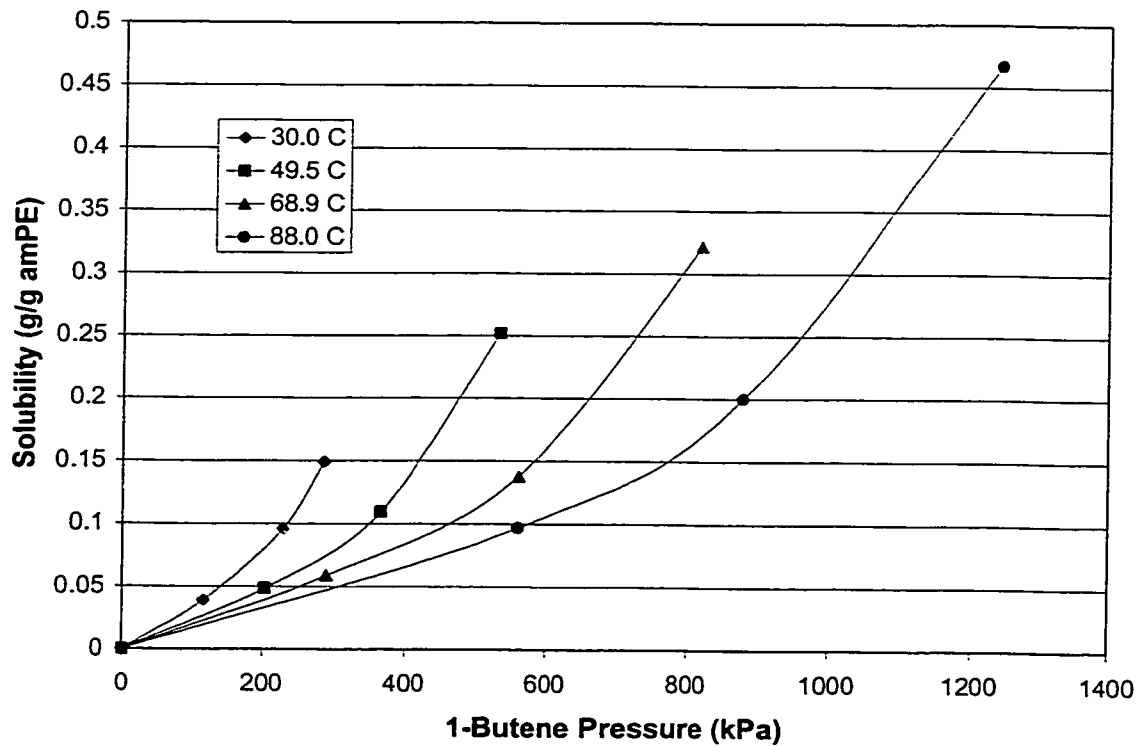
Figure 4-10 - Solubility of 1-Butene in MM029, 47% Crystalline LLDPE

exhibit the same temperature dependency, with solubility decreasing as the temperature is increased.

1-Butene was most soluble in the metallocene catalysed LLDPE sample, MM019. Because this sample had a melting temperature of approximately 85°C, the highest measurement temperature that was used was 69°C. This meant that the maximum 1-butene pressure that could be used was approximately 820 kPa. At this pressure the MM019 sample had a 1-butene solubility of 0.51 g/g amPE which was approximately 60% higher than the solubility in any of the other polyethylene samples.

Another test of the reproducibility of the experimental method is shown in Figure 4-9. In this figure, there is a sorption isotherm at 68.9°C and another one at 69.2°C. During the initial run at 68.9°C, the 1-butene cylinder ran out so that the highest pressure that could be obtained was 670 kPa. The cylinder was then refilled and the run repeated up to the maximum pressure of 820 kPa. Rather than omit the first incomplete run, it is useful to observe how close the solubility values are between the two runs. At the lowest pressure, the two values are practically identical and they are still quite close at the second pressure that was measured. Furthermore the solubility value from the first run at 670 kPa falls very close to the isotherm that was determined from the complete second run. Once again, these findings demonstrate that the experimental method used in this study is quite reproducible.

4.3.1 Comparison to Literature Values

At very low 1-butene pressures (less than 100 kPa), the sorption isotherms are practically linear and Henry's law can still be considered applicable. Yoon et al. (1996)

determined Henry's law coefficients for 1-butene in a number of different LLDPEs. It is useful to compare their results to the LLDPE samples used in this study, MM019 and MM029. At 70°C, they found polymers having densities of 0.900 g/cm^3 and 0.918 g/cm^3 to have Henry's law coefficients of 0.0095 g/(g amPE·atm) and 0.0075 g/(g amPE·atm) respectively. The samples MM019 and MM029 have densities of 0.885 g/cm^3 and 0.917 g/cm^3, similar to those used by Yoon et al. (1996). The Henry's law coefficients determined in this study were 0.024 g/(g amPE·atm) and 0.020 g/(g amPE·atm) for MM019 and MM029 respectively. These values show 1-butene to be more soluble in LLDPE than was found by Yoon et al. (1996) but the values are still of the same order of magnitude.

Because Henry's law is not applicable for the vast majority of the pressures considered in this experiment, it would be much more useful to compare 1-butene solubilities at higher pressures. Unfortunately such information is simply not available in the literature. The pressures used in this experiment are considerably greater than those used by Yoon et al. (1996) and McKenna (1998).

4.3.2 Effect of Polyethylene Crystallinity on 1-Butene Solubility

In Figure 4-5, it was shown that the solubility of ethylene in amorphous polyethylene decreased with increasing sample crystallinity. Reasons for this behaviour were suggested by Hutchinson and Ray (1990) and Doong and Ho (1991). They describe crystalline regions linked together by amorphous tie molecules, which act to constrain the amorphous polymer chains, and thus limit the amount they can swell and sorb penetrant molecules. If this explanation were correct, one would expect that the solubility of higher

α-olefins would be even more dependent on crystallinity, because sorption of these larger molecules requires even greater swelling.

Figure 4-11 shows the solubility of 1-butene in the different polyethylene samples as a function of polyethylene crystallinity.
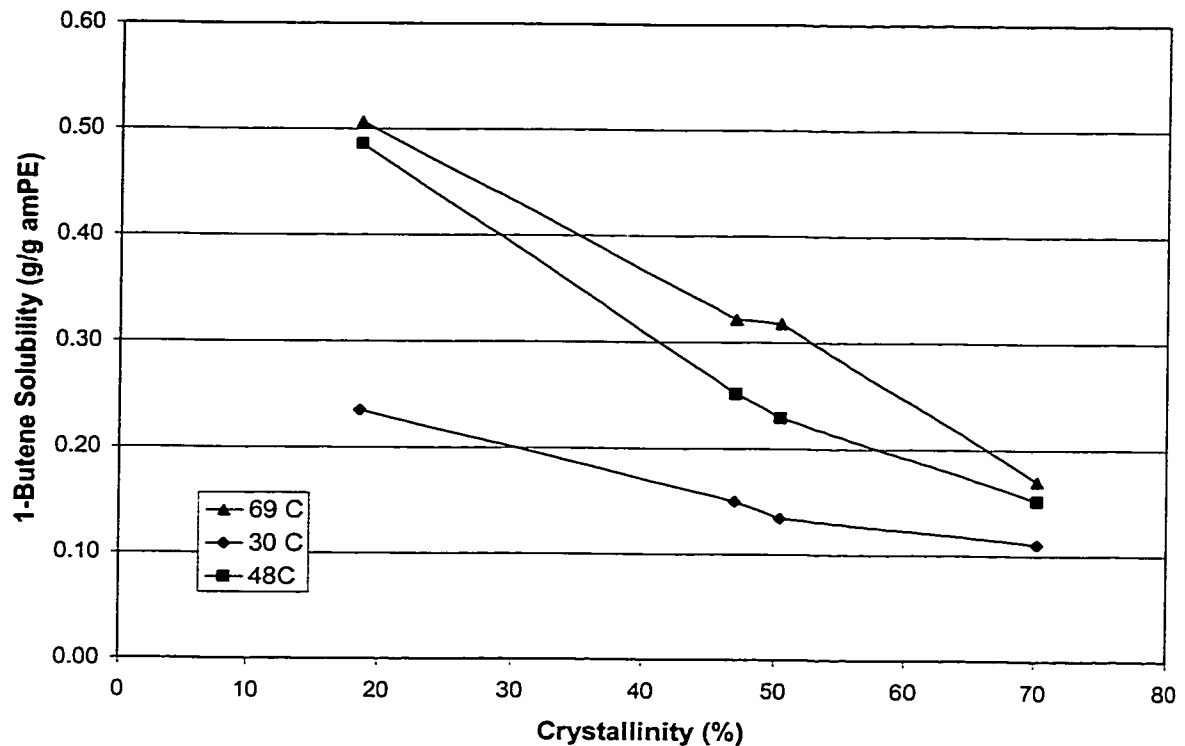
Figure 4-11 - Solubility of 1-Butene in Polyethylene Samples of Different Crystallinity at the Maximum Pressure for Each Temperature

When looking at Figure 4-11, one must remember that the solubility values at higher temperatures are measured at higher pressures. Thus, while solubility seems to increase with increasing temperature, this is not the case.

To compare the effects of crystallinity on 1-butene and ethylene solubility, it is useful to examine the percentage decrease in solubility from lowest crystallinity to highest crystallinity. The solubility of 1-butene decreases between 52% and 68% (depending on temperature) from sample MM019 to sample MM013. In contrast,

ethylene solubility decreased between 28% and 40%. Therefore, it is clear that sample crystallinity plays a greater role in the solubility of 1-butene than it does for ethylene. This conclusion is consistent with the findings of Hutchinson and Ray (1990) and Doong and Ho (1991).

4.4 1-Hexene Solubility

The last α-olefin, for which solubility in polyethylene was measured, was 1-hexene. Because of the low vapour pressure of this species, solubility measurements were carried out at only two temperatures, 69°C and 88°C. Sorption isotherms for 1-hexene in the four polyethylene samples are shown in Figures 4-12 to 4-15.
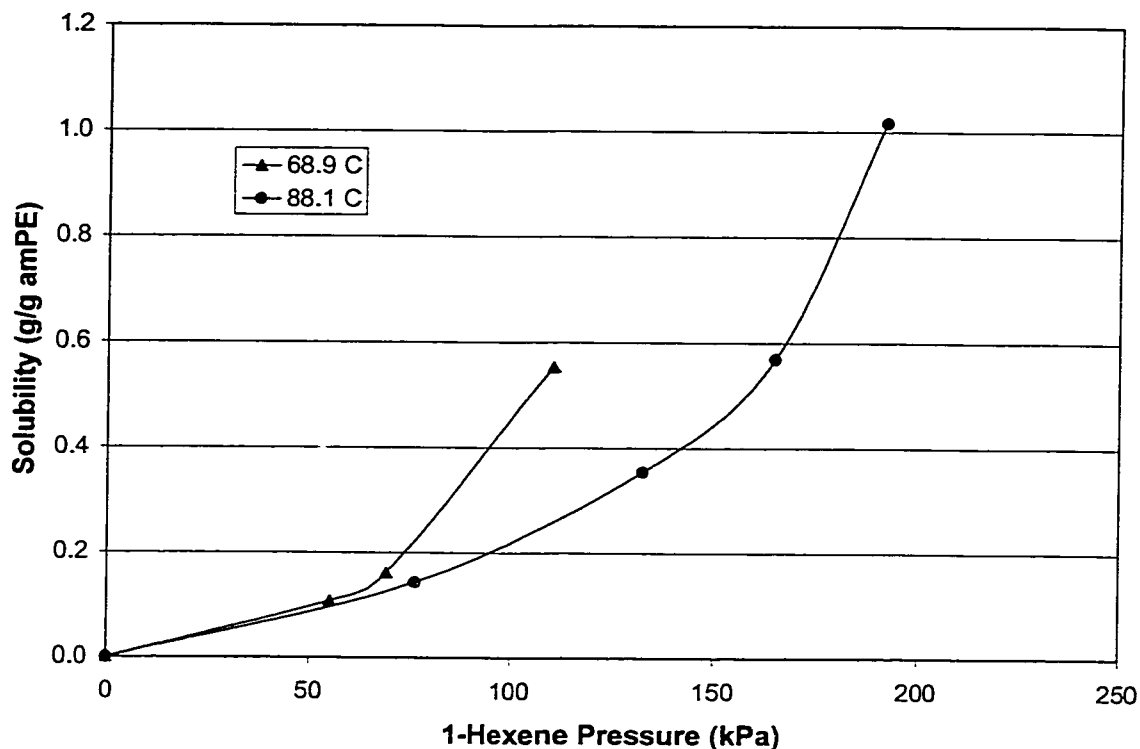
Figure 4-12 – Solubility of 1-Hexene in MM003, 50% Crystalline LDPE

The sorption isotherms for 1-hexene are similar to those seen for 1-butene. They display significant curvature and Henry's law is applicable only at the very lowest pressures, below approximately 40 kPa. 1-hexene solubility in the LDPE sample, MM003, is particularly interesting. As shown in Figure 4-12, the maximum solubility of 1-hexene in MM003 is 1.02 g/g amPE. This is remarkable, as the gas is so soluble that the mass of sorbed gas actually exceeds the amorphous mass of the sample! Because the

solubility was so high at 195 kPa, a fourth point was measured subsequently to confirm the validity of the isotherm. As can be seen in Figure 4-12, the point at 165 kPa falls on the fit line joining the other three solubility values. This smooth isotherm suggests that the solubility measured at the maximum pressure is in fact accurate.

The isotherm at 69.2°C is also of interest in Figure 4-12. The maximum 1-hexene pressure at this temperature is just over atmospheric at approximately 110 kPa. Even at this low pressure, the solubility of 1-hexene is 0.55 g/g amPE, which is much greater than that of 1-butene, and fully two orders of magnitude greater than that of ethylene at similar pressures.

Also in the 69.2°C isotherm, the first two pressures measured were very close together. This was accidental and the result of the difficulty in achieving a set pressure when working with 1-hexene. Because the pressures used are quite low and the gas uptake very high, there were significant pressure changes in the system from when the gas inlet valve is closed to when equilibrium is reached.

The solubility of 1-hexene in high-density polyethylene is shown in Figure 4-13. At both temperatures, the solubility is less than half of what it was in the low-density sample. However, 1-hexene is still much more soluble in MM013 than 1-butene or ethylene.

The effect of temperature on 1-hexene solubility in polyethylene can also be seen in Figure 4-13. At a constant pressure, solubility decreases with increasing temperature. This is the same effect that has been seen for all three α-olefin penetrants in all four polyethylene samples.
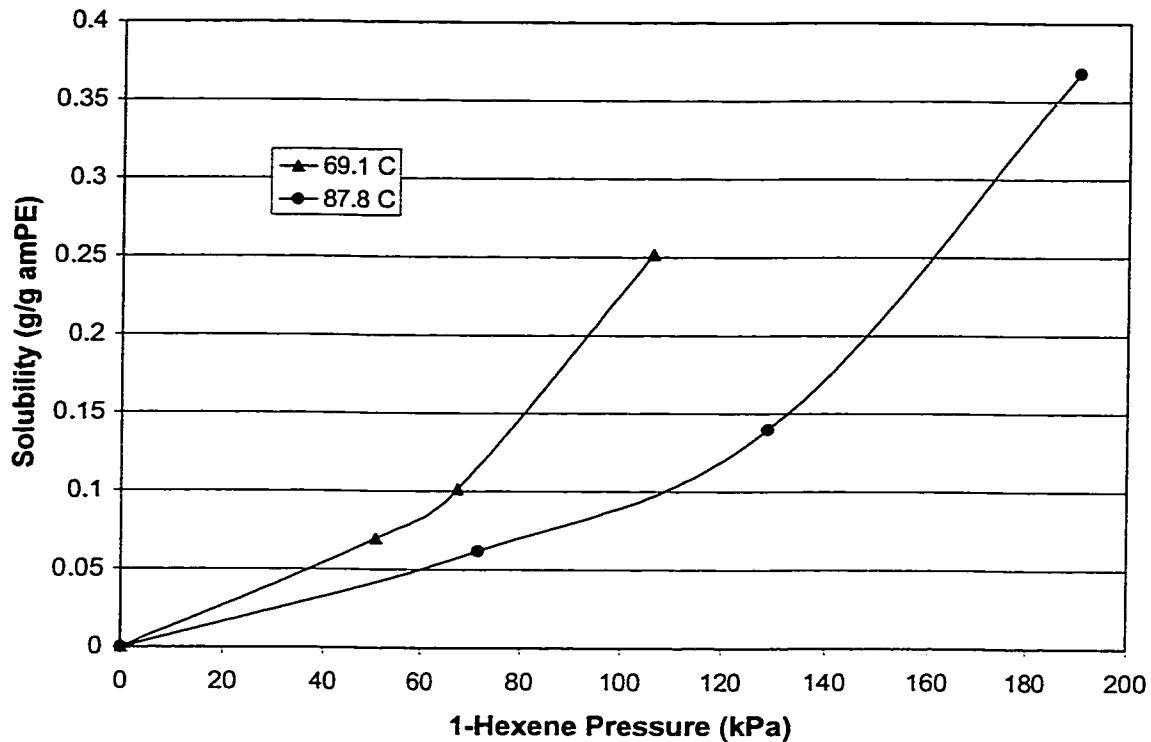
Figure 4-13 - Solubility of 1-Hexene in MM013, 70% Crystalline HDPE

The solubility of 1-hexene in the metallocene produced LLDPE sample MM019 is

shown in Figure 4-14. Because of its low crystallinity, this sample had the lowest

melting temperature and was the cause of some experimental difficulty. Although

approximately 15°C below its normal melting point, the sample melted and fell off the

hangdown wire during sorption at 69.2°C under a 1-hexene pressure of approximately

110 kPa. The weight change at the point where the sample fell off the wire is shown as

the open point on Figure 4-14. Because equilibrium was not reached for this point, a

third point was still required to generate a sorption isotherm. For this reason, solubility

was measured in a second sample of MM019 at a 1-hexene pressure of approximately 90

kPa.
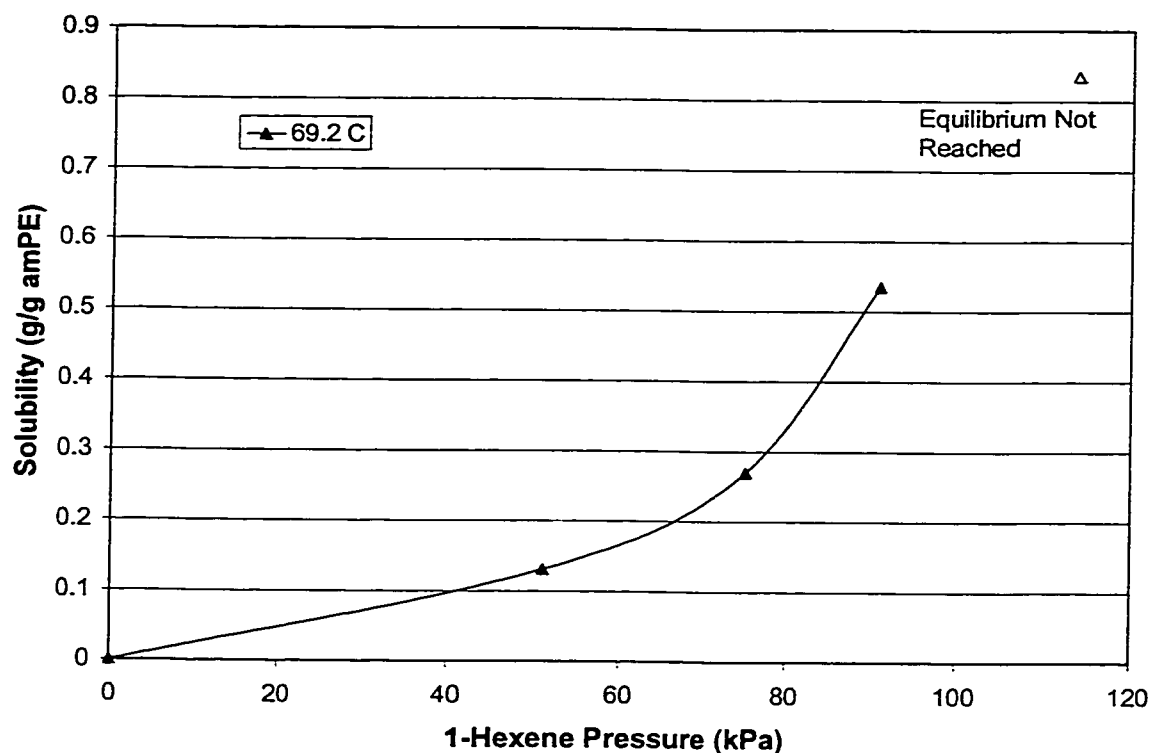
Figure 4-14 - Solubility of 1-Hexene in MM019, 18% Crystalline LLDPE

Although the experiments covered only a small range of conditions, it can still be seen from Figure 4-14 that 1-hexene was most soluble in the metallocene LLDPE sample. The fact that the sample melted indicates just how soluble the 1-hexene was; the sample sorbed so much gas that the polyethylene chains could no longer bind together and the sample lost its rigidity and melted.

The solubility of 1-hexene in the Ziegler-Natta catalysed LLDPE sample is shown in Figure 4-15. This sample had crystallinity similar to that of the LDPE sample so that one would expect the solubilities in the two samples to be similar. This was the case for the sorption isotherm at 69°C but the higher temperature isotherms were considerably different. Sample MM003 had a maximum solubility of 1.02 g/g amPE; in contrast, the maximum 1-hexene solubility in sample MM029 at 88.1 °C was 0.62 g/g amPE. This is
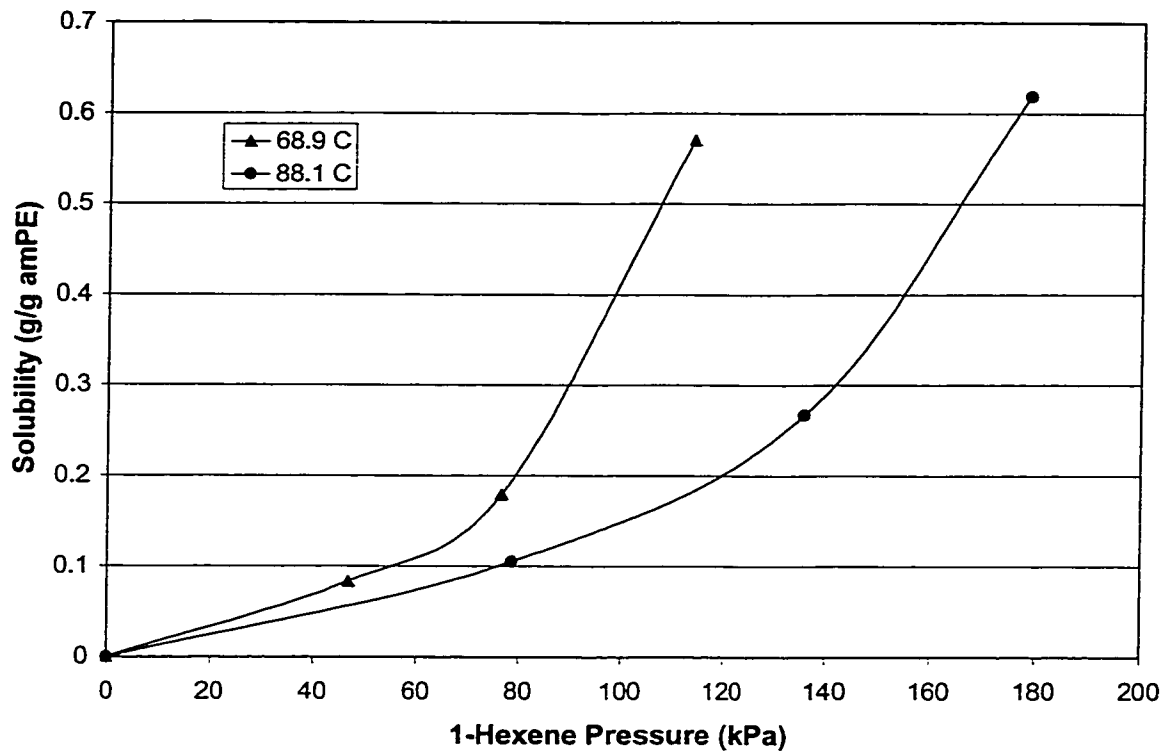
Figure 4-15 - Solubility of 1-Hexene in MM029, 47% Crystalline LLDPE

only slightly higher than the solubility at 68.9°C in the same sample. It is surprising that

the maximum solubilities at the two different temperatures would be similar because of

the considerable difference in penetrant pressure. It is possible that for this polymer,

there exists a maximum solubility, above which the amount of gas sorbed is constant and

is no longer pressure dependent. Even if this is not the case, the differences between the

sorption isotherms of MM029 and MM003 provide further evidence that molecular

structure is an important parameter for olefin solubility in polyethylenes.

4.4.1 Comparison to Literature Values

The only other research group that has studied the solubility of 1-hexene in

polyethylene is Yoon et al. (1996). They found Henry's law coefficients for a number of

linear low-density polyethylenes of different densities. For LLDPE samples having

densities of 0.900 g/cm³ and 0.918 g/cm³, they reported Henry's law coefficients of 0.092

g/(g amPE·atm) and 0.083 g/(g amPE·atm) respectively. In this study, Henry's law

coefficients of 0.24 g/(g amPE·atm) and 0.17 g/(g amPE·atm) were measured for MM019

and MM029 respectively. All of these measurements were made at approximately 70°C.

Although in the same order of magnitude, the 1-hexene Henry's law coefficients

determined in this study were significantly greater than those reported by Yoon et al.

(1996). A similar trend was seen for 1-butene.

Yoon et al. (1996) measured the solubility of 1-hexene in LLDPEs up to a

maximum 1-hexene activity of approximately 0.4. At this activity, they found 1-hexene

solubilities between 0.04 g/g amPE and 0.05 g/g amPE. In contrast, MM019 had a

solubility of approximately 0.19 g/g amPE at 69°C and a 1-hexene activity of 0.4. For

MM029, solubilities of 0.12 g/g amPE and 0.17 g/g amPE were measured at 69°C and

88°C respectively. Once again, the solubility values measured in this study are

significantly greater than those measured by Yoon et al. (1996).

4.4.2 Effect of Polyethylene Crystallinity on 1-Hexene Solubility

The solubilities of 1-hexene in the different polyethylene samples as a function of

polyethylene crystallinity are shown if Figure 4-16. Because 69°C was the only

temperature at which solubility measurements were made on all four samples, both of the

data sets in the figure were determined at this temperature. However, sample MM019

fell apart when exposed to a 1-hexene pressure of 110 kPa. The open point in Figure 4-

16 represents the solubility of 1-hexene in the sample at the time when the specimen fell
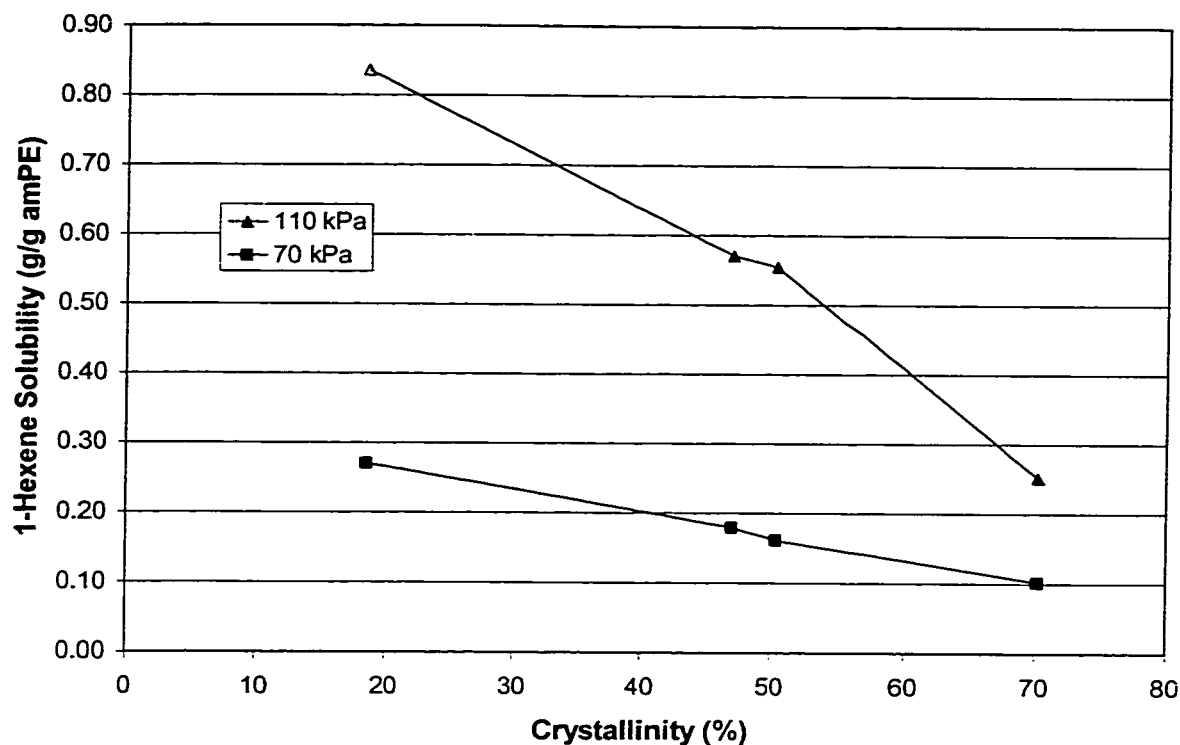
Figure 4-16 - Solubility of 1-Hexene in Polyethylene Samples of Different Crystallinity at 69°C

off the balance. While not an equilibrium solubility value, it is still representative of the amount of 1-hexene that could be sorbed under these conditions.

It can be seen from Figure 4-16 that polyethylene crystallinity is a very important parameter in determining 1-hexene solubility, even if that solubility is calculated on an amorphous mass basis. Solubilities decreased over the range of the crystallinities in this study by 62% and 70% for 1-hexene pressures of 70 kPa and 110 kPa respectively. This decrease is similar to that seen for 1-butene and significantly greater than that seen for ethylene. Therefore, the 1-hexene results confirm that sample crystallinity plays a greater role in the solubility of the higher α-olefins than it does for ethylene.

4.5 Effect of Solubility Measurement Procedure on Sample Properties

Mulder (1999) measured the crystallinity of three of the polymer samples before

and after exposure to the olefin penetrants used in this experiment. The results of these

measurements are summarised in Table 4-6

Table 4-6
Crystallinity Before and After Exposure to Penetrants (Mulder, 1999)

Sample	Crystallinity (%)			
	Initial	Exposure to Ethylene	Exposure to 1-Butene	Exposure to 1-Hexene
MM003	50.4	51.7	52.9	55.8
MM013	70.2	70.9	71.8	71.3
MM029	47.0	48.5	50.0	48.7

For all of the samples, the crystallinity increased during the elongation measurements that

were performed. It is logical to assume that because solubility measurements expose the

sample to the same pressures and temperatures as the elongation measurements, the

effects on the samples are similar.

A number of the samples displayed some visible changes after they had been

exposed to the penetrants used in this experiment, especially 1-hexene. The sample that

showed the most dramatic changes was the metallocene catalysed LLDPE, MM019.

Because this sample had a melting temperature of approximately 85°C, it was affected by

both exposure to the penetrant and also to the 69°C measurement temperature. After

completion of 1-butene solubility measurements, the MM019 sample was slightly folded

and had a much greater clarity than it did before the measurements began. As discussed

in Section 4.4, the MM019 sample "melted" when exposed to the maximum 1-hexene

pressure. A number of large bubbles formed in the sample and it completely lost its rectangular shape. The small amount of the surface which was not covered in bubbles, showed significantly increased clarity. Typically, an increase in clarity of a polymer sample is related to a decrease in crystallinity. This suggests that unlike the other samples which Mulder (1999) investigated, the crystallinity of MM019 actually decreased with exposure to the olefin penetrants. This is not an uncommon result as many polymers are typically plasticised by heavy hydrocarbon vapours (Hutchinson and Ray, 1990).

The other dramatic qualitative change was seen following exposure of the other LLDPE sample, MM029, to 1-hexene. This surface of this sample was covered with an opaque white material. The greatest concentration of this white substance was deposited on the bottom of the sample and the sample was textured so that it appeared that a liquid had flown down its side faces. Both samples MM003 and MM013 also had very small amounts of white solid forming at the bottom of the samples.

One explanation for these observations is that it is possible that the polymer samples contained some quantity of low molecular weight material. Exposure to the 1-hexene caused this material to leach out of the sample and gravity led to its accumulation at the bottom. The finding by Mulder (1999) that crystallinity increased for all of these samples is consistent with this explanation. The low molecular weight materials would be present in the amorphous phase, so that if it were removed, the crystallinity of the sample would increase.

It is also possible that the increased crystallinity of the samples after exposure to the olefin penetrants was due to a recrystallisation process. At temperatures near 90°C,

segmental motion of the polymer chains may have been sufficient for recrystallisation to take place. The presence of the olefin penetrant could also promote a recrystallisation process.

4.6 Importance of Volume Corrections

The polyethylene samples used in this study swell as they sorb the olefin penetrants and thus there is a change in sample volume over the course of an experiment. Sample volume is an important parameter as it is used to determine the buoyancy force on the sample and thus calculate the actual mass of sorbed gas. For this reason, corrections are needed in order to calculate sample volumes at the experimental temperatures and pressures. The procedure used to calculate these volume changes in the polyethylene samples is described in Section 3.3. However, these corrections require separate elongation measurements, which are quite time-consuming. It is useful then, to determine how important these corrections are, and whether or not they can be omitted from future studies.

Figures 4-17 and 4-18 show the solubility in low-density polyethylene (sample MM003) of ethylene and 1-butene respectively. In these figures, the solid points and lines represent solubility values calculated with the complete volume correction; open points and dotted lines represent solubility values determined without any volume correction. In the latter case, sample volume is determined simply by dividing the mass of the sample at room temperature by its density. By comparing the data obtained with and without the volume corrections, one can determine the importance of the correction procedure.

In Figure 4-17, the uncorrected solubility values show significant deviation from those determined using the volume correction. The deviation is greatest at high temperatures and high pressures with the maximum deviation being approximately 19%. The reason for this significant deviation is that the buoyancy force is very important in

76
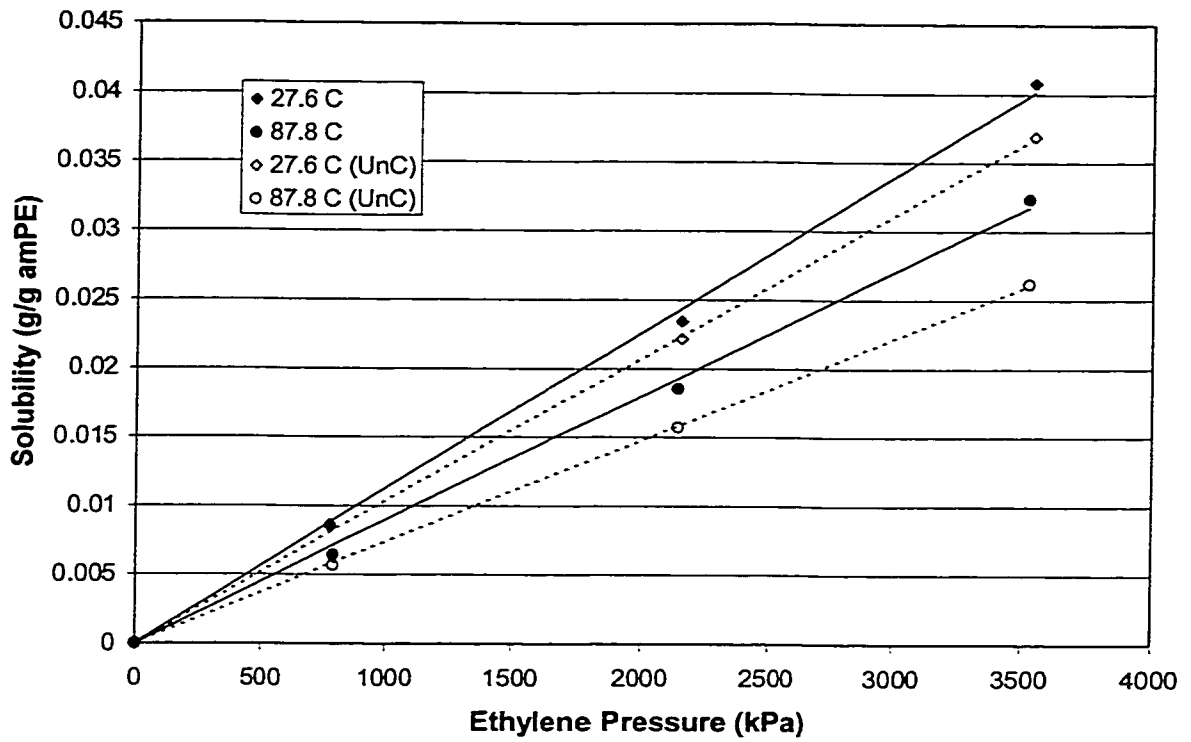
Figure 4-17 - Ethylene Solubility in MM003, With and Without Volume Corrections
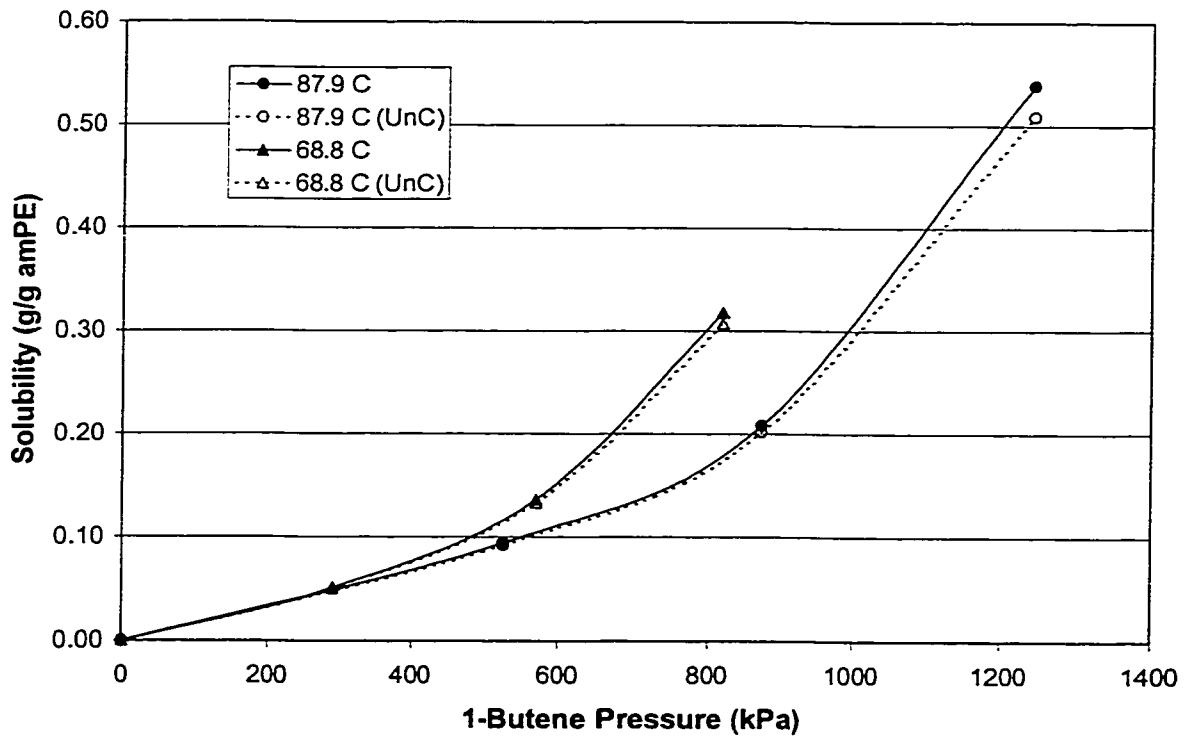
Figure 4-18 - 1-Butene Solubility in MM003, With and Without Volume Corrections

ethylene solubility measurements. With quite low uptakes of gas, the magnitude of the buoyancy force is greater than the force exerted by the mass of sorbed penetrant. Therefore, it is clear that the volume correction is needed for ethylene solubility measurements.

As shown in Figure 4-18, the deviation in the 1-butene solubility measurements is considerably less than for ethylene. At the maximum temperature and pressure, there is a 5.6% difference between the corrected and uncorrected solubilities. At lower temperatures not shown in Figure 4-18 (30°C and 49°C), the deviation was always less than 2%, and thus is small enough that it is difficult to even see on a graph of this scale. Similarly, all of the deviations for 1-hexene were less than 1%. The reason that the higher α-olefins show much smaller deviations is that the gas uptake is at least an order of magnitude greater than ethylene. Mulder (1999) found that sample elongation, and thus volume change, due to swelling increased dramatically as the molar mass of the olefin penetrant increased. However, with lower penetrant pressures and greater gas sorption, the magnitude of the buoyancy force was much less than the weight of the sorbed penetrant.

With a maximum 5.6% deviation between corrected and uncorrected solubility values, the volume correction is significant for 1-butene solubility measurement if high temperatures and pressures are used. However, the volume correction is not significant for 1-hexene solubility results. This result may be of use in future work for samples in pellet form, or with other irregular shapes, for which elongation measurements cannot be made.

4.7 Relationship Between Olefin Solubility and Sample Elongation

In order to determine the volume of swollen polymer samples, the elongation of the samples was measured during exposure to the penetrant gases at experimental temperatures and pressures. It is interesting to examine the relationship between the elongation of the samples and the masses of sorbed penetrant. Figures 4-19 to 4-21 show the relationship between sample elongation and penetrant solubility for ethylene, 1-butene, and 1-hexene respectively.
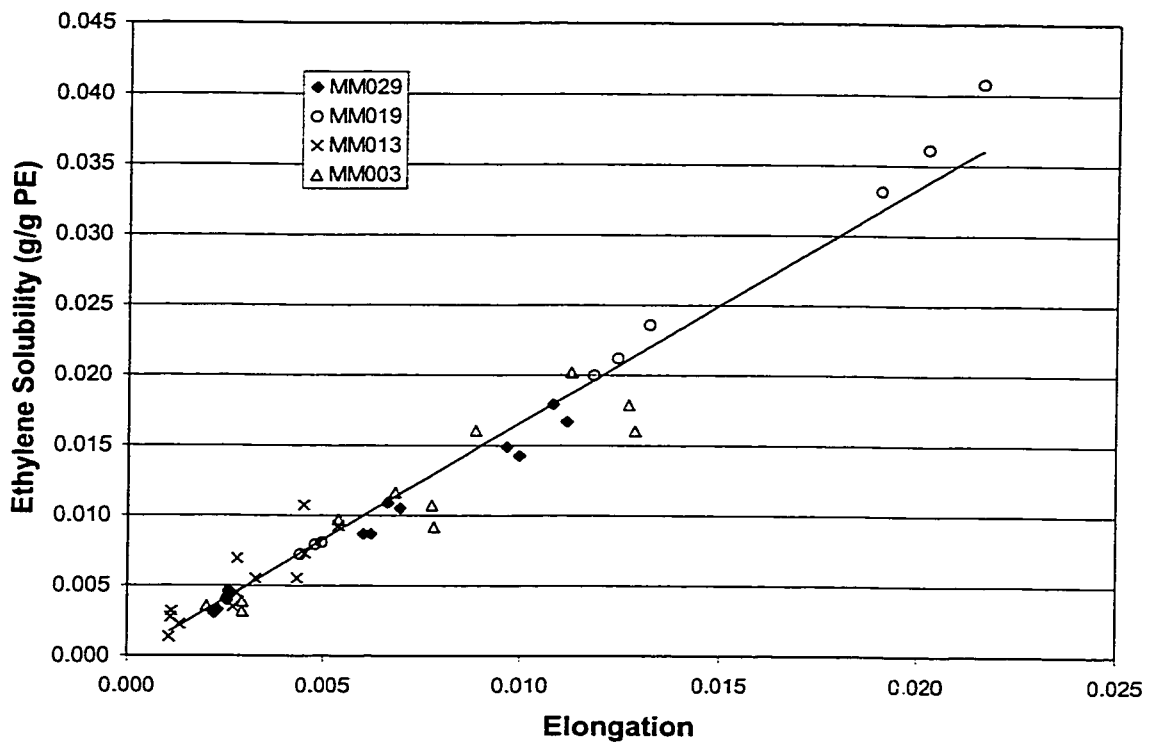
Figure 4-19 – Relationship Between Ethylene Solubility and Sample Elongation

In these figures, elongation is calculated as (equilibrium length – initial length) / initial length, with the initial lengths measured under vacuum at the experimental temperature. Solubility is measured in units of grams of penetrant per gram of polyethylene; this is a change from the unit of g/g amPE that has been used throughout this study. The reason
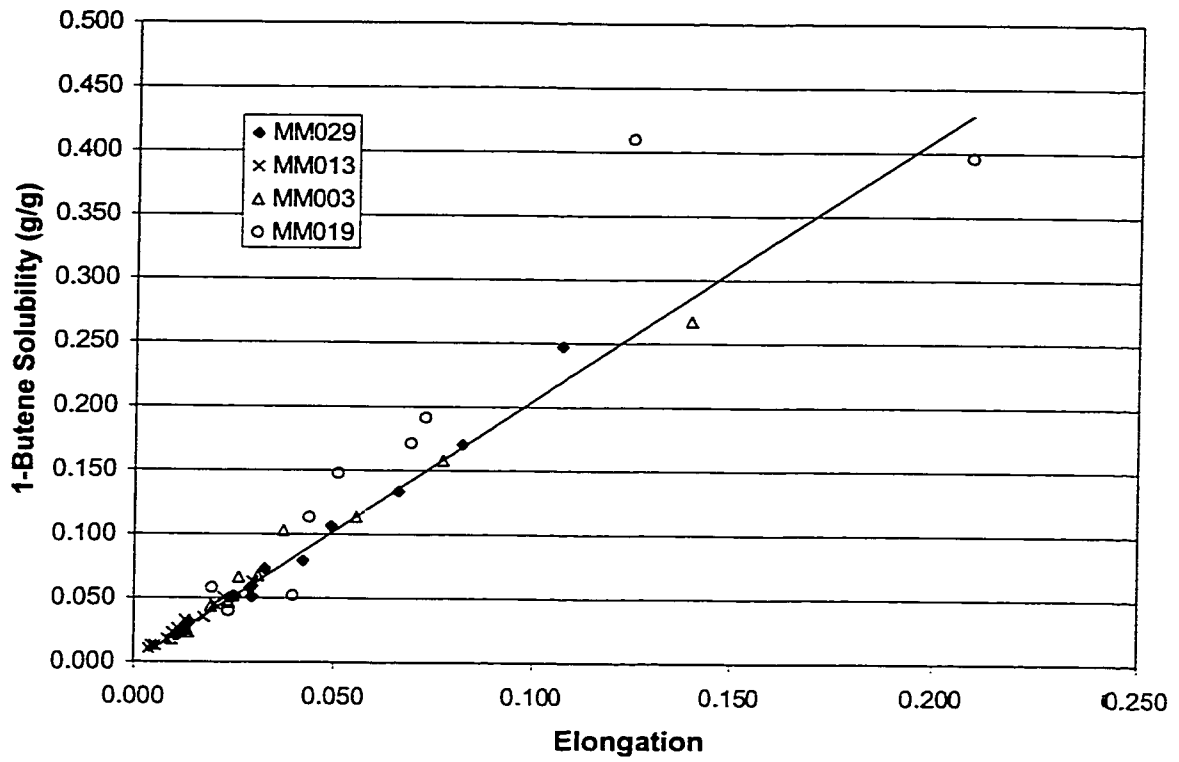
Figure 4-20 - Relationship Between 1-Butene Solubility and Sample Elongation
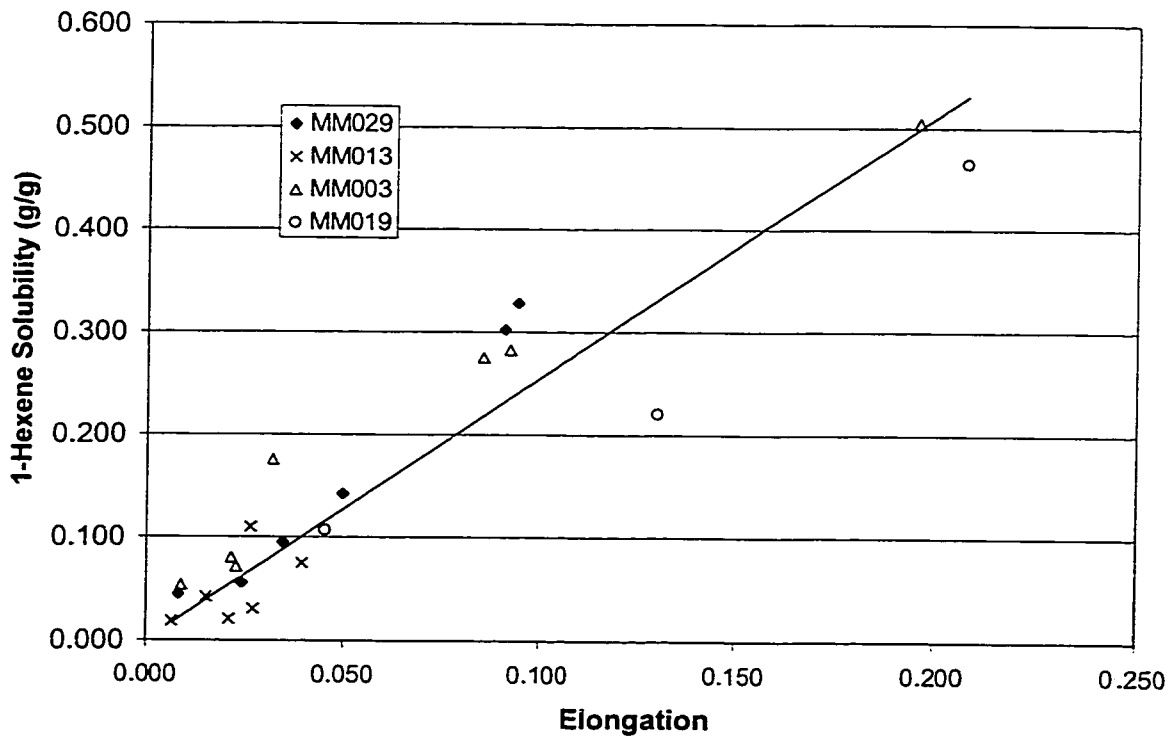
Figure 4-21 - Relationship Between 1-Hexene Solubility and Sample Elongation

that solubility is not considered using a basis of amorphous mass is that the elongation refers to the entire sample, not just the amorphous phase. One could obtain a similar plot by normalising the elongation with a basis of amorphous volume and using the amorphous solubility.

As can be seen from Figures 4-19 to 4-21, there is a linear relationship between solubility and elongation. This linear relationship generally holds over a wide range of pressures despite considerable differences in sample crystallinity, molecular structure, and temperature.

The plots in Figures 4-19 to 4-21 could be useful for a number of purposes. For film samples, such as those used in this study, it is very easy to measure the sample elongation. For these cases, one could obtain a reasonable estimation of penetrant solubility by simply measuring the elongation and then determining the corresponding solubility from the plot. This would be desirable because elongation measurements are simpler to perform than weight change measurements and one could perform elongation measurements at temperatures greater than those possible with the electrobalance.

In a contrasting case, it would be impossible to measure the elongation of a sample consisting of nascent polymer pellets. However, one could measure the weight change due to sorption, and then iteratively determine the solubility and volume correction for that sample.

Finally, the slopes of the fit lines in Figures 4-19 to 4-21 contain information relating the mass of sorbed penetrant to the volume that the penetrant occupies. From these slopes, it would be possible to determine an estimate of the molar volumes of the penetrants in polyethylene.

4.8 Solubility Modelling

One of the secondary objectives in this study was to find a mathematical model that would adequately describe the olefin solubility data that has been obtained. To be successful, the model should be useful for both interpreting existing data, and also predicting future solubility behaviour.

Modelling of ethylene solubility in polyethylene has already been discussed in Section 4.1.1. It was found that for the experimental conditions used in this study, ethylene obeys Henry's law, that is, the amount of sorbed gas is directly proportional to the ethylene pressure. Therefore, linear regression was used to fit the experimental points and represent the sorption isotherms.

However, as seen in Sections 4.3 and 4.4, 1-butene and 1-hexene do not obey Henry's law and the sorption isotherms for these gases show significant curvature. Therefore, more complicated solubility models were needed to describe their solubility behaviour.

The first model that was used to try and describe the solubility of 1-butene and 1-hexene was the Flory-Huggins equation, which was discussed in Section 2.2.3. The equation used had the form

$$\ln a_2 = \ln \phi_2 + (1 - \phi_2) + \chi_{12}(1 - \phi_2)^2 \qquad (4\text{-}1)$$

where a_2 is the activity of the penetrant, χ_{12} is the interaction parameter and ϕ_2 is the volume fraction of the penetrant. To use this model, the volume fraction and activity of the penetrant were calculated from the experimental conditions and solubilities and then plotted. Interaction parameters were then determined by fitting the data with non-linear regression using the software package POLYMATH.

82

The volume fraction of the penetrant was calculated using the equation

$$\phi_2 = \frac{SV_2^L / M_2}{SV_2^L / M_2 + V_1(T)} \tag{4-2}$$

where M_2 is the molar mass of the penetrant; S is the penetrant solubility; $V_1(T)$ is the specific volume of the polymer as a function of temperature; and V_2^L is the molar liquid volume of the penetrant. The liquid molar volume of the penetrant was estimated from the critical volume using the Tyn and Calus (1975) method:

$$V_2^L = 0.285 V_c^{1.048} \tag{4-3}$$

This equation gave volumes of 89.0 cm^3/mol and 132 cm^3/mol for 1-butene and 1-hexene respectively. Specific volumes of the polymer samples can be calculated as a function of temperature using the thermal expansion coefficients and Equation 3-3.

The activity of the penetrant is defined as the ratio of the fugacity in the gas phase at experimental temperature and pressure to the fugacity in the reference liquid state. Budzien et al. (1998a) reported the following equation to calculate the pure state liquid fugacity for a gas at any temperature and atmospheric pressure

$$\ln\left(\frac{f_L(T)}{P_c}\right) = 2.8781 - \frac{2.2399}{T_r - 0.29889} \tag{4-4}$$

where $f_L(T)$ is the liquid fugacity; P_c is the critical pressure of the species; and T_r is the reduced temperature. In order to calculate the liquid fugacity at the experimental pressures, the fugacity value obtained from Equation 4-4 was multiplied by the Poynting correction

$$f_L(T,P) = f_L(T)\exp\left[\frac{V_2^L(P - 101325)}{RT}\right] \tag{4-5}$$

Fugacity in the gas phase was calculated using fugacity coefficients obtained from generalised Lee-Kesler (1975) tables.

After the interaction parameters were determined, the Flory-Huggins equation was used to fit the olefin solubility results as a function of activity. These fit lines were compared graphically to experimental results in Figures 4-22 to 4-25.
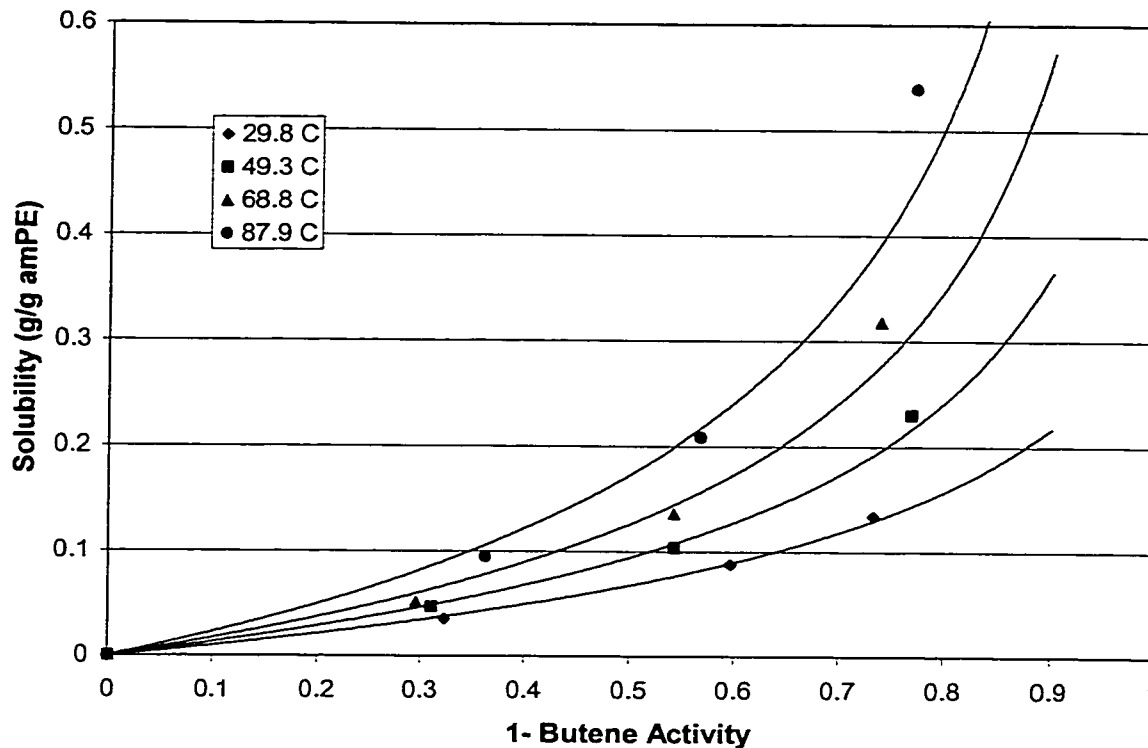
Figure 4-22 - Experimental Solubilities and Flory-Huggins Fits for 1-Butene as a Function of Activity in MM003, 50% Crystalline LDPE

It can be seen from Figure 4-22 that the experimental solubility values fall quite close to the fit lines generated using the Flory-Huggins equation. However, at high activities, the equation underpredicts the 1-butene solubility. This result was found for all four of the polyethylene samples.
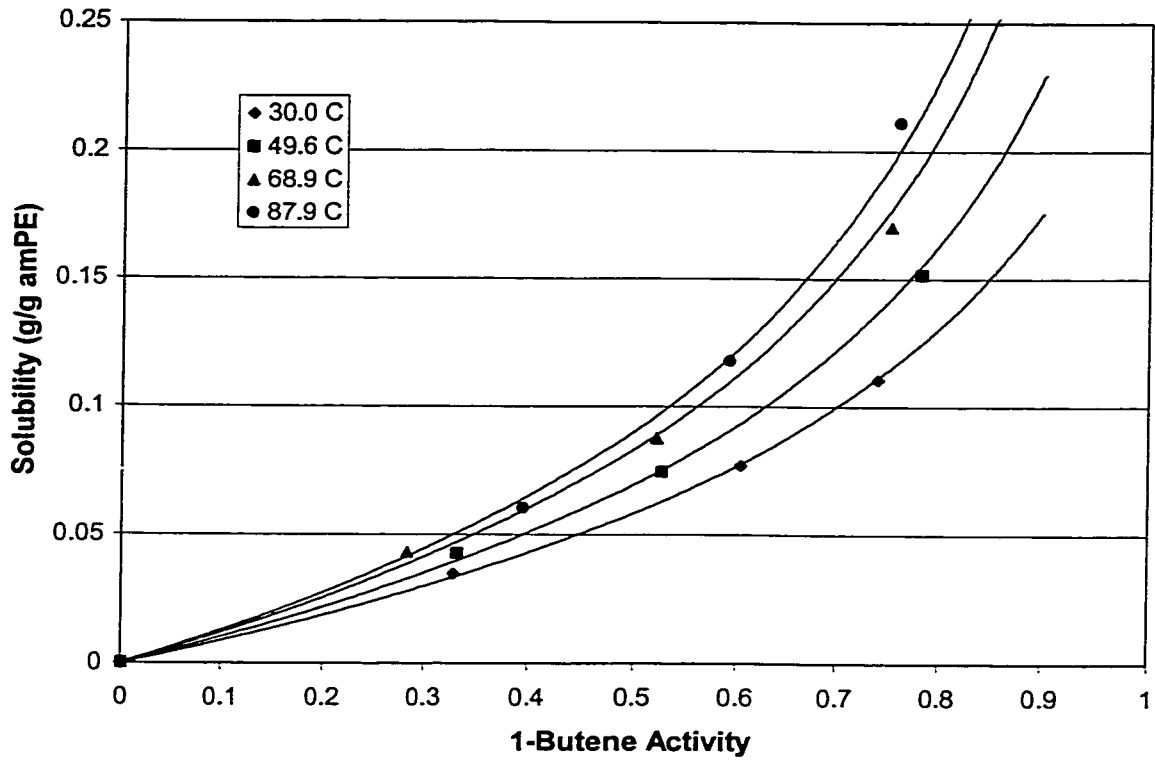
Figure 4-23 - Experimental Solubilities and Flory-Huggins Fits for 1-Butene as a Function of Activity in MM013, 70% Crystalline HDPE
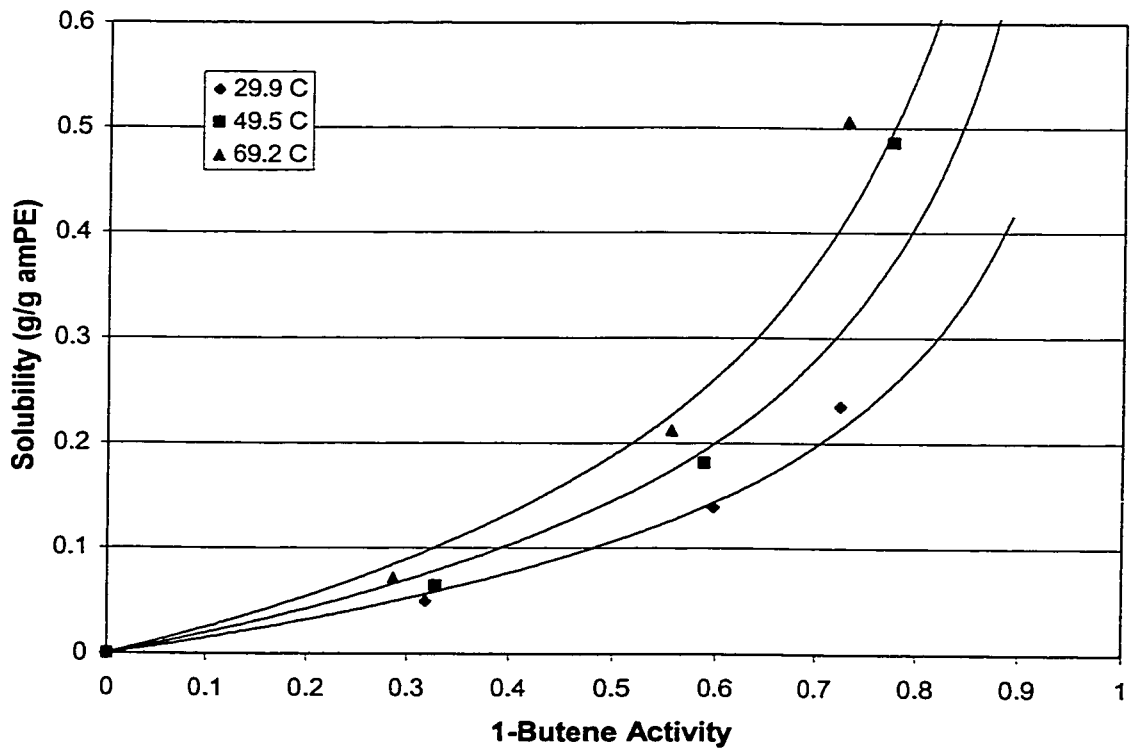
Figure 4-24 - Experimental Solubilities and Flory-Huggins Fits for 1-Butene as a Function of Activity in MM019, 18% Crystalline LLDPE
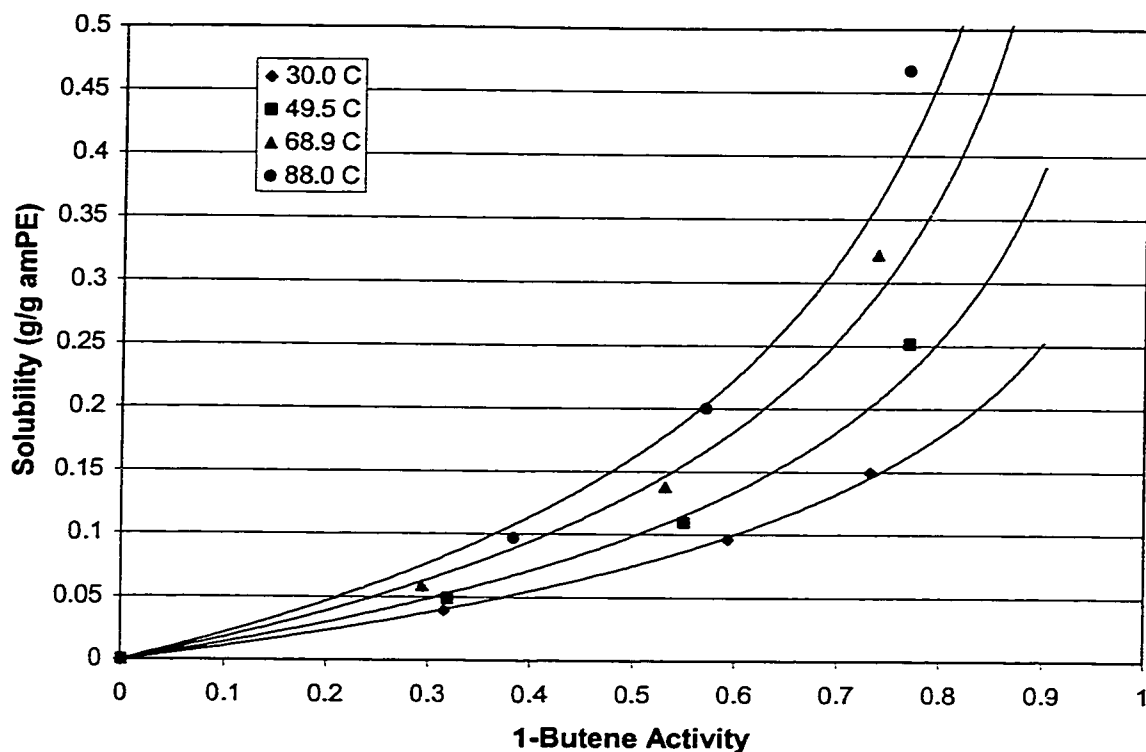
Figure 4-25 - Experimental Solubilities and Flory-Huggins Fits for 1-Butene as a Function of Activity in MM029, 47% Crystalline LLDPE

Yoon et al. (1996) reported interaction parameters between 0.98 and 1.29 for the solubility of 1-butene in LLDPE. The Flory-Huggins interaction parameters obtained for 1-butene for the four polyethylenes are listed in Table 4-7.

Table 4-7
Interaction Parameters for 1-Butene in Polyethylenes

Sample	Interaction Parameter			
	Temperature (°C)			
	30	49	69	88
MM003	0.971	0.707	0.473	0.203
MM013	1.066	0.926	0.782	0.720
MM019	0.635	0.382	0.160	not measured
MM029	0.894	0.676	0.437	0.274

The solubilities measured by Yoon et al. (1996) were lower than the ones I measured; the lower values for the interaction parameter found in this study are consistent with the higher 1-butene solubilities.

Attempts were also made to model the solubility of 1-hexene in polyethylene using the Flory-Huggins equation. However, these attempts were not successful, as the curvature of the experimental sorption isotherm was much greater than that predicted by the Flory-Huggins equation. Also, some negative values for the interaction parameter were obtained.

Ethylene / 1-Hexene Co-solubility

The final experiment that was performed in this study was an attempt to measure the solubility of a gas mixture containing ethylene and 1-hexene. Such a mixture represents an atmosphere to which polyethylene pellets would be exposed during their formation in an industrial reactor. While this experiment is only a preliminary investigation, a number of interesting findings can be reported.

The sample chosen for this experiment was MM029, the Ziegler-Natta catalysed linear low-density polyethylene, and was prepared in manner described in Section 3.2.2. The temperature used was 69°C. After evacuation, the system was filled, over a period of about 40 minutes, with 1-hexene to a pressure of approximately 113 kPa. At this point, the 1-hexene cylinder was closed and ethylene was admitted to the system until the total pressure was approximately 2175 kPa. After a 24 hour wait, ethylene was again admitted to the system until a total pressure of 3540 kPa had been reached.

The results of this experiment were quite surprising. The experimental weight changes, uncorrected for buoyancy effects, of the polyethylene sample over time as it was exposed to first 1-hexene, and then ethylene are shown in Figure 4-26. The most interesting part of this figure is the region between 0 and 50 minutes. When the 1-hexene was admitted to the system, it was immediately sorbed by the polyethylene sample and the weight increased rapidly. During this stage of the experiment, the maximum sample weight change was 0.056469 g, which was of a similar magnitude as the weight changes measured in the 1-hexene solubility experiments. However, when ethylene was admitted to the system (after approximately 40 minutes), the weight of the sample decreased
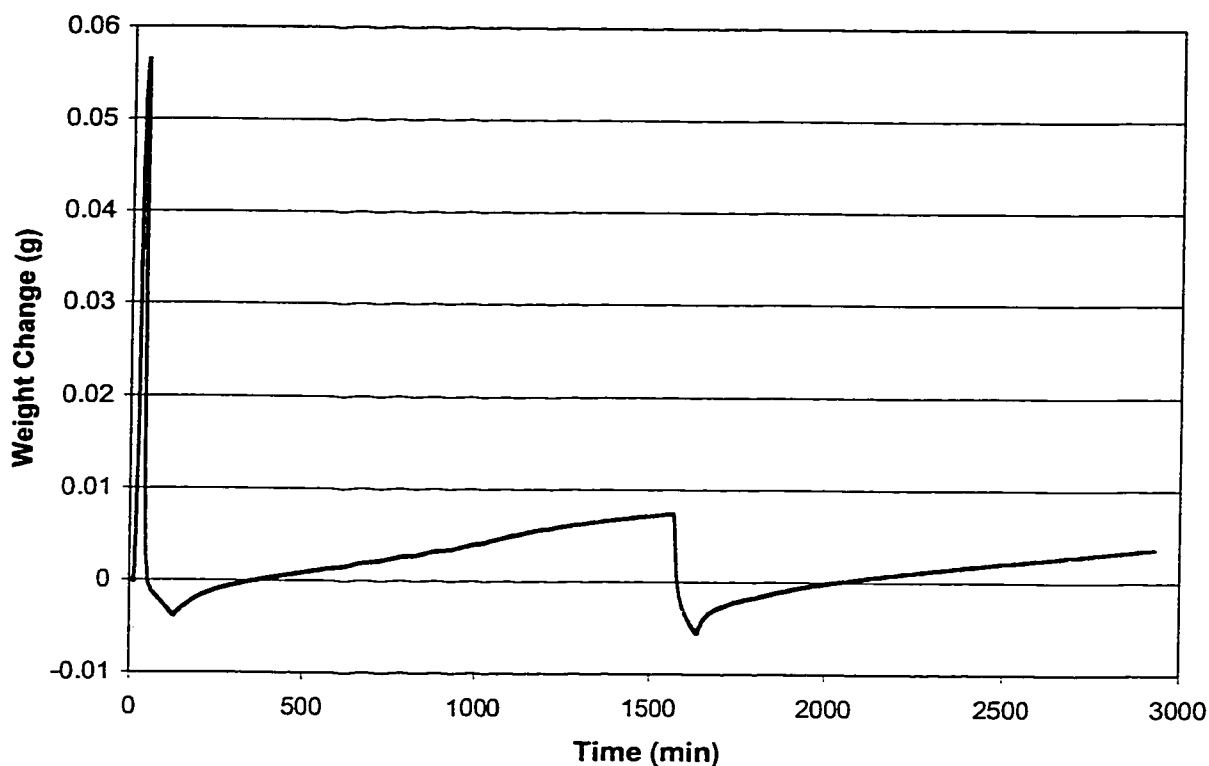
Figure 4-26 - Weight Change of Sample MM029 During Ethylene / 1-Hexene
Co-solubility Experiment at 69.1°C

rapidly. The weight change decreased to 0 in approximately 11 minutes and then became

negative as the buoyancy of the sample exceeded the weight of the absorbed gas. At the

time when the sample weight change reached 0, the total pressure in the system was

approximately 160 kPa. The sample weight then continued to decrease as the ethylene

flowed into the system. When the ethylene flow was stopped, the sample weight then

slowly increased for 24 hours. The increase in weight had not stopped when ethylene

was again admitted to the system. Following the second admission of ethylene, the

sample weight again first decreased and then increased without stopping for 24 hours.

It is very surprising that the sample weight decreased so dramatically following

the admission of ethylene. It seems that any 1-hexene that had been sorbed was displaced

almost instantaneously by ethylene. It is also surprising that the sample weight never

reached equilibrium after the ethylene flow had stopped. Most of the solubility experiments took no longer than 4 or 5 hours to reach equilibrium.

Even though equilibrium was not reached, it is still interesting to compare the amount of gas sorbed in this co-solubility experiment to the amounts sorbed in the individual ethylene and 1-hexene measurements. Figure 4-27 shows the amounts of gas sorbed in each case.
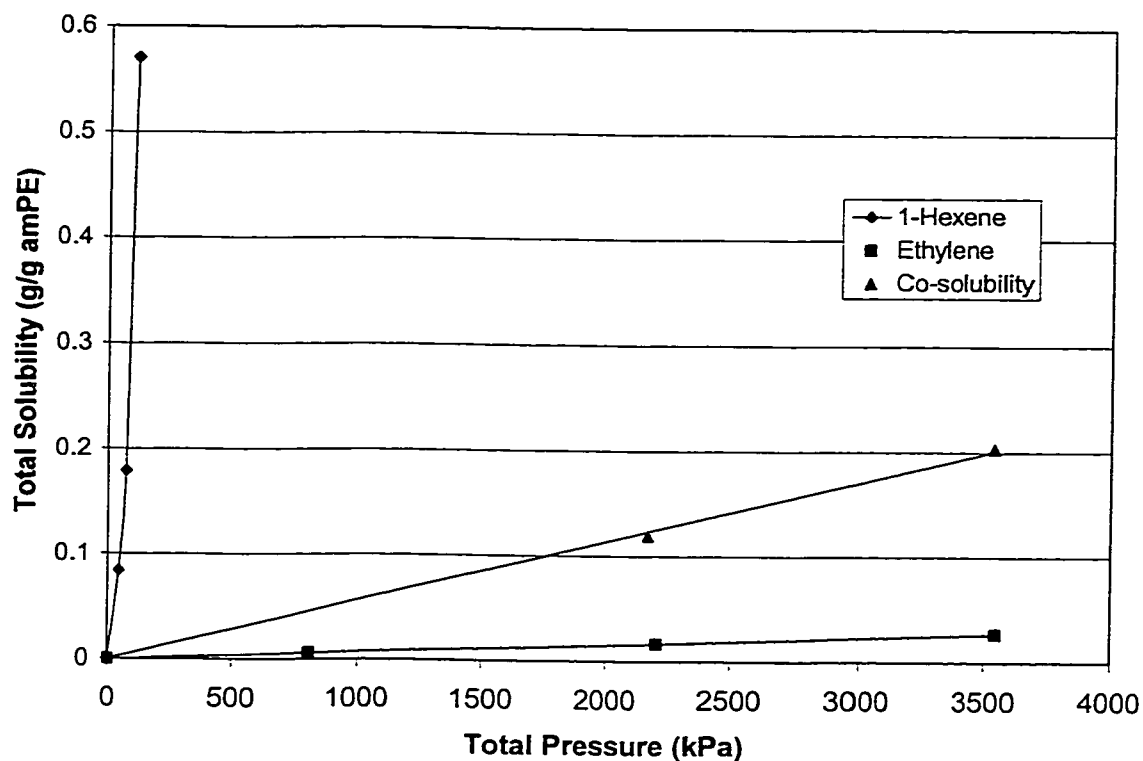
Figure 4-27 - Comparison of Sorption results for Ethylene, 1-Hexene, and Co-solubility Measurements

It can be seen from Figure 4-27 that the amount of gas sorbed in this experiment is much closer to what would be expected for an experiment with pure ethylene, than one with 1-hexene. Thus it is clear that the solubility of ethylene and 1-hexene exhibits considerable co-solubility effects and the total solubility of this gas mixture is not simply the sum of the solubilities of each pure gas.

5. Conclusions

From the results that have been presented for this study, the following conclusions can be drawn.

1. The gravimetric method described here can be accurately and reliably used to obtain data on the solubility of α-olefins in polyethylene at a variety of experimental conditions.

2. The solubility of ethylene in polyethylene obeys Henry's law at temperatures from 30°C to 90°C and ethylene pressures up to 3.5 MPa. The solubilities of 1-butene and 1-hexene do not obey Henry's law.

3. The solubility of α-olefins in polyethylene increases dramatically as the carbon number of the penetrant increases

4. At a constant pressure, olefin solubility in polyethylene decreases with increasing temperature.

5. Sample crystallinity is an important parameter in determining α-olefin solubility in polyethylene. Even when solubility is considered on a basis of amorphous mass, solubility generally decreases with increased crystallinity. However, the decrease with crystallinity is not constant, which suggests that detailed molecular structure (short and long chain branching) also plays an important role in olefin solubility.

6. The presence of ethylene appears to inhibit the sorption of 1-hexene in linear low-density polyethylene. Exposure to ethylene causes previously sorbed 1-hexene to be removed.

6. Recommendations

1. The Cahn balance is susceptible to failure caused by the high temperatures used in this experiment. While some high temperature exposure is inevitable, efforts should be made to minimise the amount of time that the balance is exposed to temperatures above ambient conditions.

2. Further efforts should be made to find a mathematical model that accurately describes the solubility behaviour of α-olefins in polyethylene.

3. Continue efforts to determine the co-solubilities of ethylene / 1-hexene and other gas mixtures. This could include introducing the gases in different order, or introducing a premixed gas sample.

4. The scope of the experiment could be extended to include diffusion studies as well as solubility. By recording the weight change of a polymer sample over time, the Cahn balance is well suited to these studies.

5. Determine olefin solubilities in nascent polyethylene pellets, rather than the film samples that were used in this experiment. This would provide data that more accurately reflects monomer solubility under reactor conditions.

7. References

Beret, S., Muhle, M. E. and Villamil, I. A., "Purging Criteria for LDPE Make Bins", *Chemical Engineering Progress*, **73(12)**, 44-49 (1977).

Beret, S. and Hager, S. L., "Ethylene Solubility and Diffusion in Low-Density Polyethylene and Ethylene Copolymers", *Journal of Applied Polymer Science*, **24**, 1787-1796 (1979).

Bu, N., Lynch, D. T. and Wanke, S. E., "Kinetics of Catalytic Gas-Phase Homopolymerization of Ethylene over $SiO_2/MgCl_2$ – Supported $TiCl_4$ Catalysts", *Polymer Reaction Engineering*, **3**, 1-22 (1995).

Budzien, J. L., McCoy, J. D., Weinkauf, D. H., LaViolette, R. A. and Peterson, E. S., "Solubility of Gases in Amorphous Polyethylene", *Macromolecules*, **31**, 3368-3371 (1998a).

Budzien, J. L., McCoy, J. D., Curro, J. G., LaViolette, R. A. and Peterson, E. S., "The Solubility of Gases in Polyethylene: Integral Equation Study of Standard Molecular Models", *Macromolecules*, **31**, 6669-6675 (1998b).

Castro, E. F., Gonzo, E. E. and Gottifredi, J. C., "Thermodynamics of the Absorption of Hydrocarbon Vapors in Polyethylene Films", *Journal of Membrane Science*, **31**, 235-248 (1987).

Castro, E. F., Gonzo, E. E. and Gottifredi, J. C., "The analysis of sorption data of organic vapors in polymeric membranes through novel theories", *Journal of Membrane Science*, **113**, 57-64 (1996).

Chiou, J. S. and Paul, D. R., "Gas Sorption and Permeation in Poly(Ethyl Methacrylate)", *Journal of Membrane Science*, **45**, 167-189 (1989).

Crank, J. and Park, G. S., "Evaluation of the diffusion coefficient for chloroform in polystyrene from simple absorption experiments", *Transactions of the Faraday Society*, **45**, 240 (1949).

Crank, J. and Park, G. S., *Diffusion in Polymers*, Academic Press, New York, New York (1968).

Curro, J. G. and Schweizer, K. S., "Theory of Polymer Melts: An Integral Equation Approach", *Macromolecules*, **20**, 1928-1934 (1987).

Curro, J. G., Honnell, K. G. and McCoy, J. D., "Theory for the Solubility of Gases in Polymers: Application to Monatomic Solutes", *Macromolecules*, **30**, 145-152 (1997).

Deas, T. M., Hofer, H. H. and Dole, M., "Solubility of Hydrogen in Polyethylene by a Semimicro Method", *Macromolecules*, **5(2)**, 223-226 (1972).

Del Nobile, M. A., Mensitieri, G., Nicolais, L. and Weiss, R. A., "Gas Transport Through Ethylene-Acrylic Acid Ionomers", *Journal of Polymer Science: Part B: Polymer Physics*, **33**, 1269-1280 (1995).

Doong, S. J. and Ho, W. S. W., "Sorption of Organic Vapors in Polyethylene", *Industrial and Engineering Chemistry Research*, **30**, 1351-1361 (1991).

Duda, J. L., Kimmerly, G. K., Sigelko, W. L. and Vrentas, J. S., "Sorption Apparatus for Diffusion Studies with Molten Polymers", *Industrial and Engineering Chemistry Fundamentals*, **12(1)**, 133-136 (1973).

Faridi, N., Hadj-Romdhane, I., Danner, R. P. and Duda, J. L., "Diffusion and Sorption in Ethylene-Propylene Copolymers: Comparison of Experimental Methods", *Industrial and Engineering Chemistry Research*, **33**, 2483-2491 (1994).

Fredenslund, A., Jones, R. L. and Prausnitz, J. M., "Group-Contribution Estimation of Activity Coefficients in Nonideal Liquid Mixtures", *AIChE Journal*, **21(6)**, 1086-1099 (1975).

Fleming, G. K. and Koros, W. J., "Dilation of Polymers by Sorption of Carbon Dioxide at Elevated Pressures. 1. Silicone Rubber and Unconditioned Polycarbonate", *Macromolecules*, **19**, 2285-2291 (1986).

Flory, P. J., *Principles of Polymer Chemistry*, Cornell University Press, Ithaca, New York (1953).

Flory, P. J., *Principles of Polymer Chemistry*, Cornell University Press, Ithaca, New York (1969).

Fried, J. R., *Polymer Science and Technology*, Prentice Hall PTR, Upper Saddle River, New Jersey (1995).

Hedenqvist, M., Angelstok, A., Edsberg, L., Larsson, P. T. and Gedde, U. W., "Diffusion of small-molecule penetrants in polyethylene: free volume and morphology", *Polymer*, **37(14)**, 2887-2902 (1996).

Hellums, M. W., Koros, W. J., Husk, G. R. and Paul, D. R., "Fluorinated Polycarbonates for Gas Separation Applications", *Journal of Membrane Science*, **46**, 93-112 (1989).

Hirose, T., Mizoguchi, K. and Kamiya, Y., "Dilation of Polyethylene by Sorption of Carbon Dioxide", *Journal of Polymer Science: Part B: Polymer Physics*, **24**, 2107-2115 (1986).

Hutchinson, R. A. and Ray, W. H., "Polymerization of Olefins Through Heterogeneous Catalysis. VIII. Monomer Sorption Effects", *Journal of Applied Polymer Science*, **41**, 51-81 (1990).

Kamiya, Y., Mizoguchi, K., Naito, Y. and Hirose, T., "Gas Sorption in Poly(vinyl benzoate)", *Journal of Polymer Science: Part B: Polymer Physics*, **24**, 535-547 (1986a).

Kamiya, Y., Hirose, T., Mizoguchi, K. and Naito, Y., "Gravimetric Study of High-Pressure Sorption of Gases in Polymers", *Journal of Polymer Science: Part B, Polymer Physics*, **24**, 1525-1539 (1986b).

Kamiya, Y., Hirose, T., Naito, Y. and Mizoguchi, K., "Sorptive Dilation of Polysulfone and Poly(ethylene terephthalate) Films by High-Pressure Carbon Dioxide", *Journal of Polymer Science: Part B: Polymer Physics*, **26**, 159-177 (1988a).

Kamiya, Y., Hirose, T., Mizoguchi, K. and Terada, K., "Sorptive Dilation of Poly(vinyl benzoate) and Poly(vinyl butyral) by Carbon Dioxide", *Journal of Polymer Science: Part B: Polymer Physics*, **26**, 1409-1424 (1988b).

Kamiya, Y., Mizoguchi, K., Hirose, T. and Naito, Y., "Sorption and Dilation in Poly(ethyl methacrylate)-Carbon Dioxide System", *Journal of Polymer Science: Part B: Polymer Physics*, **27**, 879-892 (1989a).

Kamiya, Y., Naito, Y. and Mizoguchi, K., "Sorption and Partial Molar Volume of Gases in Polybutadiene", *Journal of Polymer Science: Part B: Polymer Physics*, **27**, 2243-2250 (1989b).

Kamiya, Y., Terada, K, Naito, Y. and Wang, J. S., "Sorption, Diffusion, and Partial Molar Volumes of C_4 Hydrocarbons in Rubbery Polymers", *Journal of Polymer Science: Part B: Polymer Physics*, **33**, 1663-1671 (1995).

Kamiya, Y., Terada, K., Mizoguchi, K. and Naito, Y., "Sorption and Partial Molar Volumes of Organic Gases in Rubbery Polymers", *Macromolecules*, **25**, 4321-4324 (1992).

Koros, W. J., Paul, D. R. and Rocha, A. A., "Carbon Dioxide Sorption and Transport in Polycarbonate", *Journal of Polymer Science: Polymer Physics Edition*, **14**, 687-702 (1976).

Koros, W. J. and Paul, D. R., "Design Considerations for Measurement of Gas Sorption in Polymers by Pressure Decay", *Journal of Polymer Science: Polymer Physics Edition*, **14**, 1903-1907 (1976).

Kreituss, A., "Free-Volume Estimates in Heterogeneous Polymer Systems. I. Diffusion in Crystalline Ethylene-Propylene Copolymers", *Journal of Polymer Science: Polymer Physics Edition*, **19**, 889-905 (1981).

Kulkarni, S. S. and Stern, S. A., "The Diffusion of CO_2, CH_4, C_2H_4, and C_3H_8 in Polyethylene at Elevated Pressures", *Journal of Polymer Science: Polymer Physics Edition*, **21**, 441-465 (1983).

Lee, G. L. and Flumerfelt, R. W., "Nitrogen Solubilities in Low-Density Polyethylene at High Temperatures and Pressures", *Journal of Applied Polymer Science*, **58**, 2213-2219 (1995).

Lee, B. I. and Kesler, M. G., "A Generalized Thermodynamic Correlation Based on Three-Parameter Corresponding States", *AIChE Journal*, **21**, 510-527 (1975).

Li, N. N. and Long, R. B., "Permeation through Plastic Films", *AIChE Journal*, **15(1)**, 73-80 (1969).

Liu, C.-P.A. and Neogi, P., "Sorption of Benzene and n-Hexane in Polyethylene", *Journal of Membrane Science*, **35**, 207-215 (1988).

Lipscomb, G. G., "Unified Thermodynamic Analysis of Sorption in Rubbery and Glassy Materials", *AIChE Journal*, **36(10)**, 1505-1516 (1990).

Lundberg, J. L., Wilk, M. B. and Huyett, M. J., "Estimation of Diffusivities and Solubilities from Sorption Studies", *Journal of Polymer Science*, **57**, 275-299 (1962).

Lutzow, N., Tihminlioglu, A., Danner, R. P., Duda, J. L., De Haan, A., Warnier, G. and Zielinski, J. M., "Diffusion of toluene and n-heptane in polyethylenes of different crystallinity", *Polymer*, **40**, 2797-2803 (1999).

McKenna, T. F., "Solubility and Crystallinity Data for Ethylene/Polyethylene Systems", *European Polymer Journal*, **34(9)**, 1255-1260 (1998).

Michaels, A. S. and Parker, R. B., "The Determination of Solubility Constants for Gases in Polymers", *Journal of Physical Chemistry*, **62**, 1604 (1958).

Michaels, A. S. and Bixler, H. J., "Solubility of Gases in Polyethylene", *Journal of Polymer Science*, **50**, 393-412 (1961).

Miura, K., Otake, K., Kurosawa, S., Sako, T., Sugeta, T., Nakane, T., Sato, M., Tsuji, T., Hiaki, T. and Hongo, M., "Solubility and Adsorption of High Pressure Carbon Dioxide to Poly(Styrene)", *International Symposium on Molecular Thermodynamics and Molecular Simulation*, 371-377 (1997).

Mulder, M. H., "Solubility of Ethylene, 1-Butene and 1-Hexene in Polyethylenes", MSc. Thesis, Department of Chemical and Materials Engineering, University of Alberta, 1999.

Oishi, T. and Prausnitz, J. M., "Estimation of Solvent Activities in Polymer Solutions Using a Group-Contribution Method", *Industrial and Engineering Chemistry Process Design and Development*, **17(3)**, 333-339 (1978).

Peng, D. Y. and Robinson, D. B., "A New Two-Constant Equation of State", *Industrial and Engineering Chemistry Fundamentals*, **15**, 59-65 (1976).

Pope, D. S., Koros, W. J. and Fleming, G. K., "Measurement of Thickness Dilation in Polymer Films", *Journal of Polymer Science: Part B: Polymer Physics*, **27**, 1173-1177 (1989).

Robeson, L. M. and Smith, T. G., "The Desorption of Ethane-Butane Mixtures from Polyethylene", *Journal of Applied Polymer Science*, **11**, 2007-2019 (1967).

Robeson, L. M. and Smith, T. G., "Permeation of Ethane-Butane Mixtures through Polyethylene", *Journal of Applied Polymer Science*, **12**, 2083-2095 (1968).

Rogers, C., Meyer, J. A., Stannett, V. and Szwarc, M., "Studies in the Gas and Vapor Permeability of Plastic Films and Coated Papers", *TAPPI*, **39(11)**, 737-741 (1956).

Rogers, C. E., Stannett, V. and Szwarc, M., "The Sorption of Organic Vapours by Polyethylene", *Journal of Physical Chemistry*, **63**, 1406-1413 (1959).

Rogers, C. E., Stannett, V. and Szwarc, M., "The Sorption, Diffusion, and Permeation of Organic Vapors in Polyethylene", *Journal of Polymer Science*, **45**, 61-82 (1960).

Sada, E., Kumazawa, H., Yakushiji, H., Bamba, Y., Sakata, K. and Wang, S. T., "Sorption and Diffusion of Gases in Glassy Polymers", *Industrial and Engineering Chemistry Research*, **26**, 433-438 (1987).

Sanchez, I. C. and Lacombe, R. H., "Statistical Thermodynamics of Polymer Solutions", *Macromolecules*, **11**, 1145-1156 (1978).

Skjold-Jorgensen, S., Kolbe, B., Gmehling, J. and Rasmussen, P., "Vapor-:Liquid Equilibria by UNIFAC Group Contribution. Revision and Extension", *Industrial and Engineering Chemistry Process Design and Development*, **18(4)**, 714-722 (1979).

Stern, S. A., Mullhaupt, J. T. and Gareis, P. J., "The Effect of Pressure on the Permeation of Gases and Vapors through Polyethylene. Usefulness of the Corresponding States Principle", *AIChE Journal*, **15(1)**, 64-73 (1969).

Suwandi, M. S. and Stern, S. A., "Transport of Heavy Organic Vapors through Silicone Rubber", *Journal of Polymer Science: Polymer Physics Edition*, **11**, 663-681 (1973).

Takeuchi, Y. and Okamura, H., "Permeation of Hydrocarbon Vapors Through Polyethylene Films", *Journal of Chemical Engineering of Japan*, **9(2)**, 136-139 (1976).

Tyn, M. T. and Calus, W. F., "Estimating Liquid Molal Volume", *Processing*, **21(4)**, 16-17 (1975).

Wang, J. S. and Kamiya, Y., "Concurrent measurements of sorption and dilation isotherms and diffusivity for polysulfone membrane/carbon dioxide system", *Journal of Membrane Science*, **98**, 69-76 (1995).

Yoon, J. S., Kim, K. L., Lee, K. H. and Maing, S. J., "Diffusion Coefficient and Solubility of Vinyl Acetate Molecules in Poly(Vinyl Acetate) Matrices", *European Polymer Journal*, **28(7)**, 713-716 (1992).

Yoon, J. S., Chung, C. Y. and Lee, I. H., "Solubility and Diffusion Coefficient of Gaseous Ethylene and α-Olefin in Ethylene/α-Olefin Random Copolymers", *European Polymer Journal*, **30(11)**, 1209-1214 (1994).

Yoon, J. S., Yoo, H. S. and Kang, K. S., "Solubility of α-Olefins in Linear Low Density Polyethylenes", *European Polymer Journal*, **32(11)**, 1333-1336 (1996).

Appendix 1

Use of Cahn Balance Software

Cahn Software

The Cahn balance is controlled using a software program supplied by the company. The program is located in the directory C:\Cahn and is run with the command d100-02. When the program is loaded, it will automatically perform a diagnostic test on the balance; if the balance is in working condition, the main program menu will then appear. From the main menu, the user can choose one of three options: Setup Mode, Run Mode, or Analysis Mode.

Setup Mode

Setup Mode allows the user to control the operating parameters of the balance. From the Setup menu, select option 1, Parameters and the following screen will appear.


```
C:\cahn\d100-02.exe                                    _ □ ✕

                          SETUP PARAMETERS

     EST. MAX. RUN TIME < HR:MIN:SEC>..................[ 120:00:00  ]

     DISP. WT. RANGE (gm).......MAX [  .001      ] MIN [  -.01      ]
     DATA SAMPLING PERIOD (HR:MIN:SEC)................[ 000:00:08  ]
     BALANCE RANGE
              High Only < 10 gms/10 micogm >  ....... H




                  <PgUp>-SETUP MENU  <Esc>-MAIN MENU
                       <↑↓→←>-SELECT OPTION
```
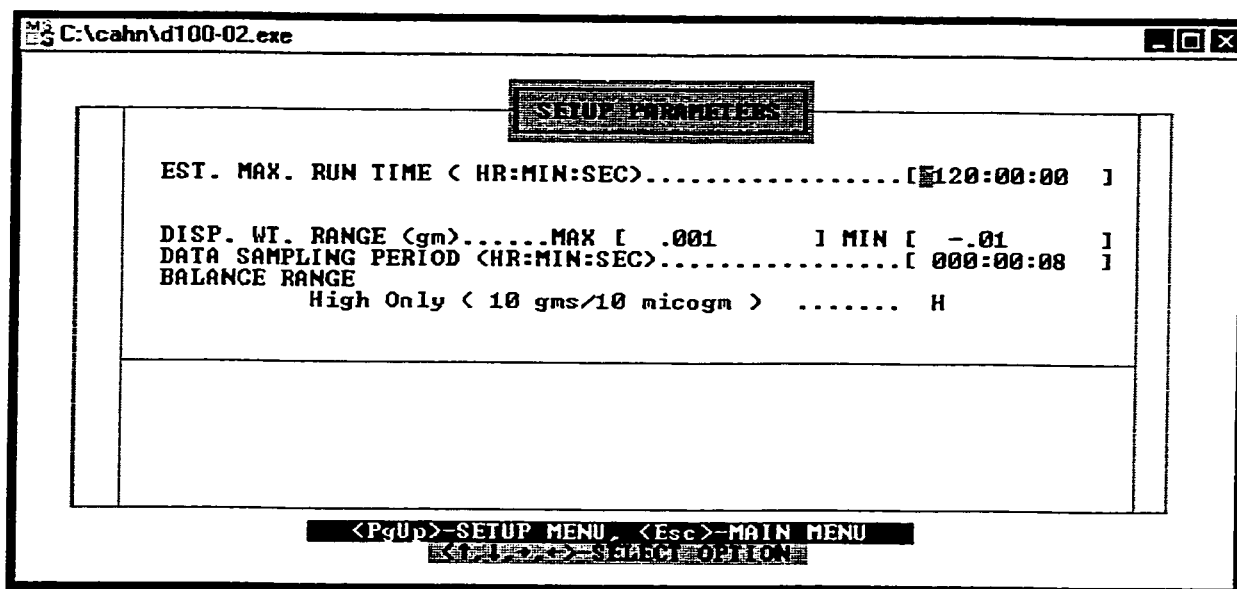
Figure A1-1 - Operating Parameters for the Cahn Balance

For the purposes of this experiment, the Max Run Time, Sampling Period, and Balance Range were not changed. The Display Weight Range was varied depending on the gas used as discussed in Section 3.2.2. The parameters used in this study were saved in the method file "newmeth.met".

Run Mode

The Run Mode is used to record weight data from the balance over a period of time. Calibration of the balance is also done using this mode. Once the user has selected Run Mode, press <↓> and the following screen will appear.

```
C:\cahn\d100-02.exe                                          [_][□][X]


                           RUN MODE


              PRESENT METHOD NAME........ newmeth.met
              DATA FILE NAME?............[ A:MM029A.DAT ]
              RUN TITLE?.................[ CAHN         ]
         ┌──────────────────────────────────────────────┐
         │      ***        BALANCE CALIBRATE       ***   │
         └──────────────────────────────────────────────┘

    TARE BALANCE?   <TYPE 'Y'>.................[■— ]
    INPUT CALIBRATION WEIGHT.......[  01.00000      ] gms
    CALIBRATE BALANCE <TYPE 'Y'>.............[ — ]
              <Esc>-MAIN MENU,  <PgDn>-RUN TEST
                       <↑ ↓>-SELECT
```
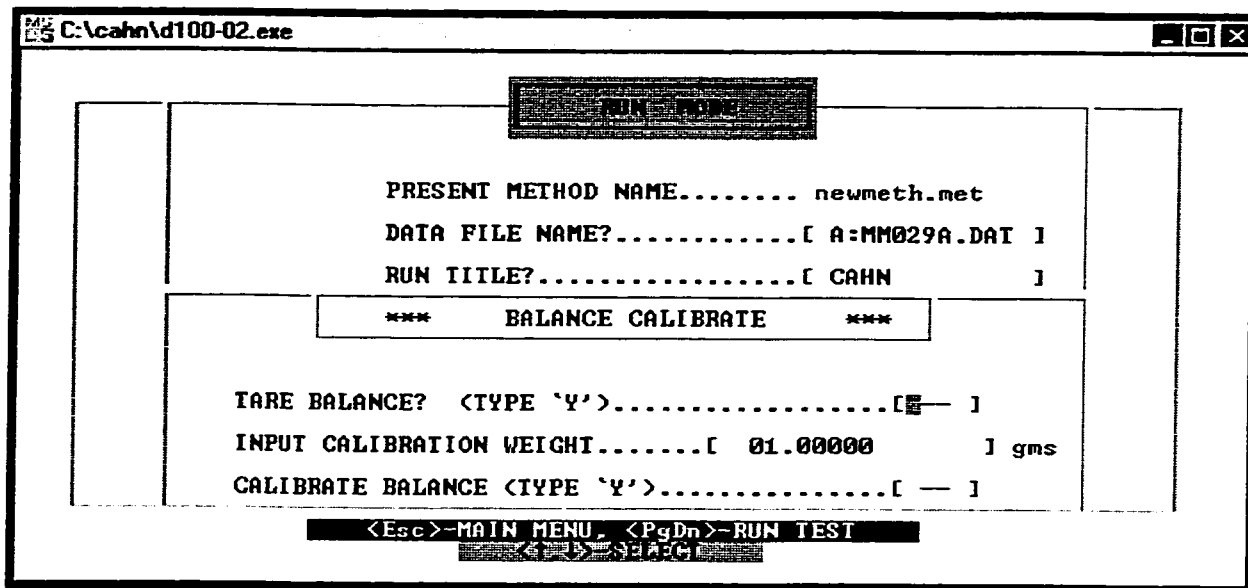
Figure A1-2 - Run Mode and Balance Calibration Menu

From this screen, the user can enter the name of the file to which the data will be saved and also a title for the run. Note that the data file entered must have the extension ".dat". To run an experiment, press <PgDn>; the user will then be asked to enter the Graph Sweep Duration time. During an experimental run, the measured weight is plotted on the screen against time; the Graph Sweep Duration determines the horizontal scale of this graph. In this study, a value of 5 hours was usually used because in most cases, sorption equilibrium was reached during this time limit.

Analysis Mode

The Analysis Mode can be used to perform a variety of functions on data that has been previously obtained. In the course of this experiment, the only analysis that was done using the Cahn software was the conversion of data files to spreadsheet files that could be loaded into Microsoft Excel. However, many of the more advanced features may be of use to future users.

The main screen of the Analysis Mode is shown in Figure A1-3.


```
MS C:\cahn\d100-02.exe - FROZEN                                    _ □ ✕

                                                           COMMAND MENU

Buffer Range..from  000:00:00      To 048:50:32
Cursor Range..from  000:00:00      To 048:50:32     AD  dition
                                                    DI  splay Parameters
                                                    ER  ase Buffer
                                                    FI  les Display
                                                    LN  Ln ←—→ Exp
                                                    LO  ad Data File From Disk
       Buffer     DATA          DATA               OF  fset
         No       File          Type              PO  Plotter
    →    1     CO291.DAT       WGT (gns)            SA  ve   on Disk
         2                                          SC  ale Factor
                                                    SM  ooth Buffer# 1 & dW/dt
                                                    SP  readsheet File (*.PRN)
                                                    ST  atistics Buffer# 1
                                                    SU  btract Buffer# 2 - # 1
                                                    SW  itch Buffers
                                                    WE  ight %

                              C▓    ]

              <PgDn>-DATA DISPLAY,<Esc>-MAIN MENU
```

Figure A1-3 - Analysis Mode Menu

A data file can be loaded into memory using the command LO. This file can then be converted into a spreadsheet file (with the extension ".prn") using the SP command. The spreadsheet file can then be read by Excel as space-delimited text.

Appendix 2

Sample Solubility Calculation

Sample Calculation

<u>Experimental Parameters:</u>

Sample: MM019 and ethylene gas
Mass of Sample: 0.4443 g
Sample Density: 0.885 g/cm^3
Sample Crystallinity: 18.5%
Temperature: 47.7 °C
Gauge Pressure: 301 psi
Atmospheric Pressure: 13.6 psi
Actual Pressure: 314.6 psi (2169083 Pa)
Weight Change: -0.00375 g
Background Buoyancy: 0.0003 g

<u>Weight Change:</u>

The equilibrium weight change of –0.00375 g was determined from Figure A2-1.
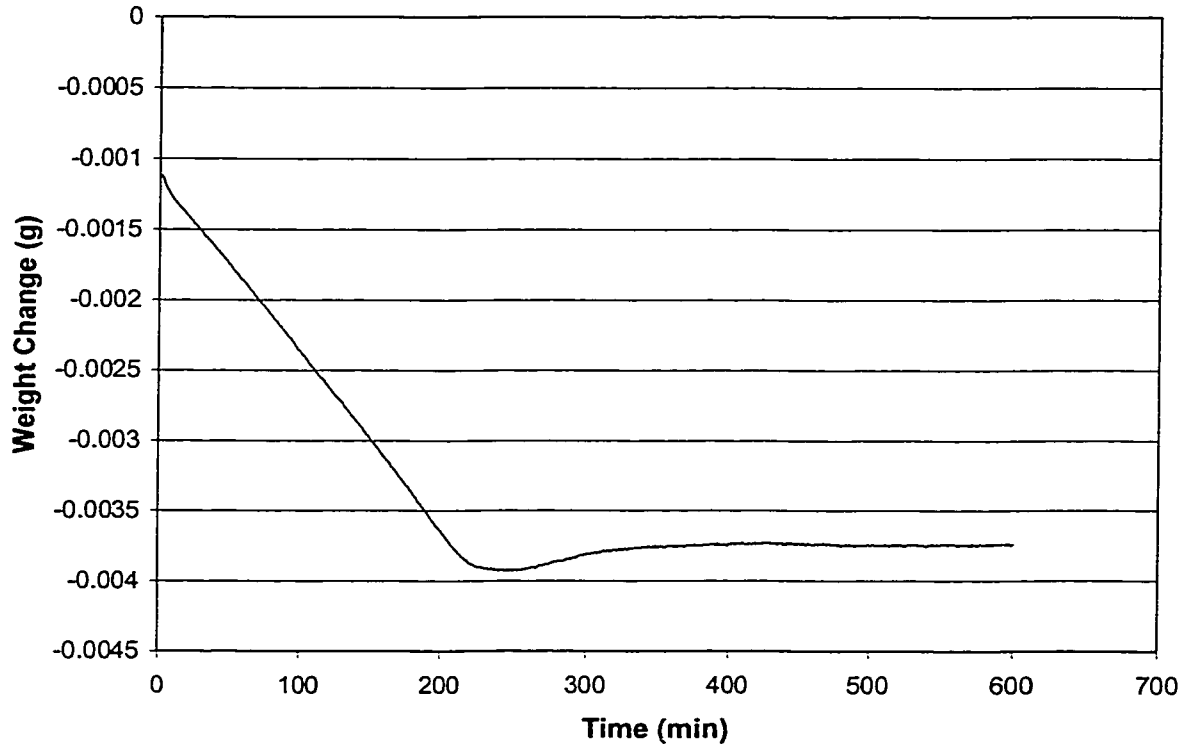
Figure A2-1 - Weight Change of Sample MM019 During Ethylene Sorption at 47.7°C
and Pressure up to 2170 kPa

The weight change behaviour shown in Figure A2-1 is typical of that seen for all ethylene solubility measurements. The initial negative weight change occurs because the buoyancy effect is greater than weight of ethylene sorbed. Note that the starting weight in this figure is –0.00112 g and not zero; the starting weight change for this measurement

was the equilibrium weight change from the previous experimental run at 790 kPa. In later experiments, all three pressures were recorded in the same data file.

Gas Density from Peng-Robinson Equation:

The original form of the equation is

$$P = \frac{RT}{v-b} - \frac{a(T)}{v(v+b)+b(v-b)}$$

which can be rewritten as

$$Z^3 - (1-B)Z^2 + (A-3B-2B)Z - (AB-B^2-B^3) = 0$$

where

$$A = \frac{aP}{R^2 T^2}$$

$$B = \frac{bP}{RT}$$

$$Z = \frac{Pv}{RT}$$

To calculate these parameters we need a number of constants for ethylene gas:
Critical Temperature (T_c): 282.344 K
Critical Pressure (P_c): 5.0408 MPa
Acentric factor (ω): 0.08294

Now the following sequence of calculations is used to find values for a(T) and b(T):

$\kappa = 0.37464 + 1.54226\omega - 0.26992\omega^2$
$\kappa = 0.37464 + 1.54226(0.08294) - 0.26992(0.08294)^2$
$\kappa = 0.500698$

$\alpha^{1/2} = 1 + \kappa(1-(T/T_c)^{1/2})$
$\alpha^{1/2} = 1 + 0.500698(1-(320.85/282.344)^{1/2})$
$\alpha = 0.934989$

The attraction parameter and Van der Waals covolume, a(T) and b(T) respectively, are then calculated using:

$$a(T) = 0.408 \frac{R^2 T_c^2}{P_c}\alpha$$

$$a(T) = 0.408 \frac{(8.31451)^2 (282.344)^2}{5.0408(1000000)}(0.934989)$$

$$a(T) = 0.417059$$

$$b(T) = 0.07 \frac{RT_c}{P_c}$$

$$b(T) = 0.07 \frac{8.3451(282.344)}{5.0408(1000000)}$$

$$b(T) = 0.00003260$$

Note that the constants 0.408 and 0.007 are those given by Bu et al. (1995). With these values, the constants A and B are calculated as:

$$A = \frac{0.417059(2169083)}{(8.31451)^2(320.85)^2}$$

$$A = 0.127115$$

$$B = \frac{0.00003260(2169083)}{(8.31451)(320.85)}$$

$$B = 0.026506$$

Now substituting in the values for A and B, equation 2 can be solved to give Z=0.896565. The specific volume of the gas is then

$$v = \frac{ZRT}{P}$$

$$v = \frac{0.896565(8.31451)(320.85)}{2169083}$$

$$v = 0.0011027 \text{ m}^3 / \text{mol}$$

The density of the gas is then

$$\rho_g = \frac{0.0280536 \text{ kg/mol}}{0.0011027 \text{ m}^3/\text{mol}}$$

$$\rho_g = 25.44 \text{ kg/m}^3$$

Thermal and Pressure Expansion Coefficient:

The pressure expansion coefficient was determined to be equal to 5.71×10^{-6} times the pressure in kilopascals. Therefore

β=(0.00000571)(2169.083)

β=0.012386

The thermal expansion coefficient (α) was 0.000263.

Sample Volume and Buoyancy Correction:

Because of a change in the buoyancy of the plastic sample when a gas is introduced to the system, the mass of absorbed gas cannot simply be determined by the measured weight change.

The buoyancy force on the sample is given by
$$F_b = \rho_{gas} g V$$
where ρ_{gas} is the gas density, V is the sample volume and g is the gravitational acceleration.

The sample volume at the experimental temperature and pressure can be obtained using
$$V_{T,P} = V_{26,0}[(1+3\alpha(T-26)](1+2\beta_{T,P})$$
where $V_{T,P}$ is the volume at experimental conditions and $V_{26,0}$ is the volume at room temperature (26 °C) and 0 psig.

The volume at room temperature can be obtained from the mass of the sample and its density.

$$V_{26,0} = \frac{0.4443\,g}{0.885\,g/cm^3}$$

$$V_{26,0} = 0.5020\,cm^3$$

Under the given experimental conditions, the volume of the sample is then
$$V = 0.5020\,cm^3[(1+3(0.000263)(47.7-26)](1+3(0.012386)$$

$$V = 0.52960\,cm^3$$

The buoyancy force is then
$$F_b = 25.44\,kg/m^3(0.00000052960\,m^3)(9.80665\,m/s^2)$$
$$F_b = 0.0001321\,N$$

For reasons of convenience that will be apparent shortly, it is useful to consider this buoyancy in terms of a mass rather than a force. If F_b is divided by g, it has a value of 0.000013473 kg or 0.013473 g.

Solubility:

The final step of calculating the gas solubility in the polymer sample is very simple. The solubility is given by

$$S = \frac{W_b + F_{b,s} - F_{b,b}}{W_s}$$

where W_b is the measured weight change, W_s is the amorphous sample weight. $F_{b,b}$ is the sample buoyancy force, and $F_{b,s}$ is the background bouyancy. The amorphous sample weight is determined by multiplying the sample weight by the amorphous volume fraction:
$$W_s = (0.4443\,g)(1-0.185)$$
$$W_s = 0.3621\,g$$

It is obvious that g is a common factor in this expression so this is why it is useful to factor it out and use all of the values in grams. Therefore the solubility can be calculated as

$$S = \frac{-0.00375\,g + 0.013473\,g - 0.0003\,g}{0.3621\,g\,amPE}$$

$$S = 0.02602\,g/g\,amPE$$

Therefore, the solubility of ethylene in the sample MM019 at 47.7 °C and 314.6 psi is 0.02602 g/g amPE.

Appendix 3

Complete Solubility Measurements

Ethylene Solubility

Table A3-1
Ethylene Solubility in MM003, Sample Mass: 0.5088 g

Temperatur (C)	Pressure (kPa)	Gas Density (kg/m³)	Weight Change (g)	Thermal Expansion Coefficient	Pressure Expansion Coefficient	Sample Volume (cm³)	Background Buoyancy (g)	Buoyancy (g)	Solubility (g/g)	Solubility (g/g amPE)
27.5	783.238	9.19114	-0.0028	0.000195	0.0024751	0.5558	0.005109	0.00014	0.004302	0.0086727
27.6	2154.59	27.6890	-0.0094	0.000195	0.0068086	0.563	0.01559	0.00026	0.011635	0.023457
27.7	3547.32	50.8636	-0.0187	0.000195	0.0112096	0.5704	0.02901	-0.00002	0.020224	0.040775
47.7	805.99	8.80816	-0.0029	0.000195	0.0028935	0.5631	0.00496	0.00013	0.003891	0.0078449
47.7	2154.59	25.2170	-0.0086	0.000195	0.0077351	0.5712	0.014404	0.0003	0.010758	0.021690
47.7	3530.09	44.7594	-0.0166	0.000195	0.0126731	0.5795	0.025937	0.00019	0.017918	0.036125
67.7	785.996	8.0262	-0.0026	0.000195	0.0019807	0.568	0.004559	0.00013	0.003556	0.0071693
67.7	2138.74	23.0939	-0.0081	0.000195	0.0053897	0.5738	0.013252	0.00025	0.009713	0.019582
67.7	3512.85	40.3256	-0.015	0.000195	0.0088525	0.5797	0.023376	0.00019	0.01607	0.032399
87.9	795.648	7.6332	-0.0026	0.000195	0.0028962	0.5762	0.004398	0.00015	0.0032	0.0064511
87.8	2140.8	21.4958	-0.0076	0.000195	0.0077926	0.5845	0.012565	0.00028	0.009208	0.018564
87.7	3526.64	37.1919	-0.0137	0.000195	0.0128371	0.5931	0.02206	0.00021	0.016057	0.032374

Table A3-2
Ethylene Solubility in MM013, Sample Mass: 0.5313 g

Temperatur (C)	Pressure (kPa)	Gas Density (kg/m³)	Weight Change (g)	Thermal Expansion Coefficient	Pressure Expansion Coefficient	Sample Volume (cm³)	Background Buoyancy (g)	Buoyancy (g)	Solubility (g/g)	Solubility (g/g amPE)
27.6	859.08	10.1411	-0.0041	0.000094	0.0010824	0.559	0.005669	0.00014	0.002764	0.009276
27.7	2186.31	28.1470	-0.0119	0.000094	0.0027548	0.5618	0.015813	0.00026	0.006969	0.023386
27.7	3561.11	51.1237	-0.0232	0.000094	0.004487	0.5647	0.028869	-0.00002	0.010745	0.036057
47.6	864.595	9.4793	-0.004	0.000094	0.0013055	0.5625	0.005332	0.00013	0.002263	0.007593
47.7	2147.7	25.1445	-0.0110	0.000094	0.0032431	0.5658	0.014226	0.0003	0.005526	0.018545
47.6	3568.7	45.3746	-0.0207	0.000094	0.0053888	0.5694	0.025835	0.00019	0.009288	0.031169
67.7	852.185	8.7254	-0.0031	0.000094	0.0010908	0.5653	0.004933	0.00019	0.003078	0.0103301
67.8	2148.39	23.2002	-0.0105	0.000094	0.00275	0.5681	0.013181	0.00025	0.0045	0.015100
67.7	3534.22	40.6103	-0.0191	0.000094	0.0045238	0.5711	0.023193	0.00019	0.007309	0.024526
88.0	852.185	8.1883	-0.0038	0.000094	0.0010397	0.5684	0.004654	0.00015	0.001364	0.0045756
87.9	2175.28	21.8596	-0.0103	0.000094	0.0026539	0.5712	0.012485	0.00028	0.003511	0.011780
87.9	3540.43	37.3263	-0.0183	0.000094	0.0043194	0.574	0.021425	0.00021	0.005542	0.018599

Table A3-3
Ethylene Solubility in MM019, Sample Mass: 0.4443 g

Temperatur (C)	Pressure (kPa)	Gas Density (kg/m³)	Weight Change (g)	Thermal Expansion Coefficient	Pressure Expansion Coefficient	Sample Volume (cm³)	Background Buoyancy (g)	Buoyancy (g)	Solubility (g/g)	Solubility (g/g amPE)
27.7	814.954	9.5851	-0.0012	0.000263	0.004955	0.5102	0.00489	0.00014	0.008103	0.0099422
27.7	2169.76	27.9007	-0.0038	0.000263	0.0131923	0.5226	0.014581	0.00026	0.02359	0.0289446
27.7	3547.32	50.8639	-0.0091	0.000263	0.0215679	0.5352	0.027224	-0.00002	0.04077	0.0500245
47.7	838.396	9.17697	-0.0011	0.000263	0.004787	0.518	0.004753	0.00013	0.007975	0.0097854
47.7	2169.07	25.4416	-0.0038	0.000263	0.012386	0.5296	0.013474	0.0003	0.021211	0.0260255
47.7	3545.25	44.9937	-0.0081	0.000263	0.0202436	0.5416	0.02437	0.00019	0.036125	0.0443253
67.7	814.954	8.33163	-0.001	0.000263	0.004401	0.5254	0.004377	0.00013	0.007242	0.0088853
67.7	2180.1	23.6065	-0.0035	0.000263	0.011773	0.5369	0.012674	0.00025	0.019994	0.024533
67.6	3526.64	40.5308	-0.0073	0.000263	0.019044	0.5481	0.022216	0.00019	0.033168	0.0406964

Table A3-4
Ethylene Solubility in MM029, Sample Mass: 0.2569 g

Temperatur (C)	Pressure (kPa)	Gas Density (kg/m³)	Weight Change (g)	Thermal Expansion Coefficient	Pressure Expansion Coefficient	Sample Volume (cm³)	Background Buoyancy (g)	Buoyancy (g)	Solubility (g/g)	Solubility (g/g amPE)
29.9	819.78	9.56467	-0.0016	0.000201	0.0025003	0.2829	0.002706	0.00014	0.003955	0.0074621
29.9	2173.21	27.6531	-0.0049	0.000201	0.0066283	0.2864	0.00792	0.00026	0.010898	0.020562
29.9	3531.47	49.8353	-0.0099	0.000201	0.010771	0.2899	0.014447	-0.00002	0.017931	0.033833
49.6	807.369	8.77495	-0.0012	0.000201	0.0025351	0.2863	0.002512	0.00013	0.004641	0.0087566
49.5	2210.44	25.7642	-0.0045	0.000201	0.0069408	0.29	0.007473	0.0003	0.01052	0.019849
49.6	3539.74	44.463	-0.0086	0.000201	0.0111148	0.2936	0.013055	0.00019	0.016718	0.031544
69.1	808.748	8.22872	-0.0014	0.000201	0.0022685	0.2894	0.002381	0.00013	0.003314	0.0062524
69.1	2210.44	23.8128	-0.0045	0.000201	0.0062003	0.2928	0.006972	0.00025	0.008727	0.016466
69.1	3545.94	40.5102	-0.0081	0.000201	0.0099464	0.296	0.011991	0.00019	0.014291	0.026965
87.9	810.817	7.78243	-0.0013	0.000201	0.0021689	0.2925	0.002276	0.00015	0.003061	0.0057754
87.9	2244.91	22.6122	-0.0042	0.000201	0.0060051	0.2958	0.00669	0.00028	0.008718	0.016449
87.9	3605.93	38.1057	-0.0074	0.000201	0.0096459	0.299	0.011394	0.00021	0.014925	0.028161

1-Butene Solubility

Table A3-5
1-Butene Solubility in MM003, Sample Mass: 0.5328 g

Temperature (C)	Pressure (kPa)	Gas Density (kg/m³)	Weight Change (g)	Thermal Expansion Coefficient	Pressure Expansion Coefficient	Sample Volume (cm³)	Background Buoyancy (g)	Buoyanc (g)	Solubility (g/g)	Solubility g/g amPE)
29.8	119.968	2.751822	0.0078	0.000195	0.0094146	0.59487	0.001637	0.00003	0.017637	0.035558
29.8	228.904	5.398088	0.02	0.000195	0.0193703	0.61215	0.003304	0.00005	0.043589	0.087882
29.9	286.13	6.859141	0.0311	0.000195	0.026067	0.62381	0.004279	0.00007	0.066327	0.133723
49.3	197.188	4.30017	0.0099	0.000195	0.0138603	0.60945	0.002621	0.00002	0.023387	0.047152
49.3	359.214	8.133288	0.0223	0.000195	0.0246679	0.62842	0.005111	0.00002	0.05141	0.103649
49.3	528.823	12.50501	0.0521	0.000195	0.0554683	0.68248	0.008534	-0.00004	0.113822	0.22948
68.8	292.335	6.082165	0.0099	0.000195	0.0130508	0.61487	0.00374	0	0.025656	0.051727
68.7	570.192	12.5617	0.028	0.000195	0.0308647	0.64645	0.008121	0	0.0677	0.136492
68.8	819.09	19.14388	0.0701	0.000195	0.0769648	0.72832	0.013943	0	0.157701	0.317945
87.9	526.066	10.69927	0.0182	0.000195	0.0237577	0.64078	0.006856	0	0.046933	0.094623
87.8	872.869	18.96745	0.0424	0.000195	0.0371525	0.66478	0.012609	0	0.103227	0.208118
87.9	1243.8	29.45712	0.1175	0.000195	0.1395563	0.84858	0.024997	0	0.26743	0.539173

Table A3-6
1-Butene Solubility in MM013, Sample Mass: 0.6116 g

Temperature (C)	Pressure (kPa)	Gas Density (kg/m³)	Weight Change (g)	Thermal Expansion Coefficient	Pressure Expansion Coefficient	Sample Volume (cm³)	Background Buoyancy (g)	Buoyanc (g)	Solubility (g/g)	Solubility g/g amPE)
30	122.726	2.815691	0.0045	0.000094	0.0037096	0.64896	0.001827	0.00003	0.010362	0.034771
30	233.041	5.497544	0.0104	0.000094	0.0096925	0.66048	0.003631	0.00005	0.022876	0.076765
30.1	290.956	6.978729	0.0155	0.000094	0.0129131	0.6667	0.004653	0.00007	0.032836	0.110189
49.6	212.357	4.642809	0.0048	0.000094	0.0053753	0.65576	0.003045	0.00002	0.012712	0.042657
49.6	350.94	7.921382	0.0083	0.000094	0.0099657	0.66465	0.005265	0.00002	0.022196	0.074483
49.5	540.544	12.81072	0.0189	0.000094	0.0203455	0.68473	0.008772	-0.00004	0.045245	0.151829
69	281.304	5.836336	0.0041	0.000094	0.004414	0.65746	0.003837	0	0.012945	0.043439
68.9	550.197	12.05907	0.0079	0.000094	0.0110349	0.67033	0.008084	0	0.026167	0.087807
68.9	836.327	19.61901	0.0174	0.000094	0.0226105	0.69286	0.013593	0	0.050725	0.170217
88	580.534	11.91842	0.0031	0.000094	0.0083345	0.66861	0.007969	0	0.018049	0.060567
87.9	913.548	20.01509	0.0078	0.000094	0.0175987	0.68672	0.013745	0	0.035145	0.117937
87.9	1225.88	28.90901	0.0179	0.000094	0.0296111	0.71023	0.020532	0	0.062887	0.211031

Table A3-7
1-Butene Solubility in MM019, Sample Mass: 0.4349 g

Temperature (C)	Pressure (kPa)	Gas Density (kg/m³)	Weight Change (g)	Thermal Expansion Coefficient	Pressure Expansion Coefficient	Sample Volume (cm³)	Background Buoyancy (g)	Buoyanc (g)	Solubility (g/g)	Solubility g/g amPE)
29.9	118.589	2.718272	0.016	0.000263	0.023657	0.52791	0.001435	0.00003	0.040113	0.049218
29.9	229.594	5.413025	0.0462	0.000263	0.0435805	0.55737	0.003017	0.00005	0.113077	0.138744
30	283.372	6.785267	0.0792	0.000263	0.0726758	0.60044	0.004074	0.00007	0.191341	0.234774
49.5	209.599	4.575655	0.0202	0.000263	0.0397162	0.56016	0.002563	0.00002	0.052249	0.064109
49.5	393.687	8.981652	0.059	0.000263	0.0508166	0.57683	0.005181	0.00002	0.147507	0.18099
49.5	535.718	12.68188	0.1619	0.000263	0.2091942	0.81464	0.010331	-0.00004	0.396209	0.486146
68.9	287.509	5.974072	0.0222	0.000263	0.019781	0.53819	0.003215	0	0.058531	0.071817
68.9	573.639	12.6367	0.0659	0.000263	0.0657288	0.60823	0.007686	0	0.16911	0.207497
68.9	666.028	14.98478	0.0913	0.000263	0.0861604	0.63937	0.009581	0	0.231871	0.284504
69.2	285.441	5.923204	0.0222	0.000263	0.0195443	0.53796	0.003186	0	0.058396	0.071652
69.2	589.497	13.01486	0.0673	0.000263	0.0690416	0.61342	0.007984	0	0.173036	0.212315
69.1	814.264	18.98353	0.1664	0.000263	0.1246494	0.69814	0.013253	0	0.413137	0.506916

Table A3-8
1-Butene Solubility in MM029, Sample Mass: 0.4413 g

Temperature (C)	Pressure (kPa)	Gas Density (kg/m³)	Weight Change (g)	Thermal Expansion Coefficient	Pressure Expansion Coefficient	Sample Volume (cm³)	Background Buoyancy (g)	Buoyanc (g)	Solubility (g/g)	Solubility g/g amPE)
30	117.899	2.702126	0.0078	0.000201	0.0109347	0.49823	0.001346	0.00003	0.020748	0.039148
30	228.904	5.393895	0.0197	0.000201	0.0293863	0.52493	0.002831	0.00005	0.050944	0.09612
30	286.82	6.874169	0.0313	0.000201	0.0421536	0.54341	0.003735	0.00007	0.079188	0.149411
49.5	203.394	4.4396	0.0091	0.000201	0.0129931	0.50709	0.002251	0.00002	0.025745	0.048575
49.5	365.419	8.279891	0.0212	0.000201	0.0289033	0.53038	0.004392	0.00002	0.057969	0.109375
49.6	532.96	12.60067	0.0515	0.000201	0.0661073	0.58489	0.00737	-0.00004	0.133515	0.251914
68.9	290.956	6.049685	0.0107	0.000201	0.0141284	0.51462	0.003113	0	0.031211	0.058888
68.9	560.539	12.31358	0.0256	0.000201	0.0326069	0.54199	0.006674	0	0.07302	0.137774
68.9	819.78	19.16946	0.0635	0.000201	0.0820124	0.61516	0.011792	0	0.170592	0.321872
88	559.85	11.45082	0.0165	0.000201	0.0252645	0.53707	0.00615	0	0.051303	0.096798
88	881.143	19.16716	0.0359	0.000201	0.0491253	0.57281	0.010979	0	0.106139	0.200262
88	1241.05	29.32864	0.09	0.000201	0.1073279	0.65998	0.019356	0	0.247692	0.467343

1-Hexene Solubility

Table A3-9
1-Hexene Solubility in MM003, Sample Mass: 0.3536 g

Temperature (C)	Pressure (kPa)	Gas Density (kg/m³)	Weight Change (g)	Thermal Expansion Coefficient	Pressure Expansion Coefficient	Sample Volume (cm³)	Buoyancy (g)	Background Buoyancy (g)	Solubility (g/g)	Solubility (g/g amPE)
69.1	55.1576	1.6657	0.0184	0.000195	0.0089493	0.4033	0.000672	0.00003	0.05371	0.1082859
69.1	68.947	2.09306	0.0276	0.000195	0.0217398	0.4184	0.000876	0.0001	0.080191	0.1616762
69.1	110.315	3.40378	0.0952	0.000195	0.085439	0.4934	0.00168	-0.00026	0.274829	0.5540907
88	75.8417	2.17812	0.0242	0.000195	0.0229435	0.4243	0.000924	-0.00001	0.071166	0.1434794
88	132.378	3.87609	0.0603	0.000195	0.0318969	0.435	0.001686	-0.00013	0.175752	0.3543394
88	164.783	4.88056	0.0972	0.000195	0.0923069	0.5069	0.002474	-0.00018	0.282478	0.5695114 *
87.9	191.673	5.73533	0.1746	0.000195	0.1957293	0.6301	0.003614	-0.00018	0.504366	1.016866

* Measured as a check because solubility at 191.7 kPa was so high

Table A3-10
1-Hexene Solubility in MM013, Sample Mass: 0.6122 g

Temperature (C)	Pressure (kPa)	Gas Density (kg/m³)	Weight Change (g)	Thermal Expansion Coefficient	Pressure Expansion Coefficient	Sample Volume (cm³)	Buoyancy (g)	Background Buoyancy (g)	Solubility (g/g)	Solubility (g/g amPE)
69.1	51.0208	1.5385	0.0117	0.000094	0.0211236	0.7139	0.001098	0.00003	0.020775	0.0697139
69.1	67.5681	2.05009	0.0172	0.000094	0.0271203	0.726	0.001488	0.0001	0.030314	0.1017251
69.1	106.178	3.27079	0.0433	0.000094	0.0394856	0.7509	0.002456	-0.00026	0.075083	0.2519568
87.8	71.7049	2.05771	0.0099	0.000094	0.006449	0.6879	0.001415	-0.00001	0.018418	0.0618052
87.8	128.931	3.77288	0.0227	0.000094	0.0153951	0.706	0.002664	-0.00013	0.041692	0.139905
87.8	190.294	5.69276	0.0628	0.000094	0.0263807	0.7282	0.004146	-0.00018	0.109614	0.3678322

Table A3-11
1-Hexene Solubility in MM019, Sample Mass: 0.2378 g

Temperature (C)	Pressure (kPa)	Gas Density (kg/m³)	Weight Change (g)	Thermal Expansion Coefficient	Pressure Expansion Coefficient	Sample Volume (cm³)	Buoyancy (g)	Background Buoyancy (g)	Solubility (g/g)	Solubility (g/g amPE)
69.2	51.0208	1.53801	0.0249	0.000263	0.0451905	0.3155	0.000485	0.00003	0.106751	0.1309823
69.2	75.1522	2.28832	0.0517	0.000263	0.130038	0.3863	0.000884	0.0001	0.22058	0.2706501
69.2	91.01	2.78355	0.1022	0.000263	0.2079899	0.4232	0.001178	-0.00026	0.464878	0.5349026 **
69.2	113.763	3.51423	0.1596	0.000263	0.3505808	0.5701	0.002003	-0.00026	0.680734	0.8352559 *

* Equilibrium not reached, sample fell off hangdown wire
** Measured as a check using second sample, mass: 0.2230 g

Table A3-12
1-Hexene Solubility in MM029, Sample Mass: 0.2853 g

Temperature (C)	Pressure (kPa)	Gas Density (kg/m³)	Weight Change (g)	Thermal Expansion Coefficient	Pressure Expansion Coefficient	Sample Volume (cm³)	Buoyancy (g)	Background Buoyancy (g)	Solubility (g/g)	Solubility (g/g amPE)
68.9	46.884	1.41194	0.0123	0.000201	0.0082496	0.3271	0.000462	0.00003	0.044591	0.0841339
68.9	76.5312	2.3315	0.0264	0.000201	0.0346128	0.3523	0.000821	0.0001	0.095028	0.1792977
68.9	113.763	3.52034	0.0846	0.000201	0.0909266	0.4062	0.00143	-0.00026	0.302524	0.5707999
88.1	78.5996	2.25856	0.0151	0.000201	0.0242992	0.3463	0.000782	-0.00001	0.055808	0.1052989
88.1	135.826	3.98054	0.0389	0.000201	0.0497048	0.3709	0.001476	-0.00013	0.141838	0.267619
88	178.573	5.31869	0.0912	0.000201	0.0942156	0.414	0.002202	-0.00018	0.328047	0.6189568